

The Kinetics of Redox Reactions of Mn(II) and Mn(III) in Aqueous Systems:
Homogenous Autoxidation of Mn(II) and the Formation and Disappearance of
Mn(III) Complexes

Thesis by
J. Kenneth Klewicki

In Partial Fulfillment of the Requirements
for the Degree of
Doctor of Philosophy

California Institute of Technology

Pasadena, California

(Submitted January 9, 1996)

c 1996

Joseph Kenneth Klewicki

All rights Reserved

ACKNOWLEDGEMENTS

I would like to thank and acknowledge all those people who have helped to make this thesis and the work underlying it possible. First of all, my gratitude goes to my advisor whose patient but firm guidance and wise advise has been an invaluable asset throughout my graduate career. To my examination committee: Janet Hering, Michael Hoffmann, Geoffrey Blake, and Glen Cass; goes my thanks for encouraging me to make this the best thesis it could be. Many others have also helped me in the lab to learn the ropes and master new techniques, especially; Mark Schlautman, Jeff Noelte, Ron Seifert, Peter Green, and Simo Pehkonen. I would also like to thank all the secretaries especially, Fran Matzen, Elaine Granger, and Linda Scott for helping me with a thousand little things that made this work so much easier.

This work would not have been possible without the financial support of the Mellon Foundation, the General Motors Gift for Environmental Research, and National Science Foundation grant #ATM-9303024.

My thanks must also go to all those who have supported me morally and spiritually throughout the last six years. To my wife, who although has only been in my life for the last three years I could not imagine having come this far without her, my undying love and gratitude for comfort, encouragement and inspiration. To my parents who have always encouraged me to go for the best even when it meant sacrifice for them, I offer my love and thanks. To Father Brian Wilson goes blessings and thanks for encouraging me develop as a person as well as a scientist. To the countless people at the Newman Center, St. Philip's Church, and the Archdioceses who have prayed with me and for me throughout the years I can only return your prayers. Lastly, but certainly not the least, I would like to thank God; who brought all of the above people into the world and my life and gave me the graces required to complete this thesis.

Abstract

The kinetics of manganese redox reactions are important for understanding redox cycles in natural waters. This study examined the kinetics of the homogenous oxidation of Mn(II) and formation and disappearance of Mn(III) complexes.

The oxidation of Mn(II) was studied to determine the homogenous oxidation rate in the absence of solid surfaces and biological activity. Experiments were conducted at 35, 45, 50, and 60°C. The pH was 8.0. The reaction solution was prepared so that at no time during the experiment was the solubility product of any solid phase exceeded. Oxidized Mn was measured using leuco crystal violet dye reagent. Measurable rates were observed for the 45, 50, and 60°C experiments. An Arrhenius expression was fitted to the rates in order to extrapolate to 25°C. The second order rate constant for the rate expression

$$-\frac{d[\text{Mn(II)}]}{dt} = k \cdot [\text{Mn(II)}] \cdot [\text{O}_2]$$

was calculated to be $6.9 \pm 1.6 \times 10^{-7} \text{ M}^{-1}\text{s}^{-1}$.

The kinetics of disappearance of Mn(III) complexes from aqueous solution were studied. Complexes of pyrophosphate ($\text{P}_2\text{O}_7^{4-}$), ethylenediaminetetracetate (EDTA), and citrate (CIT) were synthesized from MnO_4^- and a Mn(II) salt in a 1:4 ratio in the presence of excess ligand. Concentrations of Mn(III) complex were monitored spectrophotometrically. Experiments were conducted in the pH range of 6 to 9 for pyrophosphate and citrate and 3 to 9 for EDTA. The total manganese concentration was varied between 0.5 and 1.0 mM. Ligand concentrations were varied from 0.5mM to 200mM. Experiments were also conducted to examine the effects of oxygen, light, and ionic strength. Oxygen had a significant effect on only the citrate complex; ionic strength affected only the EDTA complex. Light was found to be insignificant in all cases.

The Mn(III)P₂O₇ complex was found to disappear from solution relatively slowly providing the ligand was in at least ten-fold excess. Disappearance time scales were on the order of 10⁷ s. The Mn(III)EDTA complex reacted rather rapidly with time scales on the order of 10⁴ s. There were at least two Mn(III)EDTA complexes, a protonated one more stable at low pH and an unprotonated one more stable at high pH. The pK_a of the complex appeared to be approximately 5.3. The rate of disappearance of the Mn(III)EDTA had a fractional dependence on pH, probably indicative of an unknown pH dependent intermediate in the decomposition of the complex. The rate was found to increase with increased EDTA, indicating that the rate limiting step was an outer sphere electron transfer from Mn(III)EDTA to an excess EDTA. The rate law for the reaction above pH 6 was found to be

$$-\frac{d[\text{Mn(III)EDTA}]}{dt} = k \cdot [\text{H}^+]^{0.31} \cdot [\text{EDTA}]^{1.35} \cdot [\text{Mn(III)EDTA}]$$

The Mn(III)CIT complex was found to undergo a redox cycle. The Mn(III)CIT complex was reduced, forming Mn(II). The Mn(II) was then oxidized in the presence of oxygen to re-form the Mn(III) complex. Both pH and ligand concentration were found to have fractional orders in the rate expression, largely due to the competition between the reduction and the oxidation and possibly complicated by radicals formed by the reaction.

The dissolution of MnOOH by pyrophosphate, EDTA, and citrate was studied. A MnOOH solid was synthesized by oxidizing Mn(II) with hydrogen peroxide at elevated temperatures and high pH. The solid was identified by X-ray diffraction to be β-MnOOH, with some contamination by Mn₃O₄. Throughout the dissolution process samples were removed by pipette and filtered. The filtrate was analyzed spectrophotometrically for the presence of Mn(III) complexes and total Mn. The

solids captured on the filter were analyzed by an iodine titration technique, coupled with formaldoxime measurements to determine the average oxidation state of the solids. The effects of pH and ligand concentration on rates were examined.

Pyrophosphate was found to dissolve the Mn(III) solids nonreductively, producing the Mn(III) complex in solution. The dissolution reaction rate was dependent on approximately the half power of $[H^+]$, possibly indicative of a surface binding ligand binding on the surface. No dependence on the ligand concentration was found down to a ligand:Mn ratio of 10:1, probably indicative of surface site saturation by ligand.

EDTA was found to dissolve the solids reductively with no Mn(III) solution species being observed. The dependence on $[H^+]$ was approximately one half order, possibly indicative of a surface binding.

Citrate dissolved the MnOOH solids in what appeared to be two steps. There seemed to be an initial stage of nonreductive dissolution, followed by a reductive dissolution. The rate and duration of the two different stages depended on pH. The dependence was slightly greater than first order in $[H^+]$, possibly indicating the reaction becomes controlled by reactions of the radicals produced by oxidation of the citrate.

This study has shown that Mn(III) complexes can be formed in pH conditions relevant to natural waters. These complexes can be formed either through oxidation of Mn(II) by strong oxidants in the presence of stabilizing ligands or by dissolution of Mn(III)-containing solids by stabilizing ligands. Once formed, the lifetime of these complexes will depend on the nature of the ligand and chemical characteristics of the aquatic environment. If the ligand does not rapidly reduce Mn(III) these complexes can be powerful mobile oxidants which could significantly affect the local redox environment.

TABLE OF CONTENTS

Abstract	iv
1 INTRODUCTION	1
1.1 Introduction	1
1.1.1 Mn(II)	1
1.1.2 Mn(IV)	3
1.1.3. Mn(III)	4
1.1.4 Redox Transitions	7
1.2. Scope of This Study	9
1.2.1 Homogenous Oxidation	9
1.2.2 Mn(III) Complexes	9
Chapter 1 References	10
2.1 EXPERIMENTAL METHODS	16
2.1 Introduction	16
2.1.1 Total Mn	16
2.1.2 Mn(II)	16
2.1.3 Oxidized Mn	17
2.2 Methods Used	19
2.2.1 Total Mn	19
2.2.2 Oxidized Mn	19
2.2.3 Mn(III)	21
2.2.4 pH of Zero Point of Charge	21
Chapter 2 References	23
Chapter 2 Figures	24
3.1 HIGH TEMPERATURE Mn(II) AUTOXIDATION	28
3.1 Previous Studies	28
3.2 Current Study	30
3.2.1 Solubility Considerations	30
3.2.2 Experimental Method	32
3.3 Results	34
3.3.1 45°C	34
3.3.2 50°C	34
3.3.3 60°C	34

3.3.4 Extrapolation to Room Temperature	35
3.3.5 Comparison and Discussion of Results	38
Chapter 3 References	41
Chapter 3 Tables	43
Chapter 3 Figures	44
4.1 Mn(III) SOLUTION COMPLEXES	49
4.1 Introduction	49
4.1.1 Pyrophosphate	49
4.1.2 Citrate	51
4.1.3 Ethylenediaminetetracetate (EDTA)	52
4.1.4 This Study	52
4.2 Experimental	53
4.2.1 Complex Preparation	54
4.2.2 Experimental Monitoring	54
4.3 Results and Discussion	55
4.3.1 Pyrophosphate	55
4.3.1.1 Effect of pH	55
4.3.1.2 Effect of Ligand Concentration	63
4.3.2 EDTA	65
4.3.2.1 Effect of pH	65
4.3.2.2 Effect of Ligand Concentration	69
4.3.2.3 Effect of Light and Ionic Strength	71
4.3.3 Citrate	72
4.3.3.1 Effect of pH	72
4.3.3.2 Effect of Oxygen on Reformation of the Mn(III) Complex	73
4.3.3.3 Effect of Ligand Concentration	75
4.4 Conclusions	77
4.4.1 Pyrophosphate	78
4.4.2 EDTA	78
4.4.3 Citrate	78
Chapter 4 References	79
Chapter 4 Mechanisms	81
Chapter 4 Tables	85
Chapter 4 Figures	89

5.1 MnOOH DISSOLUTION BY LIGANDS	110
5.1 Introduction	110
5.1.1 Mn(III) Solid Phases	111
5.1.2 MnOOH Reactions	112
5.1.3 This Study	113
5.2 Experimental	113
5.2.1 Solids Preparation	113
5.2.2 Solids Characterization	113
5.2.3 Experimental Procedures	115
5.3 Results and Discussion.....	115
5.3.1 Pyrophosphate	115
5.3.1.1 Effect of pH.....	115
5.3.1.2 Effect of Solids Concentration	118
5.3.1.3 Effect of Ligand	122
5.3.1.4 Oxidation State	122
5.3.2 EDTA	123
5.3.3 Citrate	126
5.4 Conclusions	130
5.4.1 Pyrophosphate	130
5.4.2 EDTA	130
5.4.3 Citrate	131
Chapter 5 References	131
Chapter 5 Mechanisms	134
Chapter 5 Tables	136
Chapter 5 Figures	137
6.1 SUMMARY AND CONCLUSIONS	152
6.1 Important Findings of This Study	152
6.1.1 Mn Oxidation	152
6.1.2 Mn(III)	152
6.1.3 MnOOH Dissolution	153
6.2 Implications of This Study	154
6.2.1 Surface Waters	155
6.2.2 Ground Waters	159
6.2.3 Other Potential Environments for Mn(III) Complexes	160
6.3 Directions for Future Research	161
6.3.1 Mn(II) Oxidation	161

6.3.2 Mn(III) Solution Complexes	161
6.3.3 MnOOH Dissolution	163
Chapter 6 References	164
Chapter 6 Tables	165
Chapter 6 Figures	170
APPENDICES	174
Appendix A	174
Tables	174

List of Tables

Table 3.1: Comparison of Homogenous Rate Constants of Autoxidation of Mn(II) at 25°C	43
Table 4.1: Some Properties of Ligands Used in This Study	85
Table 4.2 First Order Fit Parameters for Mn(III)P ₂ O ₇ Dissappearance: [P ₂ O ₇] = 25mM	86
Table 4.3 First Order Fit Parameters for Mn(III)P ₂ O ₇ Dissappearance: pH = 7.8	86
Table 4.4 First Order Fit Parameters for Mn(III)EDTA Dissappearance: [EDTA] = 25mM	87
Table 4.5 First Order Fit Parameters for Mn(III)EDTA Dissappearance: pH= 6.8	87
Table 4.6 First Order Fit Parameters for Mn(III)CIT Dissappearance: [CIT]=0.2M	88
Table 4.7 First Order Fit Parameters for Mn(III)CIT Dissappearance: pH ₀ = 6.0	88
Table 5.1: Redox Characterization of Synthesized Mn Solids	136
Table 6.1: Rate Constants for Mn(III)L Disappearance	165
Table 6.2: Rate Constants for MnOOH Dissolution	168
Table 6.3: Rate Constants and Expressions Used for Box Model	169
Table A1: Acidity Constants of Ligands Used in This Study	174
Table A2: Stability Constants of Mn(II) and Mn(III) Complexes	175
Table A3: Equilibrium Constants of Mn Solids	175
Table A4: Band Gap Energy of β-MnO ₂	175

List of Figures

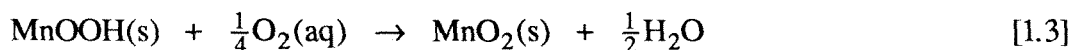
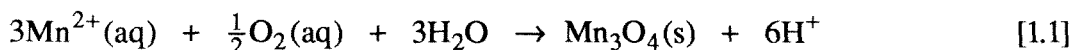
Figure 2.1: Formaldoxime Calibration Curve	24
Figure 2.2: Leuco Crystal Violet Calibration Curve	25
Figure 2.3: Top View of Electrophoretic Mobility Device	26
Figure 2.4: Sample Data for Electrophoretic Mobility Measurements	27
Figure 3.1: Mn(II) Speciation	44
Figure 3.2: 50°C Oxidation Reactor pH	45
Figure 3.3: Oxidation of Mn(II) at 45°C.....	46
Figure 3.4: Oxidation of Mn(II) at 50°C.....	47
Figure 3.5: Oxidation of Mn(II) at 50°C.....	48
Figure 4.1a: Disappearance of Mn(III)P ₂ O ₇ Complex - Dependence on pH	89
Figure 4.1b: Disappearance of Mn(III)P ₂ O ₇ Complex - Dependence on pH	90
Figure 4.2: ΔG of Disproportionation of Mn(III)P ₂ O ₇ Complex	91
Figure 4.3: Disappearance of Mn(III)P ₂ O ₇ Complex - Dependence on Ligand	92
Figure 4.4: Disappearance of Mn(III)EDTA Complex - Dependence on pH	93
Figure 4.5: Half life for Mn(III)EDTA Complex Disappearance	94
Figure 4.6: Rate Constants for Mn(III)EDTA Complex Dissappearance	95
Figure 4.7a: Disappearance of Mn(III)EDTA Complex - Dependence on Ligand....	96
Figure 4.7b: Disappearance of Mn(III)EDTA Complex - Dependence on Ligand ...	97
Figure 4.8: Rate Constants for Mn(III)EDTA Complex Disappearance	98
Figure 4.9: Disappearance of Mn(III)EDTA Complex - Dependence on Light	99
Figure 4.10: Disappearance of Mn(III)EDTA Complex - Dependence on I	100
Figure 4.11a: Disappearance of Mn(III)CIT Complex - Dependence on pH	101
Figure 4.11b: Disappearance of Mn(III)CIT Complex - Dependence on pH	102
Figure 4.12: Rate Constants for Disappearance of Mn(III)CIT Complex	103
Figure 4.13a: Disappearance of Mn(III)CIT Complex - Dependence on Oxygen ..	104
Figure 4.13b: Disappearance of Mn(III)CIT Complex - Dependence on Oxygen ..	105
Figure 4.14: Oxidation of Mn(II) in the Presence of Citrate	106
Figure 4.15a: Disappearance of Mn(III)CIT Complex - Dependence on Ligand	107
Figure 4.15b: Disappearance of Mn(III)CIT Complex - Dependence on Ligand ...	108
Figure 4.16: Rate Constants for Disappearance of Mn(III)CIT Complex	109
Figure 5.1: Proposed Cycle for Formation and Loss of Mn(III) Complexes	137
Figure 5.2: X-ray Diffraction Patterns of Synthesized Solids	138
Figure 5.3: Standard X-ray Diffraction Patterns of Mn(IV) Minerals	139
Figure 5.4: Standard X-ray Diffraction Patterns of Mn(III) Minerals	140
Figure 5.5: Standard X-ray Diffraction Patterns of MnOOH Minerals	141

Figure 5.6: Dissolution of MnOOH by P_2O_7 - Dependence on pH	142
Figure 5.7: Dissolution of MnOOH by P_2O_7 - Solids Oxidation State	143
Figure 5.8: Rate Constants for Dissolution of MnOOH by P_2O_7	144
Figure 5.9: Dissolution of MnOOH by P_2O_7 - Dependence on Solids.....	145
Figure 5.10: Dissolution of MnOOH by P_2O_7 - Solids Oxidation State	146
Figure 5.11: Dissolution of MnOOH by EDTA - pH 8.0	147
Figure 5.12: Dissolution of MnOOH by EDTA - pH 7.0	148
Figure 5.13: Dissolution of MnOOH by CIT - pH 7.8	149
Figure 5.14: Dissolution of MnOOH by CIT - pH 6.3	150
Figure 5.15: Dissolution of MnOOH by CIT - Solids Oxidation State	151
Figure 6.1a: Mn Cycle without Knowledge of Mn(III) Solution Species	170
Figure 6.1b: Mn Cycle with Knowledge of Mn(III) Solution Species	171
Figure 6.2a: Box Model Results for an Mn(II)-MnOOH-MnO ₂ System	172
Figure 6.2b: Box Model Results for an Mn(II)-MnOOH-Mn(III)L-MnO ₂ System	173

INTRODUCTION

1.1 Introduction

Manganese is one of the most important metals in the earth's crust. It is the second most abundant heavy metal in the earth's crust (1) yet it becomes even more significant because it is an essential nutrient for both plant and animal life. Mn has been found to be an essential component of the photosystem II enzyme, one of the primary enzymes responsible for electron transfer during photosynthesis(2). Herein lies one of the chief reasons for the importance of Mn in the environment, its access to several stable or quasi-stable oxidation states under natural conditions, namely the (II), (III), and (IV) oxidation states. The most common species for these redox states include $\text{Mn}^{2+}(\text{aq})$, $\text{Mn}(\text{II})(\text{OH})_2(\text{s})$, $\text{Mn}(\text{II})\text{CO}_3(\text{s})$, $\text{Mn}(\text{III})\text{OOH}(\text{s})$, $\text{Mn}(\text{II})\text{Mn}_2(\text{III})\text{O}_4(\text{s})$, and $\text{Mn}(\text{IV})\text{O}_2(\text{s})$. The oxidation of aqueous $\text{Mn}(\text{II})$ to $\text{Mn}(\text{IV})\text{O}_2(\text{s})$ is a process that involves all three oxidation states. The sequence of Mn^{2+} oxidizing to Mn_3O_4 to MnOOH to MnO_2 has been shown by Hem (3). Assuming oxygen is the sole source electron acceptor the balanced equations become:



The access to 3 different oxidation states allows Mn to act as a catalyst for many oxidation/reduction processes such as photosynthesis. Mn can also play an important part in the redox cycles of many other elements including carbon and some transition metals.

1.1.1 Mn(II)

$\text{Mn}(\text{II})$ is the most common oxidation state of manganese found in most natural systems including the oceans, rivers, and lakes. This points to one of the important features of $\text{Mn}(\text{II})$, its ability to act as a reservoir for electrons. This is evident because $\text{Mn}(\text{II})$ is so

abundant despite being thermodynamically unstable with respect to Mn(III,IV) oxyhydroxides in most oxic environments. The reason for this metastability is the comparative ease of transferring an electron to Mn compared with the difficulty of transferring an electron away.

Electron transfer to oxidized forms of Mn from many common electron donors to form Mn(II) has been found to be rapid for many electron donors (4 - 7). These reactions typically take place on time scales of minutes to hours.

Mn(II) on the other hand reacts only very slowly with the most common electron acceptor, oxygen, to give oxidized forms of Mn. In fact, in the absence of solids and bacteria, half-lives for the autoxidation of Mn(II) have been measured ranging from years to essentially nonreactive in the range of conditions found in natural waters (8 - 10). Even in the presence of biological mediation or solids the half lives are still on the order of days to weeks, much longer than for most redox reactions(9,11 - 13). The end result is that Mn(II) ends up serving as a pool for electrons between oxygen and various organic and inorganic electron donors.

Another important characteristic of Mn(II) is its solubility. $Mn^{2+}(aq)$, the most common form of Mn(II), as well as most other Mn(II) complexes, is much more soluble than the common forms of Mn(III) and Mn(IV) found in natural systems. In fact filtration is often used to distinguish between aqueous Mn(II) and Mn oxides. Despite its high solubility in comparison with oxidized Mn, $Mn^{2+}(aq)$ is still relatively insoluble. For example under typical conditions found in oceanic waters the maximum concentration of Mn^{2+} that can be present without exceeding the solubility of $MnCO_3$ is ten micromolar(10). Although natural concentrations are typically much below this level it is an important consideration in laboratory work. In fact it has been suggested that many of the known kinetic studies on Mn(II) oxidation do not report the proper constants for homogenous oxidation but rather report faster rates because of the supersaturation in many of these experiments with respect to Mn(II) solid phases(8).

1.1.2 Mn(IV)

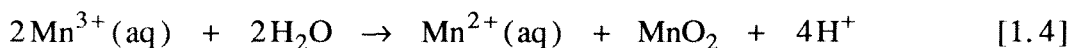
Mn(IV) is the thermodynamically stable oxidation state of Mn in most oxic environments. The most common form of Mn(IV) is MnO₂(s). MnO₂ has several common mineral forms such as, δ-MnO₂ and α-MnO₂, which are found as coatings on many natural particles and can also be found as MnO₂ colloidal particles. The fact that Mn(IV) oxides are insoluble has allowed studies to examine the cycling between oxidized Mn and Mn(II) in natural systems. Although it can be difficult to differentiate between different Mn minerals, it has been shown that there is a cycle in the ocean and other redox active bodies of water(14-16). Mn(II) is oxidized in oxic upper waters by either microbial oxidation or solids catalysis of autoxidation. The formed oxidized Mn particles then settle through the water column. In anoxic bottom waters Mn oxide particles are reductively dissolved, releasing Mn(II). The Mn(II) then diffuses upwards until it passes above the oxic/anoxic boundary where it is oxidized and again settles to the bottom waters.

Such cycling of Mn particles is of interest not only with respect to Mn but also for the cycling of other trace elements. Many other trace elements have been found to be affected by the cycling of Mn. One way Mn oxide particles affect the cycles of other elements is through their strong oxidizing potentials. Mn(IV) oxides are strong oxidizers with reduction potentials exceeding 1 V versus the standard hydrogen electrode(17). Although potentials are lower at circumneutral pH, Mn is still one of the most significant oxidants present in many systems, especially in suboxic zones. MnO₂(s) has been found capable of oxidizing a number of organic compounds as well as trace metals such as Cr(III)(5-6,18-19).

In addition to acting as a strong oxidant Mn(IV) affects other elemental cycles by acting as a carrier. Many trace metals have been found to adsorb preferentially to Mn oxide particles. Thus when Mn oxide particles dissolve they also release many other trace metals as well. Plumes of metals such as Cd, Ni, Cu, and Cr have been found associated with the reduction of Mn oxide particles(20).

1.1.3 Mn(III)

Mn(III) has long been thought to be of little importance in natural systems because of its instability with respect to disproportionation, the reaction of 2 Mn(III) species to give one Mn(II) species and one Mn(IV) species:



Nevertheless, there has been interest in Mn(III) in the laboratory because of its strong oxidizing ability. The hexaquo Mn(III) ion has a standard reduction potential of 1.5 V versus the standard hydrogen electrode(17)



This high reduction potential has led to interest in the use of Mn(III) as an oxidant for many different compounds.

Most of the earliest work with Mn(III) was done in highly acidic media. This was necessary to shift the equilibrium of Reaction 1.4 sufficiently to the left so the Mn(III) was present long enough to react with the reductant. Often ligands such as pyrophosphate and oxalate were used with the acid to give additional stabilization to the Mn(III)(aq) species. Early studies showed Mn(III) could oxidize such compounds as chloride, bromide, α -hydroxybutyric acid, di-butylphenols, N-alkylphenothiazines, and NO₂(21-26). Eventually, studies began to find that in oxidation of some organic complexes little additional stabilization of the Mn(III) was needed, as the organic seemed to form a Mn(III) complex which was stable on the time scale of reaction. As it became evident that organic compounds could stabilize Mn(III) with respect to disproportionation, complexation became a more common form of stabilization, in some cases even allowing work at pHs above the commonly used acidic media of pH 0 - 2. Mn(III) complexes with compounds

such as urea and porphyrins were found able to oxidize species such as Ni(II) complexes, H₂O₂, Co(II) complexes, EDTA, NTA, IDA, NCS⁻, and organic dyes(27-32).

Mn(III) complexes first became of interest in the natural environment in the field of biology. The interest arose from work showing that certain plant enzymes involved in oxidation processes contained Mn(33-35). Further study found that these enzymes could be mimicked using Mn(II), a Mn(III) stabilizing ligand such as P₂O₇ and an oxidant such as H₂O₂. When the photosystem II enzyme was found to contain 4 Mn atoms which apparently react between the (II), (III), and (IV) oxidation states, interest in oxidized Mn complexes increased greatly. Many organic Mn(III) and Mn(IV) complexes have been synthesized in an effort to mimic the photosystem II enzyme(36-40). Another enzyme was also found in lactic acid bacteria and white rot fungi which catalyzed the oxidation of lignin. This too was found to work through the oxidation of Mn(II) to Mn(III) by H₂O₂ and the stabilization of the Mn(III) by organic ligands(41-43). An enzyme-like substance containing Mn and citrate has also been found in soil(44).

Mn(III) was also found to be an important intermediate in the reaction of Mn(II) and MnO₄⁻ in the presence of oxalate. Several investigators have examined this reaction and have found the mechanism to involve the oxidation of Mn(II) to Mn(III). The Mn(III) formed a complex with the oxalate which then degraded via internal electron transfer(45-46).

Another area where interest in Mn(III) arose was in atmospheric chemistry. Studies examining the catalytic effect of Mn on oxidation of S(IV) by oxygen found that Mn(III) was an intermediate. A mechanism was shown which involved oxidation of Mn(II) to Mn(III) by oxygen, followed by oxidation of S(IV) by Mn(III) complexes(47-50).

The finding that Mn(III) can be a long lived intermediate in natural systems has led to a greater interest in complexes of Mn(III) for their own sake with the possibility being raised of their existence and contribution to redox cycling in natural systems. Several Mn(III) complexes have been synthesized and characterized in the lab. Among these are

complexes with pyrophosphate, citrate, EDTA, CyDTA, biphenyl, salicylate, and porphyrin(51-60) . Most work to date on such compounds has been concerned with physical characterization. Molar absorptivities have been found for complexes with citrate, pyrophosphate, and EDTA(51,55,56). A wide variety of Mn(III) complexes with aliphatic alcohols, polyalcohols, and carboxylic acids have been studied electrochemically giving reduction potentials for each complex(61-62). Structural information has been reported for citrate, EDTA, P_3O_{10} , tris(acetylacetonate) and some porphyrin complexes (53,54,55,58,63-64). Equilibrium constants have been reported for EDTA and pyrophosphate although there is some disagreement about these constants(55-56).

Less work has been done to characterize the kinetic behavior of such complexes. One group has examined the reduction of the citrate complex both by citrate alone and in the presence of hydrogen peroxide(65-66). They have also examined the autoxidation of the Mn(II) complex to the Mn(III) complex in the presence of citrate at high pH(67). Although these studies report kinetic data, no effort was made to control pH and therefore the constants reported have an unknown pH dependence. Barek et al. have examined reactions of Mn(III) sulfate with citrate and oxalate. They however do not report any rate constants and give only qualitative and stoichiometric data(50). Recently Kostka et al. have examined the reduction of Mn(III) pyrophosphate complexes by Mn reducing bacteria, using lactate or formate as electron donors, as well as S(IV) and Fe(II)(68).

One study has tried to examine the existence of Mn(III) complexes in natural systems (69). The study measured samples in the Chesapeake Bay using formaldoxime, polarography, and o-tolidene. They claim that formaldoxime measures only the Mn(II) while polarography measures total dissolved Mn. o-Tolidene measures total oxidizing equivalents of the species in the water. They found that total dissolved Mn was greater than Mn(II) and that there was oxidizing capacity of the water despite the absence of Fe(III) and H_2O_2 . They attribute this oxidizing capability to dissolved Mn(III). There is some debate over this finding however. The same result could be explained by very small Mn oxide

particles. Also, not all oxidants were ruled out from being the source of the oxidizing capacity. Although the study certainly raises the possibility of existence of such compounds the question is far from answered.

1.1.4 Redox transitions

Although each redox state of Mn holds interest in its own right it is the transitions between redox states that hold the most interest. Such redox reactions are of great interest as they can often affect and even control cycling of Mn as well as the forms and transport of other elements. In some environments the redox reactions of Mn can control the redox state of the local environment. This is true in suboxic zones where oxygen is depleted and other contaminant oxidants such as hexachloroethane are absent. Here Mn(III/IV) now becomes the strongest oxidant, and the reduction and oxidation of Mn(III/IV) determines the redox conditions of the local environment. Also, in the case of some trace elements, Mn is the only oxidant powerful enough to oxidize certain compounds. For example, Mn(III/IV) is the only oxidant which can oxidize Cr(III) on a time scale relevant under natural conditions (70-73).

Redox transitions are also important in determining the form and transport of both Mn and other compounds. Because Mn(III) and Mn(IV) form solid oxides they are much less mobile than Mn(II). Mn(III) complexes, however, would be a much more mobile oxidant than a solid oxide of Mn(III) or Mn(IV). Reduction of oxidized Mn solids can also be important in determining the fate of adsorbing organics and trace metals(74). Therefore in natural systems it is important to know both the oxidation state and the physical state of Mn and the time scales for transition between the various states.

The time scales of such redox transitions are important in determining the fate of pollutants. For example a sluggish reaction could mean that certain organics are unaffected by Mn oxides even if the reaction is thermodynamically favorable. Even when the reduction reaction is rapid, if the oxidation of Mn(II) is slow then the ability of the Mn(III/IV) to oxidize is limited to the amount of oxidized Mn present, as each Mn oxide can take up at the

most two electrons per manganese. If on the other hand the oxidation of Mn(II) is rapid and the reduction of oxidized Mn is also rapid then there exists the possibility of a catalytic cycle. Here manganese acts as a shuttle for electrons, accepting them from various reductants and losing them again to oxygen. As long as oxygen is present in this case Mn will continue to oxidize the reductant catalytically provided other conditions of the reaction remain constant.

The oxidation of Mn(II) to Mn oxides by oxygen is one of the most studied of these reactions. Early work noted that the reaction was slow except at very high pH(75). Later studies found the reaction to be autocatalytic in nature and to have a 2nd order dependence on hydroxide ion(76,9). Once the autocatalytic nature was found, the focus shifted to the nature of the catalysis. It was found that oxide surfaces were the cause of the increased oxidation rate. Rate constants and rate laws were reported for these processes in the 1980's(9-13). Recent work has focused largely on the mechanistic details of oxidation at the surface. Spectroscopic studies have found different mechanisms depending on the surface involved. Reactions have been found to form either uniform precipitates over the entire surface or precipitates that propagated along step imperfections on mineral surfaces(76-77). A great deal of work has also been done to measure the oxidation rate of Mn(II) by microbes. Studies have found greatly accelerated rates of oxidation in natural systems on the time scales of hours to days(78-81). Some work was also done examining the products of the oxidation of Mn(II). It was found that oxidation proceeded through Mn₃O₄ to MnOOH and only very slowly to MnO₂(3,82-88). It has been found for these Mn(III) containing products that Mn(III) dominates the surface and any Mn(II) present is in the interior(81). Very little work has been done to examine the homogenous oxidation rate. A few studies have been done around pH 9 in NH₃ buffers(9-10). One study has examined air oxidation at pH 8 in the absence of solids and bacteria and found none on a time scale of 7 years(8).

1.2.0 Scope of this Study

This study has examined some of the unanswered questions concerning redox transitions of Mn(II) and Mn(III). The kinetics of reactions of Mn(II), Mn(III), and Mn(IV) have been studied to better determine which processes may be significant in various natural environments.

1.2.1 Homogenous Mn(II) autoxidation

The first of these questions is: what is the homogenous oxidation rate of Mn(II)? This is important for determining the relative importance of biological activity and solids for rapid cycling and will allow some prediction of required time of Mn oxidation in areas where neither biological activity nor solids catalysis is present. Studies have been done at elevated temperatures to allow the experiments to be completed in reasonable amounts of time with concentrations allowing reasonable degrees of accuracy. Using a number of higher temperatures allows calculation of the activation energy for the reaction. The activation energy is then used to extrapolate to lower temperatures.

1.2.2 Mn(III) complexes

The next question is the time scale for existence of the Mn(III) oxidation state as a solution species in the environment. To address this question the rates of disappearance of Mn(III) complexes have been studied. The effects of pH, oxygen, ligand, and metal concentration have been studied to determine what conditions might allow Mn(III) to exist as a meta-stable species. Such species, although as yet not directly detected in natural environments, would be extremely significant even if only stable for a time scale of minutes to hours because of their strong oxidizing ability and high mobility.

The last question concerning natural occurrence of Mn(III) complexes concerns possible sources for formation of Mn(III). Although biological processes are certainly one possible source, the possibility of leaching of Mn(III) from the solid phase has not been addressed. The existence of Mn(III) oxides as long lived intermediates and the dominance

of Mn(III) at surface sites suggest that Mn(III) may indeed be available for complexation and release into solution. This study examined the kinetics of such processes and the factors which affect those kinetics.

References

- (1) Faure, G. *Principles and Applications of Inorganic Geochemistry: a Comprehensive Textbook for Geology Students*; McMillan Publishing Company: New York, 1991, pp 862.
- (2) Brudwig, G. W.; Crabtree, R. H. *Progress in Inorganic Chemistry* **1989**, *37*, 99 - 142.
- (3) Hem, J. D. *Geochimica et Cosmochimica Acta* **1981**, *45*, 1369 - 1374.
- (4) Stone, A. T. PhD Thesis, California Institute of Technology, 1983.
- (5) Stone, A. T.; Morgan, J. J. *Environmental Science and Technology* **1984**, *18*, 617 - 624.
- (6) Stone, A. T.; Morgan, J. J. *Environmental Science and Technology* **1984**, *18*, 450 - 456.
- (7) Johnson, C. A.; Xyla, A. G. *Geochimica et Cosmochimica Acta* **1991**, *55*, 2861 - 2866.
- (8) Diem, D.; Stumm, W. *Geochimica et Cosmochimica Acta* **1984**, *48*, 1571 - 1573.
- (9) Davies, S. H. R. PhD Thesis, California Institute of Technology, 1985.
- (10) Morgan, J. J.; Stumm, W. *Abstracts of the American Chemical Society* **1963**, *145*, 13 - 16.
- (11) Davies, S. H. R.; Morgan, J. J. *Journal of Colloid and Interface Science* **1989**, *129*, 63 - 77.
- (12) Sung, W.; Morgan, J. J. *Geochimica et Cosmochimica Acta* **1981**, *45*, 2377 - 2383.
- (13) Wilson, D. E. *Geochimica et Cosmochimica Acta* **1980**, *44*, 1311 - 1317.

- (14) Lewis, B. L.; Landing, W. M. *Deep Sea Research* **1991**, *38 supplement 2*, S773 - S803.
- (15) Tebo, B. M. *Deep Sea Research* **1991**, *38 supplement 2*, S883 - S905.
- (16) Nealson, K. H.; Myers, C. R.; Wimpee, B. B. *Deep Sea Research* **1991**, *38 supplement 2*, S907 - S920.
- (17) *CRC Handbook of Chemistry and Physics*; 71 ed.; Lide, D. R., Ed.; CRC Press: Boca Raton, 1974.
- (18) Kieber, R. J.; Helz, G. R. *Environmental Science and Technology* **1992**, *26*, 307 - 312.
- (19) Johnson, C. A.; Xyla, A. G. *Geochimica et Cosmochimica Acta* **1991**, *55*, 2861 - 2866.
- (20) German, C. R.; Holliday, B. P.; Elderfield, H. *Geochimica et Cosmochimica Acta* **1991**, *55*, 3553- 3558.
- (21) Taube, H. *Journal of the American Chemical Society* **1948**, *70*, 1216 - 1220.
- (22) Wells, C. F.; Barnes, C. *Transactions of the Faraday Society* **1971**, *67*, 3297 - 3305.
- (23) Taube, H. *Journal of the American Chemical Society* **1948**, *70*, 3928 - 3935.
- (24) Pelizzetti, E. *Journal of the Chemical Society: Dalton Transactions* **1980**, 484 - 486.
- (25) Jones, T. E.; Hamm, R. E. *Inorganic Chemistry* **1975**, *14*, 1027 - 1030.
- (26) Poh, B. L.; Stewart, R. *Canadian Journal of Chemistry* **1972**, *50*, 3432 - 3442.
- (27) Hage, R. *Nature* **369**, 637 - 639.
- (28) Macartney, D. H. *Inorganica Chimica Acta* **1987**, *127*, 9 - 13.
- (29) Banfi, S.; Legramandi, F.; Montanari, F.; Pozzi, G.; Quici, S. *Journal of the Chemical Society: Chemical Communications* **1991**, 1285 - 1287.
- (30) Gangopadhyay, S.; Ali, M.; Scha, S. K.; Banerjee, P. *Journal of the Chemical Society : Dalton Transactions* **1991**, 2729 - 2734.

- (31) Gangopadhyay, S.; Saha, S. K.; Banerjee, P. *Transition Metal Chemistry* **1991**, *16*, 355 - 357.
- (32) Bhat, I. K.; Sherigara, B. S.; Pinto, I. *Transition Metal Chemistry* **1993**, *16*, 163 - 166.
- (33) Kenten, R. H.; Mann, P. J. G. *Biochemical Journal* **1952**, *52*, 125 - 130.
- (34) Kenten, R. H.; Mann, P. J. G. *Biochemical Journal* **1952**, *50*, 360 - 369.
- (35) Kenten, R. H.; Mann, P. J. G. *Biochemical Journal* **1955**, *61*, 279 - 286.
- (36) Gamelin, D. R.; Kirk, M. L.; Stemmer, T. L.; S.Pal; Armstrong, W. H.; Pennner-Hahn, J. E.; Solomon, E. I. *Journal of the American Chemical Society* **1994**, *116*, 2392 - 2399.
- (37) Vites, J. C.; Lynam, M. M. *Coordination Chemistry Reviews* **1994**, *131*, 95 -126.
- (38) Brudwig, G. W.; Crabtree, R. H. *Progress in Inorganic Chemistry* **1989**, *37*, 99 - 142.
- (39) Manchanda, R.; Thorpe, H. H.; Brudvig, G. W.; Crabtree, R. H. *Inorganic Chemistry* **1991**, *30*, 494 - 497.
- (40) Thorpe, H. H.; Sarneski, J. E.; Kulawiec, R. J.; Brudvig, G. W.; Crabtree, R. H.; Papaefthymiou, G. G. *Inorganic Chemistry* **1991**, *30*, 1153 - 1155.
- (41) Aitken, M. D.; Irvine, R. L. *Archives of Biochemistry and Biophysics* **1990**, *276*, 405 - 414.
- (42) Glenn, J. K.; Gold, M. H. *Archives of Biochemistry and Biophysics* **1985**, *242*, 329 - 341.
- (43) Archibald, F. S.; Fridovich, I. *Archives of Biochemistry and Biophysics* **1982**, *214*, 452 - 463.
- (44) Loll, M. J.; Bollag, J. M. *Soil Biology and Biochemistry* **1985**, *17*, 115 - 117.
- (45) Jones, T. J.; Noyes, R. M. *Journal of Physical Chemistry* **1983**, *87*, 4686 - 4689.

- (46) Barek, J.; Berka, A.; Civivosa, D. *Collection of Czechoslovakian Chemical Communications* **1984**, 49, 954 - 962.
- (47) Siskos, P. A.; Peterson, N. C.; Huie, R. E. *Inorganic Chemistry* **1984**, 23, 1134 - 1137.
- (48) Coichev, N.; Eldik, R. v. *Inorganica Chimica Acta* **1991**, 185, 69 - 73.
- (49) Berglund, J.; Fronaeus, S.; Elding, L. I. *Inorganic Chemistry* **1993**, 32, 4527 - 4538.
- (50) Powell, R. T.; Oskin, T.; Ganapathisubramanian, N. *Journal of Physical Chemistry* **1989**, 93, 2718 - 2721.
- (51) Duke, F. R. *Journal of the American Chemical Society* **1947**, 69, 2885 - 2888.
- (52) Ganapathisubramanian, N. *Journal of Physical Chemistry* **1988**, 92, 414 - 417.
- (53) Carrell, H. L.; Glusker, J. P. *Acta Crystallographica* **1973**, B29, 638 - 640.
- (54) Glusker, J. P.; Carrell, H. L. *Journal of Molecular Structure* **1973**, 15, 151 - 160.
- (55) Ciavatta, L.; Palombari, R. *Gazzeta Chimica Italiana* **1983**, 113, 557 - 562.
- (56) Yoshino, Y.; Ouchi, A.; Tsunada, Y.; Kujima, M. *Canadian Journal of Chemistry* **1962**, 40, 775 - 783.
- (57) Macartney, D. H.; Thompson, D. W. *Inorganic Chemistry* 28, 2195 - 2199.
- (58) Meunier, B.; Caralho, M. d.; Batolini, O.; Momenteau, M. *Inorganic Chemistry* **1988**, 27, 161 - 164.
- (59) Manchanda, R.; Thorpe, H. H.; Brudvig, G. W.; Crabtree, R. H. *Inorganic Chemistry* **1991**, 30, 494 - 497.
- (60) Perlepes, S. P.; Blackman, A. G.; Huffman, J. C.; Christou, G. *Inorganic Chemistry* **1991**, 30, 1665 - 1668.
- (61) Magers, K. D.; Smith, C. G.; Sawyer, D. T. *Inorganic Chemistry* **1978**, 17, 515 - 523.
- (62) Yamaguchi, K. S.; Sawyer, D. T. *Israeli Journal of Chemistry* **1985**, 25, 164 - 176.

- (63) Aranda, M. A. G.; Chaboy, J.; Bruque, S. *Inorganic Chemistry* **1991**, *30*, 2394 - 2397.
- (64) Stutts, B. R.; Marionelli, R. S.; Day, V. W. *Inorganic Chemistry* **1979**, *18*, 1853 - 1858.
- (65) Guindy, N. M.; Basily, E. K.; Milad, N. E. *Journal of Applied Chemistry and Biotechnology* **1974**, *24*, 407 - 413.
- (66) Guindy, N. M.; Daoud, J. A.; Milad, N. E. *Egyptian Journal of Chemistry* **1977**, *20*, 131 - 139.
- (67) Milad, N. E.; Guindy, N. M.; Helmy, F. M. *Egyptian Journal of Chemistry* **1971**, *14*, 571 - 580.
- (68) Kostka, J. E.; Luther, G. W.; Neelson, K. H. *Geochimica et Cosmochimica Acta* **1995**, *59*, 885 - 894.
- (69) Luther, G. W.; Bhattacharya, A.; Nuzzio, D. In *American Geophysical Union Ocean Sciences Meeting*; 1992; 012D-3
- (70) Kieber, R. J.; Helz, G. R. *Environmental Science and Technology* **1992**, *26*, 307 - 312.
- (71) Johnson, C. A.; Xyla, A. G. *Geochimica et Cosmochimica Acta* **1991**, *55*, 2861 - 2866.
- (72) Fendorf, S. E.; Zasoski, R. J. *Environmental Science and Technology* **1992**, *26*, 79 - 85.
- (73) Fendorf, S. E.; Zasoski, R. J.; Burau, R. G. *Journal of the Soil Science Society of America* **1993**, *57*, 1508 - 1515.
- (74) Stone, A. T.; Godfredsen, K. L.; Deng, B. In *Chemistry of Aquatic Systems: Local and Global Perspectives*; G. Bidoglio, Ed.; Kluwer Publishers: Dordrecht Netherlands, 1993.
- (75) Nichols, A. R.; Walton, J. H. *Journal of the American Chemical Society* **1942**, *64*, 1866 - 1870.

- (76) Junta, J. L.; Hochella, M. F. J.; Harris, D. W.; Edgell, M. In *Proceedings of the 7th international symposium on water rock interaction*; 1992; pp .
- (77) Junta, J. L.; Hochella, M. F. J. *Geochimica et Cosmochimica Acta* **1994**, *58*, 4985 - 4999.
- (78) Tebo, B. M.; Emerson, S. *Biogeochemistry* **1986**, *2*, 149 - 161.
- (79) Tebo, B. M.; Emerson, S. *Applied and Environmental Microbiology* **1985**, *50*, 1268 - 1273.
- (80) Tebo, B. M.; Nealson, K. H.; Emerson, S.; Jacobs, L. *Limnology and Oceanography* **1984**, *29*, 1247 - 1258.
- (81) Emerson, S.; Kalthorn, S.; Jacobs, L.; Tebo, B. M.; Nealson, K. H.; Rosson, R. A. *Geochimica et Cosmochimica Acta* **1982**, *46*, 1073 - .
- (82) Hem, J. D.; Roberson, C. E.; Fournier, R. B. *Water Resources Research* **1982**, *18*, 563 - 570.
- (83) Kessick, M. A.; Morgan, J. J. *Environmental Science and Technology* **1975**, *9*, 157 - 159.
- (84) Hem, J. D.; Lind, C. J. *Geochimica et Cosmochimica Acta* **1991**, *55*, 2435 - 2451.
- (85) Murray, J. W.; Dillard, J. G.; Giovanoli, R.; Moers, H.; Stumm, W. *Geochimica et Cosmochimica Acta* **1985**, *49*, 463 - 470.
- (86) Hem, J. D.; Lind, C. J. *Geochimica et Cosmochimica Acta* **1983**, *47*, 2037 - 2046.
- (87) Hem, J. D. *Chemical Geology* **1978**, *21*, 199 - 218.
- (88) Stumm, W.; Giovanoli, R. *Chimia* **1976**, *30*, 423 -426.

EXPERIMENTAL METHODS

2.1 Introduction

2.1.1 Total Mn

In order to examine the redox reactions of manganese in aqueous solution, methods are needed to detect all three oxidation states as well as total Mn. A number of reliable methods exist for detection of total manganese. For concentrations down to the micromolar level, several spectrophotometric methods are available. These were compared in a paper by Morgan in 1965 and include the formaldoxime method and the permanganate method as the most common (1). Concentrations at the micromolar level or lower require more sophisticated methods. Although some spectrophotometric techniques can be used by adding a preconcentration step, such as adsorption onto a cation exchange column or through the use of kinetic techniques, in general mass spectrometry is the most widely used technique for low concentrations of Mn (2). ICP-MS mass spectrometers can detect nanomolar levels with relative ease, and with proper cleanroom techniques and preconcentration steps, detection can go even lower.

2.1.2 Mn(II)

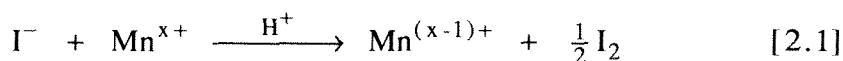
Unfortunately, fewer techniques exist for the detection of specific oxidation states of Mn. Mn(II) is probably the easiest oxidation state to detect. Several methods exist that can detect Mn(II) at micromolar or submicromolar levels. ESR is one method that is specific for Mn(II) (3,4). Several methods also exist which are based on the catalytic behavior of Mn in oxidation reactions. By measuring the extent of catalysis of a dye oxidation reaction the amount of Mn(II) can be calculated(5,6). Despite the existence of such methods, in the field a common way of determining Mn(II) is by difference. Since Mn(II) is usually the most abundant form of Mn it is often easier to determine oxidized Mn and total Mn and subtract to find Mn(II). This

can yield accurate measurements of Mn(II) providing the method for detecting oxidized Mn is accurate.

2.1.3 Oxidized Mn

Even fewer sensitive techniques exist for detection of oxidation states above Mn(II). The earliest studies used solubility differences between Mn(II) species and Mn(III) and Mn(IV) oxides. Often the samples were filtered and total Mn measurements were done for both the filtrate and the filtered solids. The filtrate was then considered to be Mn(II) and the filtered Mn was considered as Mn oxide solids of either the (III) or (IV) state. Most early studies used 0.2 μ m filters. Later it was realized that smaller pore sizes are needed to exclude colloidal Mn oxides. Although this method is effective if small enough pore size filters are used, it does not differentiate between III and IV solids, it does not include the possibility of soluble oxidized Mn and does not take into account the possibility of Mn(II) adsorption to oxide surfaces.

A more specific approach for detection of Mn(III) and Mn(IV) is offered by redox based techniques. These techniques are also unable to differentiate Mn(III) and Mn(IV). Instead they measure the equivalents of oxidizing capacity greater than Mn(II). Therefore the total concentration obtained from one of these techniques is equal to the concentration of Mn(III) plus twice the concentration of Mn(IV). The simplest of these techniques is the iodine titration method. This technique involves adding iodide and sulfuric acid to a solution of oxidized Mn. The Mn(III/IV) then oxidizes the iodide according to the reaction:



where $x = 3$ or 4 . If $x = 4$ then the reaction will proceed twice to give Mn^{2+} . The formed iodine is then titrated with standardized thiosulfate. The total equivalents of oxidized Mn are then obtained from:

$$[Mnox] = \frac{V_{S_2O_3} * N_{S_2O_3}}{V_s} \quad [2.2]$$

where $[Mnox]$ is equivalents of oxidized Mn per liter, $V_{S_2O_3}$ is the volume of thiosulfate added, $N_{S_2O_3}$ is the normality of thiosulfate added, and V_s is the volume of sample. This technique has been used mainly for measuring oxidation states of solids. It has not been used for soluble Mn(III) or Mn(IV) complexes. Attempts to do so in this study proved unreliable because of poor endpoint resolution.

There are also several dyes which work on a redox basis. These dyes consist of a colorless compound which, when it loses one electron, forms a colored compound which can then be measured using spectrophotometry. Such dyes include o-tolidene, leuco crystal violet, leuco malachite green, and leuco beurbelien blue(1,5,7). o-tolidene is the most popular of these dyes as it seems to be the most stable. Leuco crystal violet (LCV) has a higher molar absorbance than the o-tolidene and is able to reach a lower detection limit; it is generally less stable, however, and must be remade frequently to avoid blank problems. All of the redox based methods are subject to interferences from other strong oxidants such as Fe(III), Cr(VI), H_2O_2 , and O_3 . In general, however, these are only important if the concentration of oxidant is much greater than the concentration of Mn. Even in these cases the reaction with other oxidants is generally much slower than the reaction with Mn.

To date, there are no techniques that can distinguish the (III) or (IV) states of Mn. Detection of these oxidation states is limited to those compounds which have measurable absorbances. Most Mn(III) complexes do absorb in the UV-visible region;

however, they also have low molar absorptivities which do not allow for detection much below the hundred micromolar level.

2.2 Methods used

2.2.1 Total Mn

This study used the formaldoxime method for determining total Mn. The method was chosen for its simplicity of use and the ability to do measurements in real time as opposed to storing samples for later analysis. The method is also able to detect all 3 oxidation states of Mn, including solids if given adequate time for dissolution. For the concentrations used in this study the molar absorptivity of the formaldoxime was more than adequate to measure total Mn. The only case where formaldoxime was not used was with EDTA. This was because the formaldoxime could not compete with the EDTA to complex the Mn and no color was formed. Therefore in experiments where EDTA was used all total Mn measurements were done using the ICP-MS.

The formaldoxime method required sample volumes from 0.05ml to 2 ml, depending on the expected concentration of Mn. The sample was added to a 1 cm quartz spectrophotometric cell and the volume was then made up to 3 ml with pH 9.1 NH_3 buffer. The buffer consisted of 10.7 g of NH_4Cl and 2.9 g of NaOH in 100 ml of deionized distilled water. 0.05 ml of dye were then added to the solution and about 5 minutes was allowed for the color to form. The absorbance was measured at 450 nm. A calibration curve for formaldoxime is shown in Figure 2.1.

2.2.2 Oxidized Mn

In experiments examining the oxidation of Mn(II), the leuco crystal violet dye was chosen to measure oxidized Mn. It was chosen because the increased absorptivity was required for the low concentrations of Mn used. Concentrations of Mn were held low so as to avoid supersaturation with respect to rhodocrosite (MnCO_3) precipitation. The dye solution is made using 0.01 g. of the leuco crystal violet dye

with 9 ml of deionized distilled water and 1 ml of 1 M HCl. The dye solution was prepared in small volumes and made fresh every day because it oxidizes slowly in the presence of oxygen, leading to blank problems. This oxidation by oxygen is slow, however, and does not interfere with Mn measurements. The method consisted in adding 0.5 ml of the dye solution, to 1.25 ml of pH 4.0 acetate buffer and 25 ml of sample in a 10 cm. spectrophotometric cell. The absorbance was then measured at 591 nm. A sample calibration curve is shown in Figure 2.2. A calibration was done each time the method was used because of the instability of the dye and problems with blank reproducibility. Calibrations were done using a Mn oxide synthesized by adding MnO_4^- and Mn(II) in a 1:1.5 ratio. Interference studies were done with Cr(VI), Fe(III), H_2O_2 , and Cu(II). Only Cr(VI) and Fe(III) produced any significant interference, and this was only an increase of 0.05 absorption units for concentrations of interfering metal on the order of hundreds of micromolar. Even this increase was slow and could be distinguished from the much quicker formation of color due to Mn. For this reason all measurements were taken within 5 minutes of adding the dye.

In cases where the oxidized Mn concentration is expected to be below 100nM, such as in many natural environments, an extraction technique was used to concentrate the sample. The method is an adaptation of the one proposed by Kessick et. al.(7). 25 ml of sample are added to a 60 ml polyethylene bottle with 1.25 ml of buffer and 0.5 ml of dye. Then 5 ml each of isobutanol and toluene are added. The mixture is then shaken vigorously for about 30 seconds. The organic layer is allowed to separate and then is pipetted into a spectrophotometric cell and the absorbance at 591 nm is measured.

For experiments involving Mn oxide solids the iodine titration method was used in conjunction with the formaldoxime method to determine the average oxidation state of the solid. The method is an adaptation of the Winkler method for determining oxygen. It was adapted to the examination of Mn oxide particles by

Murray et. al.(8). The method involves adding a sample of filtered solids to 50 ml of deionized distilled water. To that was added 1 ml of NaI solution and 2 ml of 20% H₂SO₄. The solution was stirred until all the solids were dissolved. The yellow colored solution was titrated using 0.1N Na₂S₂O₃. When the solution became a very pale yellow a few drops of starch solution were added to give a sharper endpoint determination. Before use the thiosulfate was standardized every day using a 0.1N I₂ solution. After the titration the solution was measured for total Mn by the formaldoxime method. The method was found to work well with solids but presented difficulty with Mn(III) complexes because of poor end point resolution due to an apparent reformation of the complex during titration.

2.2.3 Mn(III)

All Mn(III) complex concentrations were measured spectrophotometrically. The ligands were chosen for the known absorptivities of their Mn(III) complexes in the UV-visible range. Samples were taken directly from the vessel, filtered if necessary, and then absorbance was measured at the appropriate wavelength. Several different spectrophotometers were used for this study. A Shimadzu double beam spectrophotometer with a 10 cm quartz cell was used for the oxidation experiments. A Shimadzu portable spectrophotometer was used for the solution phase Mn(III) work using either a 5 or 10 cm quartz cell. A Hewlett Packard diode array spectrophotometer was used for the solid dissolution experiments.

2.2.4 pH of zero point of charge

pH_{ZPC} (isoelectric pH) of the MnOOH particles was determined using an electrophoretic mobility cell to measure particle velocities at different pHs. The velocity measurements were done using a Rank Brothers Mark II electrophoretic mobility cell. A diagram of the cell appears in Figure 3. It consists of a thin rectangular glass cell across which an electric potential can be applied. Particles were viewed through an eyepiece which could be focused to within 0.001 cm. and had a

grid superimposed. Particles could then be timed for the length of time it took to cross one grid space. Care had to be taken because particle movement sets up currents in the cell. The fluid moves in the direction of the particles in the center of the cell and then returns along the walls. In order to obtain the true particle velocity it is necessary to find the stationary surface where the drag and velocity cancel each other and the fluid is motionless. According to theory the stationary surfaces are given by the equation:

$$\frac{s}{d} = 0.5 - \left[0.0833 + \frac{32d}{\pi^5 l} \right]^{\frac{1}{2}} \quad [2.3]$$

where s is the position of the stationary surface, d is the thickness of the cell, and l is the length of the cell. According to the formula these surfaces should be 0.2mm from the cell walls in the instrument used. The stationary surface was hard to find, however, because it was not always easy to determine the exact location of the cell wall. The only way to determine the cell wall location was to try to focus on imperfections in the glass, as it is clear and otherwise undistinguishable from the water in the cell and the bath. It was not always easy to distinguish glass imperfections from out-of-focus particles. Therefore the location of the surface was checked. One way of checking the surface location was by measuring the mobility with the cell polarity in alternating directions. Because the stationary points should be unaffected by direction of flow they should be the least affected by changing polarity. Points away from the stationary point may be affected especially because the electrical current changes much faster than the water currents. Also, by knowing the cell walls are 1mm apart then it can be calculated that the stationary surfaces should be 0.6mm apart, which is another check. Therefore measurements were made all the way across the cell and the points where the mobilities were nearly equal in both

polarity directions and were about 0.6mm apart were used to obtain the mobility. A sample plot of mobility versus position in the cell is shown in Figure 2.4. It can be noted that although particles were not visible across the entire 1mm thickness of the cell and thus could lead to an erroneous identification of the stationary surface, using this method does indeed locate stationary planes that are 0.6mm apart as predicted by theory.

References

- (1) Morgan, J. J.; Stumm, W. *Journal of the American Water Works Association* **1965**, *57*, 107 - 119.
- (2) Nakayama, E.; Suzuki, Y.; Fujiwara, K.; Kitano, Y. *Analytical Sciences* **1989**, *5*, 129 - 139.
- (3) Carpenter, R. *Geochimica et Cosmochimica Acta* **1983**, *47*, 875 - 885.
- (4) Boughriet, A.; Oudanne, B.; Wartel, M. *Marine Chemistry* **1992**, *37*, 146 - 169.
- (5) Resing, J. A.; Mottl, M. J. *Analytical Chemistry* **1992**, *64*, 2682 - 2687.
- (6) Janjic, T. J.; Milanovic, G. A.; Celap, M. B. *Analytical Chemistry* **1970**, *42*, 27 - 29.
- (7) Kessick, M. A.; Vuceta, J.; Morgan, J. J. *Environmental Science and Technology* **1972**, *6*, 642 - 644.
- (8) Murray, J. W.; Balistrieri, L. S.; Paul, B. *Geochimica et Cosmochimica Acta* **1984**, *48*, 1237 - 1247.

Figure 2.1

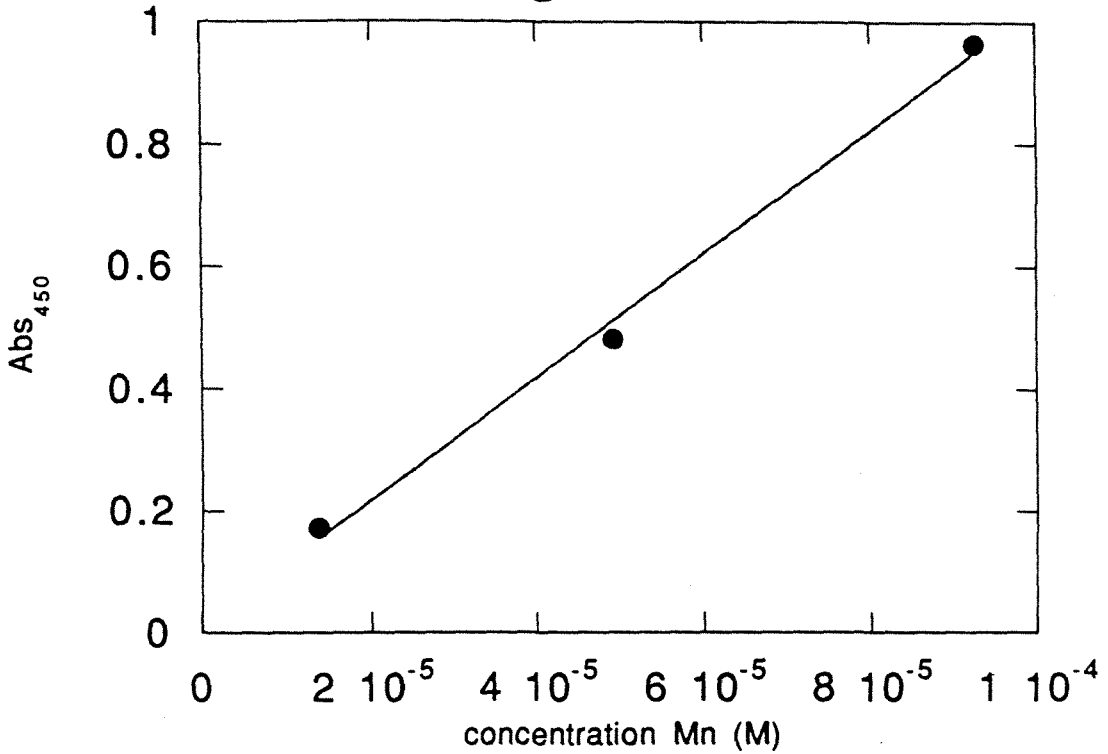


Figure 2.1. Formaldoxime Calibration Curve. The absorbance of formaldoxime dye at 450 nm versus the concentration of total Mn present. Regression line used for calculating concentrations is shown. Measurements were done using a 1 cm quartz cell on a Hewlett Packard diode array spectrophotometer. Mn was added as the Mn(NO₃)₂ salt.

Figure 2.2

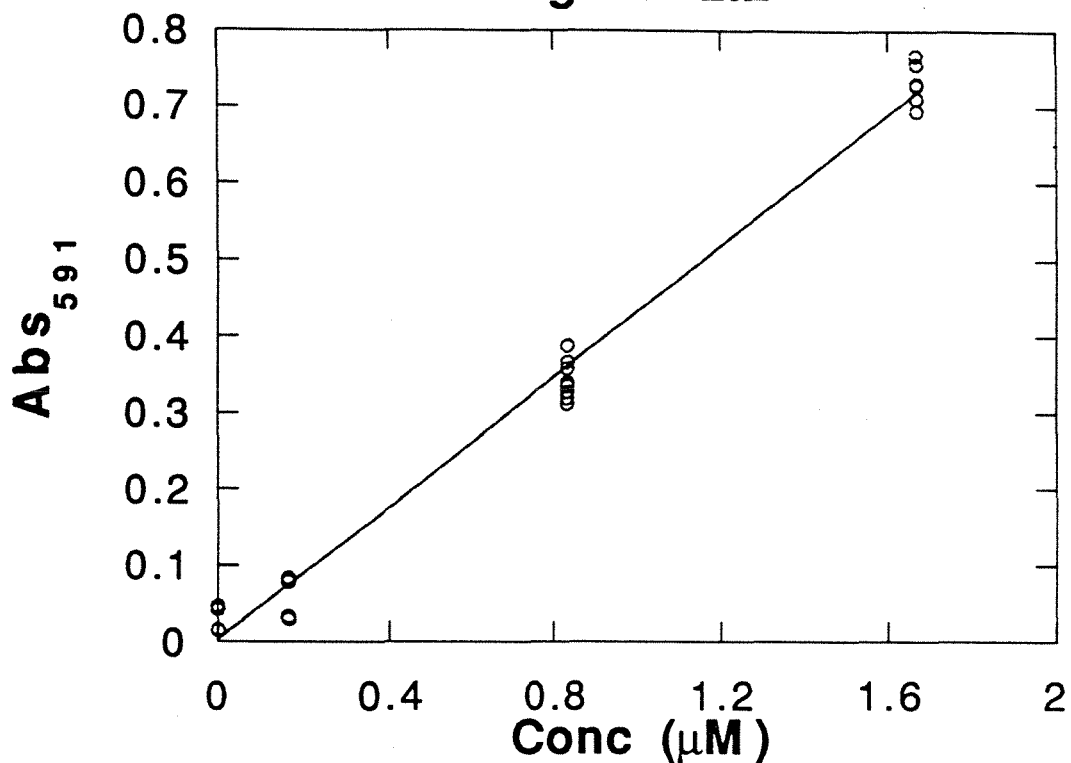


Figure 2.2 Leuco Crystal Violet Calibration Curve. The absorbance at 591 nm of the leuco crystal violet dye versus the total equivalents of oxidized Mn. A regression line is shown for the data. Differences in points at the same concentration show the scatter in blank values. Oxidized Mn was added as a Mn oxide produced by reacting Mn(II) with MnO_4^- in a 1:1.5 ratio.

Figure 2.3
Top View of electrophoretic mobility device

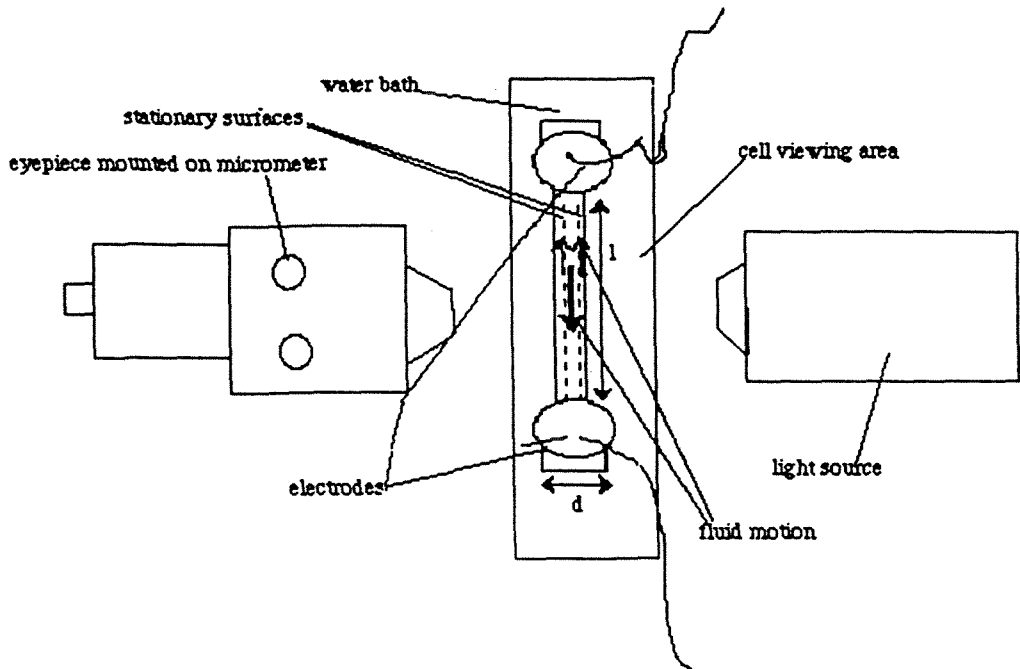


Figure 2.3. Top view of electrophoretic mobility device. Current is passed through the electrodes in either end of the rectangular cell. The entire cell is immersed in a cooling bath. The position of the eyepiece can be positioned with the use of a micrometer.

Figure 2.4

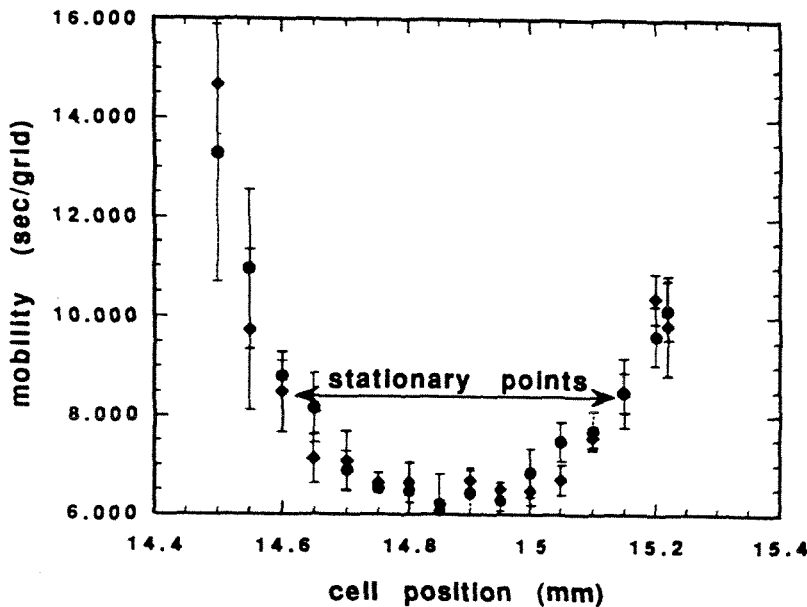


Figure 2.4. Sample data for electrophoretic mobility measurements. The time it took Mn oxide particles to cross one grid space versus the lateral position in the cell. Cell position is in mm and is on an arbitrary scale. The ●s represent mobilities measured with the positive charge on the right electrode. The ◆s represent mobilities measured with the positive charge on the left electrode. The exact positions of the cell walls on this scale are unknown, but are probably around 14.4 and 15.4 mm. The cell thickness is 1mm. The actual particle mobility is the mobility at the stationary planes. These planes were chosen according to the criteria discussed in section 2.2.4 to be at 15.15mm and 14.6mm. The inverse velocity is 8.5 sec/grid which gives a mobility of 0.117 grid/sec. The planes are close to being 0.6mm apart as predicted by theory

HIGH TEMPERATURE Mn(II) AUTOXIDATION

3.1 Previous Studies

Oxidation of Mn has been of much interest in the study of the geochemical cycling of Mn, as it is one of the determining factors in Mn removal from the water column. Most early studies were laboratory based. Nichols and Walton studied the reaction at pH 8.4 - 9.6 and found the reaction faster at higher pH and dependent on oxygen concentration(1). Later Morgan found the reaction to be autocatalytic and also found the rate to be second order with respect to hydroxide ion. Morgan proposed the rate law (2):

$$\frac{d[\text{Mn(II)}]}{dt} = -k_1[\text{OH}^-]^2[\text{O}_2][\text{Mn(II)}] - k_2[\text{Mnox}][\text{OH}^-]^2[\text{O}_2][\text{Mn(II)}] \quad [3.1]$$

where [Mnox] is the concentration of oxidized Mn and k_2 is much larger than k_1 . Studies by Hem (3) and Sung and Morgan (4) identified the source of the autocatalysis as the surface of the formed Mn oxide. It was found that the reaction was catalyzed by both the surface of formed Mn oxides and the surface of Fe oxides. The rate equation was found to depend on the available oxide surface area and could be made pseudo first order with respect to Mn(II) if the solid surface area was high enough. Later Davies and Morgan (5) showed that other oxide surfaces, such as Al_2O_3 , could catalyze the reaction and that competing cations could slow the reaction rate. They proposed a rate equation for the heterogenous oxidation of the form:

$$\frac{d[\text{Mn(II)}]}{dt} = \frac{k \cdot a \cdot p\text{O}_2 \cdot \langle =\text{SOH} \rangle \cdot [\text{Mn}^{2+}]}{[\text{H}^+]^2} \quad [3.2]$$

where a is the concentration of solids in g/l, and $\langle =\text{SOH} \rangle$ is the concentration of surface hydroxyl sites in moles/g solids. Wilson (6) also showed the existence of

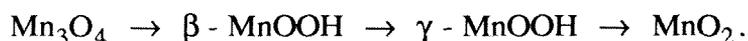
surface catalysis by MnO_2 as well as the ability of organics to inhibit the reaction. These studies made it evident that the amount of surface sites available for binding Mn(II) is an important factor in determining the rate of reaction. It also became apparent that in the absence of mineral surfaces the homogenous reaction of Mn(II) with dissolved oxygen was extremely slow.

The Hochella group (7,8) and others recently began to explore the nature of the autocatalysis by surfaces. Using spectroscopic and microscopic techniques they examined mineral surfaces and studied the oxidation by oxygen on them. They found two major types of oxidative growth of Mn oxides on the surface. One consisted of a uniform layer of precipitate and the other of precipitation and growth along steps and ridges. The type of precipitation and growth observed depended on the mineral surface. Fe surfaces tended to produce layers while silicate surfaces gave ridges of Mn(III) oxides.

Studies examining the oxidation of Mn in the field found that many oxidation rates in natural environments were much faster than could be explained by invoking surface catalysis (9-13). It was soon found that several microorganisms catalyze the oxidation of Mn(II) . Tebo and Emerson (11) found that binding sites were an important component of the rate equation. Half lives for oxidation by microorganisms were found to be from 12 hours to a few days, much faster than the time scale of weeks for surface catalysis. Thus in many natural systems Mn cycling can be controlled by microorganisms.

The products of abiotic Mn(II) oxidation were found to be mostly Mn(III) containing oxides. Stumm and Giovanoli (14) found the product of oxidation at pH 9 to be $\gamma\text{-MnOOH}$ and postulated a Mn_3O_4 intermediate. They also noted the product was colloidal and would be difficult to detect in natural environments. Hem examined the nature of the products of Mn(II) oxidation(15-17). He found a sequence which went from Mn(II) to Mn_3O_4 to $\beta\text{-MnOOH}$ and then very slowly to MnO_2 . At low

temperatures the Mn_3O_4 phase was not formed and $MnOOH$ was found to form directly from $Mn(II)$. A spectroscopic study by Murray et. al. (18) confirmed the sequence:



They also found that $Mn(III)$ dominated the surface of the hausmanite intermediate, showing that the oxidation is a surface process.

The reaction of $Mn(II)$ with oxygen in a homogenous system is so slow that it has not been well studied. Some of the earlier experiments using ammonia buffers were undersaturated with respect to solid phases (2,5) and homogenous oxidation constants were estimated. Some question has been raised, however, whether in the adding of the ammonia, the pH rose above 9 and caused a temporary supersaturation with respect to $Mn(OH)_2$. Diem and Stumm (19) did a study where a homogenous solution at pH 8.4 was monitored for 7 years and found no measurable quantity of oxidized Mn in the absence of surfaces or bacteria.

3.2.0 Current Study

This study has examined the homogenous autoxidation of $Mn(II)$ at high temperatures in order to determine more accurately the homogenous oxidation rate of $Mn(II)$. This allows better quantification of the effects of catalysis and enables better calculations of required times in oxidation reactions.

3.2.1 Solubility Considerations

Great care had to be taken to insure that the system remained undersaturated with respect to all solid phases. At a pH of 8 this is not too much of a problem for $Mn(OH)_2$. This study; however, used a CO_2 buffer. Therefore steps had to be taken to avoid supersaturation with respect to $MnCO_3$. Carbon dioxide - bicarbonate buffers were used because they buffer well in the region of interest, do not bind either Mn^{2+} or the products appreciably in aqueous solution, and are representative of the chemical environment of most natural waters. A solubility diagram for the carbonate

system is shown in Figure 3.1. The main phase near pH 8 is MnCO_3 . The $^cK_{SO}$ of MnCO_3 at 25°C and $I = 0.5\text{mM}$ is $10^{-10.3}$. The ionic strength comes largely from the NaHCO_3 added as buffer which is present at a concentration of 0.48mM . Therefore for an open system:

$$\log(^cK_{SO}) = \log\left([\text{Mn}^{2+}] \cdot [\text{CO}_3^{2-}]\right) = \frac{\log\left([\text{Mn}^{2+}] \cdot P_{\text{CO}_2} \cdot K_H \cdot K_1 \cdot K_2\right)}{[\text{H}^+]^2} \quad [3.3]$$

Where K_H is the Henry's Law constant of CO_2 and K_1 and K_2 are the first and second proton dissociation constants of H_2CO_3^* . So for exposure to the atmosphere and a pH of 8.0 the saturation concentration for Mn is:

$$\log[\text{Mn}^{2+}] = -10.3 - 2 \cdot 8 + 3.5 + 1.5 + 6.3 + 10.3 = -4.7 \quad [3.4]$$

Therefore the maximum allowed concentration of Mn is $10^{-4.7}$ or 2×10^{-5} M. Concentrations were kept at 10^{-5} M for all experiments. Care also had to be taken in order to prevent a temporary supersaturation during mixing. To avoid this the reaction was started by adding a slightly acidic concentrated Mn(II) solution to a larger volume of buffered water at a pH just above 8. The acidified solution was made by adding to one liter of water 0.037 g NaHCO_3 along with 2.7 ml of 0.0186 M $\text{Mn}(\text{NO}_3)_2$ in 10% HNO_3 . The reactor was equilibrated with 1250 ml of $\text{CO}_2/\text{HCO}_3^-$ buffer, made by adding 0.046 g NaHCO_3 to 1.25 l of water, giving a solution of pH 8.1. Once the buffer in the reactor reached equilibrium, 250 ml of the acidified Mn solution was added to the reactor. Generally there was an acid spike as the Mn was added to begin the reaction. The spike normally took a few hours to rebound to the desired pH of 8.0. There was some drift in the pH after the pH of 8.0 was attained, but the pH was within ± 0.1 pH units of 8.0 for most of the experiment. One exception

was the 60°C run. Here there was a significant rise in pH, of about a half a pH unit, over the experiment. This may have been caused by concentration of alkalinity due to evaporation.

The reactor pH for the 50°C experiment is shown in Figure 3.2 and is typical of the pH behavior of solution during the oxidation experiments. It shows an acid spike to pH 7.44 at time zero followed by a rebound to pH 8.1. That spike and rebound is followed by another depression to pH 7.85 and a slow rise to pH 8.1. The second drop after the initial spike and recovery could be caused by protons produced by oxidation of Mn, by an increase in CO₂ taken into the solution, or by error in the pH meter. The increase in CO₂ is unlikely as it would require a 50% increase in P_{CO₂} to achieve that significant a pH drop. The acidity from oxidation is also an insufficient explanation. Even if all the Mn were oxidized it could not account for that large a pH change. Therefore it would seem this downward drift is error in the pH meter itself. The later upward drift is most likely a concentration of the alkalinity by evaporation. It would take approximately a 40% concentration of alkalinity to account for the observed rise. The concentration factors observed ranged from 33 to 47% in the experiments. Therefore the upward drift can be accounted for by evaporation, although the pH meter instability must also be considered.

3.2.2 Experimental Method

All reactions were run in a jacketed glass reaction vessel. Temperature was controlled to within 0.2 °C by a circulating water bath. The reactor had a lid to keep out atmospheric fallout of dust and other particle sources and also to limit evaporation. Evaporation was found to be significant in the 45°C run. Therefore for all subsequent runs a condenser was attached to the top of the reactor. Even with the condenser in place there was significant evaporative loss. The water was weighed before and after the experiment and the evaporative loss determined. Concentrations were corrected assuming a constant loss rate. The loss rate of water ranged from 7 to

13 g of water per day. The loss corrections were made by multiplying the measured concentration by the ratio of volume of water in the reactor at the time of the measurement to the total initial volume of the reactor. Reactions were started by first bringing 1250 ml of the buffer solution to the desired temperature. The reactor was stirred, with a magnetic stir bar, strongly enough so there was a slight vortex at the surface of the solution. Once pH reached equilibrium, which typically took about a day, the Mn was added and the experiment begun.

Samples were withdrawn daily to monitor the extent of oxidation. Each sample was 25 ml and withdrawn using an acid cleaned glass pipette. Samples were then acidified using 90 μ l of 0.1 M HNO₃ and stored at room temperature. The acidification and lower temperature preserved the samples from further oxidation until they could be analyzed for oxidized Mn. The final pH of the preserved samples was about 5 which is sufficient to stop oxidation but not so low as to cause reduction of oxidized Mn.

The pH was monitored using a radiometer glass electrode. The instrument has a temperature knob which was used to calibrate the electrode for higher temperatures. The electrode was calibrated in pH 7 and pH 10 buffers at room temperature with the temperature knob set at 25°C. The knob was then turned to the appropriate temperature for the experiment being conducted. The corrections for the temperature dependence on the slope of pH versus voltage was then automatically accounted for by the instrument.

Oxidized Mn was detected by the LCV method described previously. Standards were run with each analysis, including blanks at the beginning and the end of an analysis run. Experiments were typically conducted for a period of 2 to 3 months.

3.3.0 Results

3.3.1 45°C

Runs were conducted at 35, 45, 50, and 60 °C. No appreciable oxidation was found at the 35°C run over 3 months. All other runs showed some oxidation over the duration of the experiment. Figure 3.3 shows the concentration of Mn(II) versus time for the 45°C experiment. There is some scatter in the data, probably due to scatter in blank values and instrumental noise. Yet there is a definite trend above the noise that indicates that oxidation did indeed occur. An exponential fit was done to the data in order to determine the initial pseudo first order rate. Several outlying points were discarded from the curve fit to determine the rate constant. These were all points that were much higher in absorbance than the rest of the points. This is most likely due to either blank problems with the LCV or contamination with oxidized Mn. With those points omitted the first order rate constant is $1.7 \pm 0.3 \times 10^{-9} \text{ s}^{-1}$. The correlation coefficient r^2 was 0.67.

3.3.2 50°C

Figure 3.4 shows the data for the 50°C run. This run had much less scatter in the data; two points were still omitted from the curve fit, however. The pseudo first order rate constant for this run was $2.9 \pm 0.6 \times 10^{-9} \text{ s}^{-1}$. The correlation coefficient r^2 was 0.75.

3.3.3 60°C

Figure 3.5 shows the data for the 60°C run. Unfortunately, this run had considerable scatter and shows much less of a trend than the previous data set. Several factors contribute to the scatter. One is the drift in pH which could cause significant changes in the oxidation rate itself. The second is the volume change caused by evaporation. This effect contributes to the flattening of the data. Before the volume corrections were made the data did show a marked increase in oxidized Mn over the course of the experiment. However; when the volume corrections were

applied, it turned out that the increase was largely a concentration effect due to evaporation. For example at 25 days there were 0.41 μM of oxidized Mn measured in the sample, but at this point 375 g of water had already been lost due to evaporation. Therefore, correcting for volume, the actual concentration of oxidized Mn would have been 0.32 μM if no evaporation had occurred. Still, some oxidation should have still been noticeable even with the volume corrections. However; that oxidation was obscured by the last problem which was high blanks. Observing the first point which should be close to ten micromolar shows that the blank is greater than the total amount of oxidation observed in the 50°C run. The blank problem could be caused by several different factors. There may actually be some contamination of the reactor or the reagents used with oxidized Mn or the LCV reagent may have been oxidized by some oxidant other than Mn, such as oxygen. These problems make it very difficult to determine a rate constant. If a statistical fit is done through the data the least squared error turns out to be larger than the rate constant. Therefore no rate constant was determined for this data.

3.3.4 Extrapolation to room temperature

All the rate constants calculated are pseudo first order rate constants. As shown in equation 1 the homogenous rate law is also dependent on the oxygen and hydroxide concentration. The pseudo first order fit is valid at a particular temperature because pH, and therefore hydroxide concentration, is held constant through use of the buffer. Dissolved oxygen concentration is also in large excess of the concentration of Mn(II). If the reactor is in equilibrium with the atmosphere, then oxygen concentrations are on the order of 10^{-4}M , an order of magnitude greater than the Mn concentration. Therefore the pseudo first order rate equation holds.

To properly determine the rate constants the observed pseudo first-order rate constants must be interpreted in terms of reduced metal ion speciation, e.g. MnOH^+ and $\text{Mn}(\text{OH})_2^0$, and the oxygen concentration as suggested by the work of

Millero(20), Davies(21), and Wehrli(22). For example the equilibrium concentration of $\text{Mn}(\text{OH})_2^0$ is

$$[\text{Mn}(\text{OH})_2^0] = \alpha_2 \cdot [\text{Mn}]_T \quad [3.5]$$

where α_2 is approximately

$$\alpha_2 = \frac{{}^*\beta_2}{[\text{H}^+]^2} \quad [3.6]$$

If it is assumed that $\text{Mn}(\text{OH})_2^0$ reacts the quickest with oxygen then the rate expression can be written

$$\frac{d[\text{Mn}(\text{II})]_T}{dt} = -k_2' \cdot K_{\text{HO}_2} \cdot P_{\text{O}_2} \cdot \frac{{}^*\beta_2}{[\text{H}^+]^2} [\text{Mn}(\text{II})]_T \quad [3.7]$$

where K_{HO_2} is the Henry's Law constant for oxygen in Matm^{-1} and P_{O_2} is the partial pressure of oxygen in atm. Therefore the first-order rate constant is

$$k^* = k_2' \cdot K_{\text{HO}_2} \cdot P_{\text{O}_2} \cdot \frac{{}^*\beta_2}{[\text{H}^+]^2} \quad [3.8]$$

at fixed pH, temperature, and P_{O_2} , the rate is

$$\frac{d[\text{Mn}(\text{II})]_T}{dt} = -k \cdot [\text{O}_2] \cdot [\text{Mn}(\text{II})]_T \quad [3.9]$$

with

$$k = \frac{k^*}{K_{\text{H}_2\text{O}_2} \cdot P_{\text{O}_2}} \quad [3.10]$$

and k has units of $\text{M}^{-1}\text{s}^{-1}$. This assumes the fastest reacting species is $\text{Mn}(\text{OH})_2^0$. To be precise rate constants of the same form as equation 4.8 would have to be included for each possible $\text{Mn}(\text{II})$ species. The different species rate constants would then need to be resolved by a series of experiments over a wide pH range. Since this study was conducted at a single pH it will be assumed that equation 3.7 is adequate to describe the reaction.

Unfortunately, reliable data on $^*\beta_2$ for Mn^{2+} are not available, nor is a ΔH° value to permit evaluating the temperature dependence. At this point it is only possible to evaluate the influence of temperature to a limited degree. Applying equations 3.8 and 3.9 the following second order rate constants were calculated for 45 and 50°C respectively.

$$(8.3 \pm 1) \times 10^{-6} \text{ M}^{-1}\text{s}^{-1}$$

$$(1.5 \pm 0.3) \times 10^{-5} \text{ M}^{-1}\text{s}^{-1}$$

These constants incorporate the influence of temperature on O_2 solubility. They depend on temperature in two ways: the influence of temperature on $^*\beta_2$ and the influence of temperature on the oxidation process itself.

Because there are only two reliable rate constants a statistical fit to an Arrhenius expression would be statistically meaningless. Therefore the 25°C rate constant was estimated by plugging the high and low values of the two rate constants into an Arrhenius expression. This will give the range of possible activation energies and rate constants possible in light of this data. It was found that the activation energy for the process ranged between $85 \text{ kJ}\cdot\text{mol}^{-1}$ and $113\text{kJ}\cdot\text{mol}^{-1}$. The second order rate constant at 25°C ranged between $8.5 \times 10^{-7} \text{ M}^{-1}\text{s}^{-1}$ and $5.3 \times 10^{-7} \text{ M}^{-1}\text{s}^{-1}$. Assuming

equilibrium with the atmosphere and pH of 8.0, equation 3.10 gives a pseudo first-order rate constant between $1.3 \times 10^{-10} \text{ s}^{-1}$ and $2.0 \times 10^{-10} \text{ s}^{-1}$. This gives a half life for oxidation between 110 and 170 years. Such a long half life would certainly explain why Diem and Stumm (19) did not see any appreciable oxidation in their experiments which only ran about 7 years.

3.3.5 Comparison and discussion of results

This rate constant is about two orders of magnitude greater than any previously reported homogenous rate constants determined in other studies. Table 1 lists rate constants from studies by Davies (20) and Morgan (21). These rate constants are pseudo first order constants. The range of constants is from 10^{-5} s^{-1} to 10^{-8} s^{-1} . The lowest value is the $<3 \times 10^{-8} \text{ s}^{-1}$ reported by Davies (20) at pH 8.35. If a second order dependence on pH is assumed then the rate reported by Davies would be on the order of 10^{-9} s^{-1} at a pH of 7.9 to 8.0. If on the other hand a dependence on the 2.6 order is assumed as suggested by Davies (20) then the rate obtained by extrapolating Davies rates to pH 8.0 would be even closer. Given the relatively large uncertainty in this study as well as Davies, the two results would seem to agree. This would suggest that the pH dependence of the reaction may be greater than second order and is still unknown. It also shows that previous homogenous experiments done in ammonia buffers were not affected by supersaturation with respect to solids phases. The results of Diem and Stumm (19) may just be a result of such small oxidation that it was undetectable by the method used.

One area where error could have skewed the results is in gas transfer from the atmosphere into the reactor. This could have an effect either way. If other atmospheric oxidants are transferred into the reactor in appreciable amounts then this could artificially raise the measured rate. If on the other hand the rate of oxygen transfer were slow enough this could lower the rate. The main oxidants of concern are hydrogen peroxide and ozone. Hydrogen peroxide can typically reach levels on the

order of 1 ppb in urban atmospheres(23). Ozone can reach levels on the order of 100 ppb(23). The simplest approach to determine the potential effect of these gases on the oxidation of Mn is to assume equilibrium with the atmosphere is maintained throughout the experiment. The Henry's Law constants for H₂O₂ and O₃ are 10⁵ and 10⁻² respectively(23). If the solution is in equilibrium with the atmosphere these constants would yield solution concentrations of 0.1mM for H₂O₂ and 1nM for O₃. The concentration of ozone in solution would be far below the amount of oxidation of Mn observed and therefore even at equilibrium ozone would not be a problem. Hydrogen peroxide on the other hand could be present on concentration levels near that of oxygen and could interfere with the results. Therefore it is important to estimate how long it will take to attain equilibrium for hydrogen peroxide as well as oxygen.

Using the two film model the overall resistance to transfer is equal the resistance of the transfer across the gas film in series with the resistance across the liquid film. This is given by the relation:

$$\frac{1}{K_L} = \frac{1}{k_l} + \frac{1}{k_g \cdot H} \quad [3.11]$$

where K_L is the overall resistance to transfer, k_l is the liquid film resistance, k_g is the gas phase resistance, and H is a unitless Henry's law constant. According to Roberts and Dandliker a typical k_l for a moderately stirred vessel is on the order of 10⁻³ cm/s (24). k_g values are typically about 2 to 3 orders of magnitude higher than k_l values (25). Therefore for this estimate values of 10⁻³ and 10⁻¹ cm/s will be used for k_l and k_g respectively. These values would give overall resistances of 4 x 10⁻⁸ cm·s⁻¹ for hydrogen peroxide and 10⁻³ cm·s⁻¹ for oxygen. The overall flux rate is given by:

$$\text{flux} = K_L \cdot \frac{A}{V} \cdot (C_g - C_l) \quad [3.12]$$

where A is the surface area of transfer and V is the volume of the vessel, and C_g and C_l are the gas and liquid phase concentrations respectively. A/V is simply equal to the depth of the liquid in the reactor. The time scale for transfer of gaseous reactants into the reactor then is given by:

$$\tau = \frac{h}{K_L} \quad [3.13]$$

where h is the height of liquid in the reactor in centimeters. Assuming an average depth of 10 cm depth throughout the course of the experiment gives time scales of 2.8 hours for oxygen and 2900 days for hydrogen peroxide. This is a result of the oxygen being liquid phase controlled and the hydrogen peroxide being gas phase controlled. Therefore there should be sufficiently fast transfer of oxygen into the reactor that it would be at equilibrium concentrations of 2×10^{-4} M at the beginning of the experiment. Once this concentration is reached the oxidation does not proceed enough to significantly deplete this concentration. Hydrogen peroxide on the other hand should transfer into the reactor only very slowly and therefore should not have a significant effect on the oxidation of Mn(II). It should also be noted that even if this calculation seriously underestimated the transfer of hydrogen peroxide to the reactor the error caused by contamination by hydrogen peroxide would be positive causing faster oxidation than by oxygen alone. Therefore even if peroxide is a significant oxidant then the homogenous oxidation rate is even slower than reported here.

One other possible source of error is the tendency of Mn oxide particles to stick to surfaces. If this occurred it would give low oxidized Mn values and an artificially low rate constant. Although there was no evidence of this, it would be

difficult to detect such adherence with such low concentrations of oxidized Mn. Although this could lower the rate constant, it would most likely only be a 10 or 20% correction.

Therefore although there is still some uncertainty in the exact rate constant, it is evident that past studies in ammonia buffers have yielded accurate rate constants. It would also appear that the pH dependence of the oxidation reaction may be greater than second order as previously thought. The process is indeed very slow and is negligible in most natural systems in the absence of biological or surface catalysis.

References

- (1) Nichols, A. R.; Walton, J. H. *Journal of the American Chemical Society* **1942**, 64, 1866 - 1870.
- (2) Morgan, J. J.; Stumm, W. *Abstracts of the American Chemical Society* **1963**, 145, 13 - 16.
- (3) Hem, J. D. *Geochimica et Cosmochimica Acta* **1981**, 47, 1369 - 1374.
- (4) Sung, W.; Morgan, J. J. *Geochimica et Cosmochimica Acta* **1981**, 45, 2377 - 2383.
- (5) Davies, S. H. R.; Morgan, J. J. *Journal of Colloid and Interface Science* **1989**, 129, 63 - 77.
- (6) Wilson, D. E. *Geochimica et Cosmochimica Acta* **1980**, 44, 1311 - 1317.
- (7) Junta, J. L.; Hochella, M. F. J.; Harris, D. W.; Edgell, M. In *Proceedings of the 7th international symposium on water rock interaction*; 1992; pp .
- (7) Junta, J. L.; Hochella, M. F. J.; Harris, D. W.; Edgell, M. In *Proceedings of the 7th international symposium on water rock interaction*; 1992; pp .
- (8) Junta, J. L.; Hochella, M. F. J. *Geochimica et Cosmochimica Acta* **1994**, 58, 4985 - 4999.
- (9) Tebo, B. M. *Deep Sea Research* **1991**, 38 supplement 2, S883 - S905.

- (10) Tebo, B. M.; Emerson, S. *Biogeochemistry* **1986**, 2, 149 - 161.
- (11) Tebo, B. M.; Emerson, S. *Applied and Environmental Microbiology* **1985**, 50, 1268 - 1273.
- (12) Tebo, B. M.; Nealson, K. H.; Emerson, S.; Jacobs, L. *Limnology and Oceanography* **1984**, 29, 1247 - 1258.
- (13) Emerson, S.; Kalhorn, S.; Jacobs, L.; Tebo, B. M.; Nealson, K. H.; Rosson, R. *A. Geochimica et Cosmochimica Acta* **1982**, 46, 1073 -
- (14) Stumm, W.; Giovanoli, R. *Chimia* 1976, 30, 423 -426.
- (15) Hem, J. D.; Roberson, C. E.; Fournier, R. B. *Water Resources Research* **1982**, 18, 563 - 570.
- (16) Hem, J. D.; Lind, C. J. *Geochimica et Cosmochimica Acta* **1983**, 47, 2037 - 2046.
- (17) Hem, J. D. *Chemical Geology* **1978**, 21, 199 - 218.
- (18) Murray, J. W.; Dillard, J. G.; Giovanoli, R.; Moers, H.; Stumm, W. *Geochimica et Cosmochimica Acta* **1985**, 49, 463 - 470.
- (19) Diem, D.; Stumm, W. *Geochimica et Cosmochimica Acta* **1984**, 48, 1571 - 1573.
- (20) Millero, F. J. *Geochimica et Cosmochimica Acta* **1985**, 49, 547-553.
- (21) Davies, S. H. R. PhD Thesis, California Institute of Technology, 1985.
- (22) Wehrli, B. In *Aquatic Chemical Kinetics: Reaction Rates of Processes in Natural Waters*; W. Stumm, Ed.; John Wiley & Sons: New York, 1990; pp 311 - 337.
- (23) Seinfeld, J. H. *Atmospheric Chemistry and Physics of Air Pollution*; John Wiley & Sons Inc.: New York, 1986.
- (24) Roberts, P. V.; Dandliker, P. G. *Environmental Science and Technology* **1983**, 17, 484 - 489.
- (25) Schwarzenbach, R. P.; Gschwend, P. M.; Imboden, D. M. *Environmental Organic Chemistry*; John Wiley & Sons Inc.: New York, 1993.

Table 3.1
Comparison of Homogenous Rate Constants for
Autoxidation of Mn(II) at 25°C

pH	Pseudo first order constant (sec ⁻¹)
9.0 ^a	6.0 x 10 ⁻⁶
9.3 ^a	2.8 x 10 ⁻⁵
9.5 ^a	7.0 x 10 ⁻⁵
8.35 ^b	<3 x 10 ⁻⁸
8.95 ^b	1.5 x 10 ⁻⁶
9.04 ^b	2.8 x 10 ⁻⁶
9.25 ^b	9.5 x 10 ⁻⁶
8.0 ^c	1.6 ± 0.4 x 10 ⁻¹⁰

^a Morgan PhD Thesis, Harvard University 1964

^b Davies PhD Thesis, California Institute of Technology 1985

^c This Study

Figure 3.1
Mn(II) speciation

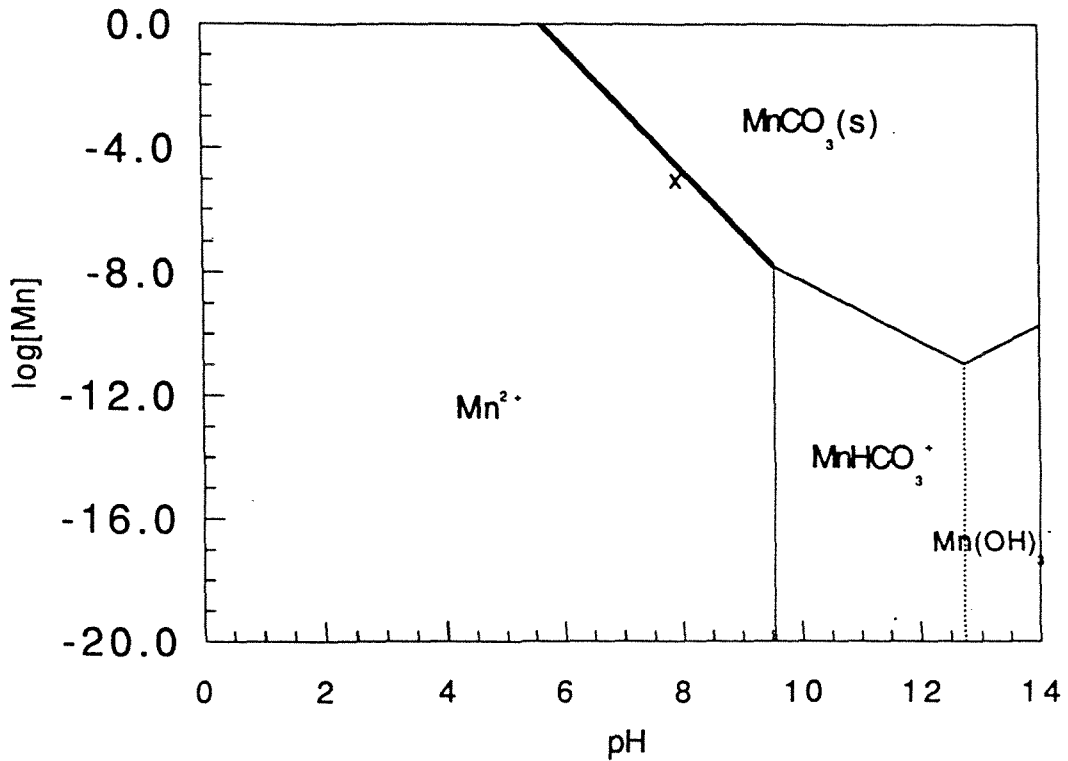


Figure 3.1. Mn(II) Speciation. Phase diagram for the Mn-CO₃-H₂O system. Showing $\log[Mn]$ versus pH. The system is open to the atmosphere and the partial pressure of CO₂ is $10^{-3.5}$ atm. All constants are for $I = 0.5$ mM.

Figure 3.2

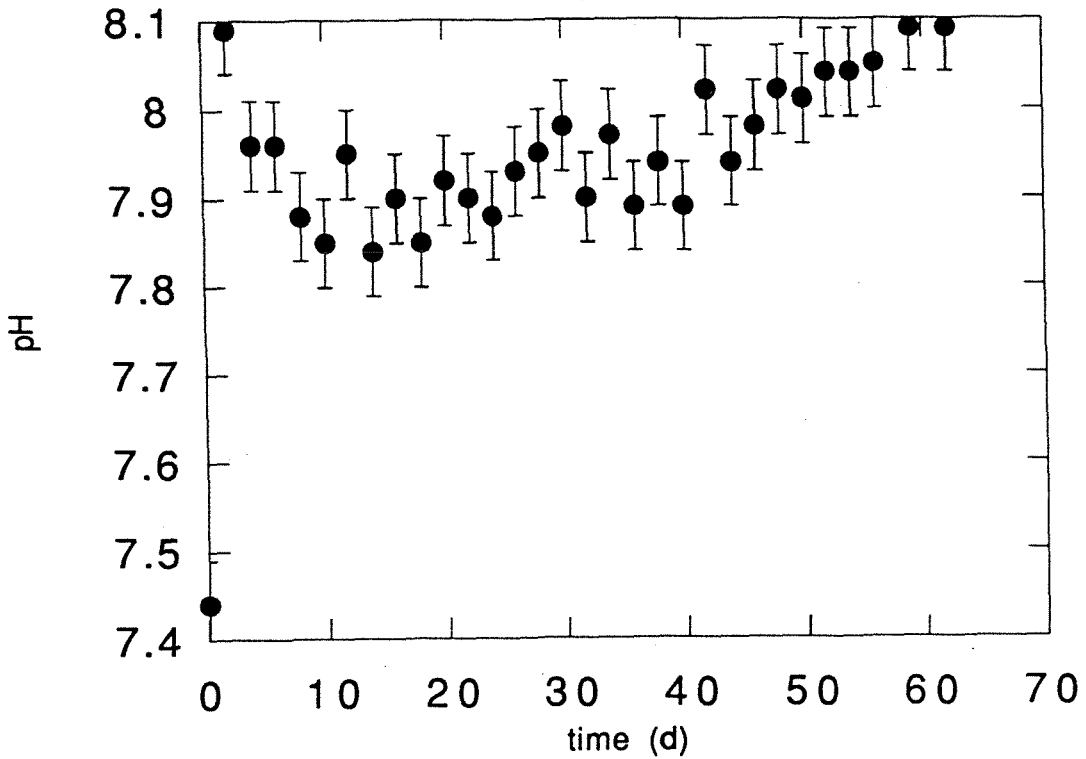


Figure 3.2. 50°C Oxidation reactor pH. The pH variations are typical of the reactor pH throughout the oxidation experiments, with the exception of the 60°C data which showed a much larger upward drift. The data here shows a sharp acid spike at $t = 0$ which rebounds within a day. There is a slight upward drift over the course of the experiment.

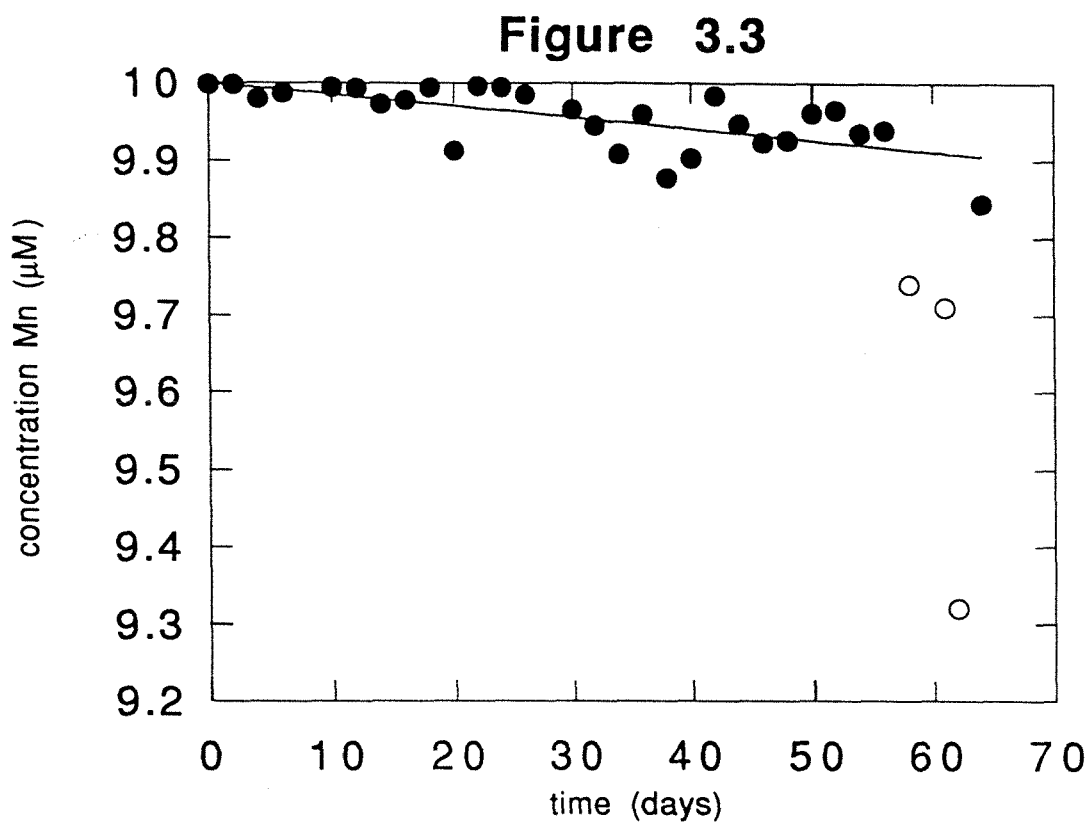


Figure 3.3. Oxidation of Mn(II) at 45°C. Plot of Mn(II), calculated by difference, versus time. Open circles were omitted from the curve fit.

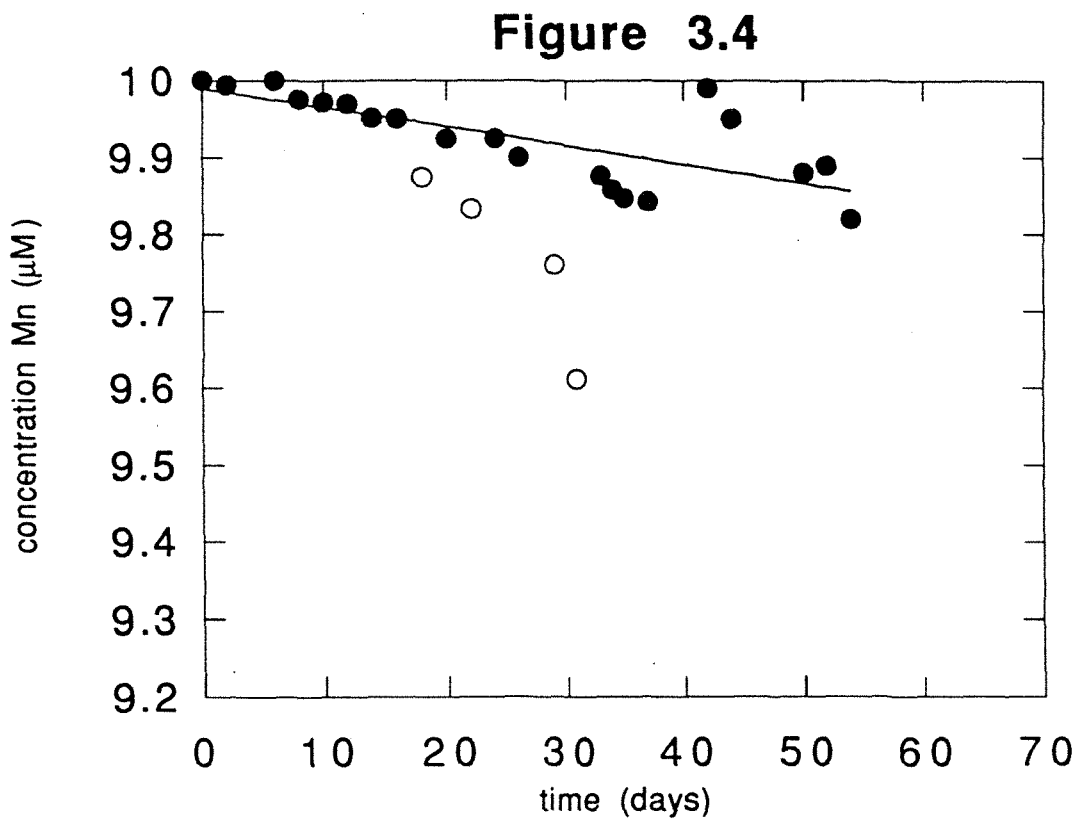


Figure 3.4. Oxidation of Mn(II) at 50°C. Plot of Mn(II), calculated by difference, versus time. Open circles were omitted from the curve fit.

Figure 3.5

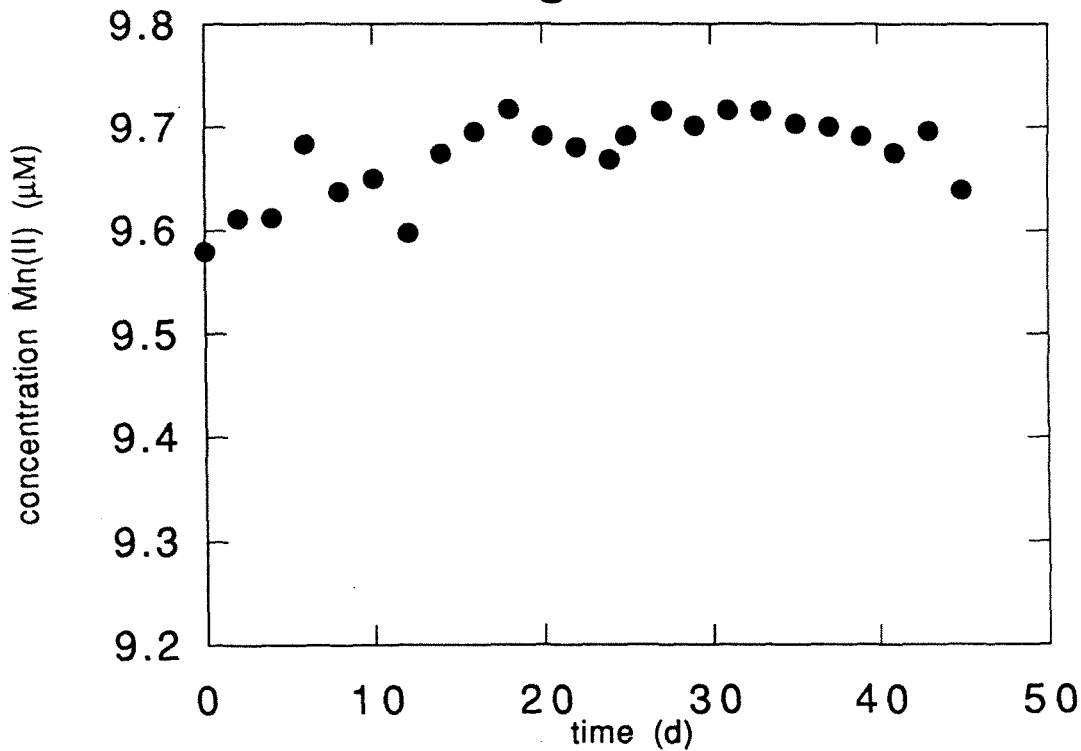


Figure 3.5. Oxidation of Mn(II) at 60°C. Plot of Mn(II), calculated by difference, versus time. Open circles were omitted from the curve fit. It is evident there is a high blank problem which has largely obscured the results.

Mn(III) COMPLEXES

4.1 Introduction

Mn(III) has long been thought to be a short lived and unstable oxidation state of Mn in water. The hexaquo Mn^{3+} ion has a standard reduction potential of 1.5 V. versus the standard hydrogen electrode(1). The disproportionation reaction is also known to be favored under most conditions



Despite its apparent instability, its tendency to react quickly through either reduction or disproportionation reactions, Mn(III) has been of interest in the laboratory because of its high reduction potential. The high reduction potential made it an interesting oxidant for many species. The interest in using Mn(III) as a strong oxidant was great enough to drive laboratory studies to find ways of stabilizing Mn(III). Stabilization here is defined as slowing down the disproportionation reaction enough to allow reactions with other species.

The overall interest and study of Mn(III) complexes was outlined in the introductory chapter. The Mn(III) stabilizing ligands which are of most interest for this study are pyrophosphate, citrate, and ethylenediamine tetracetate (EDTA). These ligands were chosen because of their relatively well defined characterization and their differing chemical properties. A comparison of the properties of these ligands can be found in Table 4.1.

4.1.1 Pyrophosphate

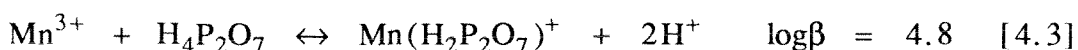
Pyrophosphate($\text{P}_2\text{O}_7^{4-}$) is the simplest of the ligands used not only in structure but also in the number of possible chemical reactions it can undergo. It is the smallest of the polyphosphate chains, which have been found naturally in lake sediments and are involved in biological reactions(2). $\text{P}_2\text{O}_7^{4-}$ has no redox chemistry, its only loss

mechanism being hydrolysis to form orthophosphate or polymerization to give longer chains. Pyrophosphate was one of the earliest ligands found to stabilize Mn(III) complexes. It has been used in many experiments in order to examine oxidation of other compounds by Mn(III)(3-5). Pyrophosphate has also been found to stabilize Mn(III) in several enzymatic biological reactions(6-9).

The Mn(III) pyrophosphate complex has been fairly well characterized. The presence of $P_2O_7^{4-}$ has been found to stabilize the Mn(III) by dropping the Mn(III)/Mn(II) reduction potential from 1.5V for the hexaquo ion to 1.15V for Mn(III) in a $P_2O_7^{4-}$ medium(10). Equilibrium constants have been reported by Ciavatta and Palombari(11) and Gordienko et al.(12). These two groups disagree on the constants and the predominant species. Gordienko et al.(12) report constants for $MnP_2O_7^-$ and $Mn(P_2O_7)_2^{5-}$. They report log K's for these species of 16.68 and 31.85. e.g.,



At the conditions they worked at, 25°C and I = 0.3M, this would mean $Mn(P_2O_7)_2^{5-}$ is the predominant species under conditions of excess pyrophosphate. Ciavatta and Palombari report constants for the species $MnH_2P_2O_7^+$, $MnHP_2O_7^0$, $MnH_4(P_2O_7)_2^-$, and $MnH_5(P_2O_7)_2^0$. The log β 's they report are: 4.8, 4.2, 6.5, and 6.7, respectively. e.g.,



These constants would imply that the protonated species are more important. Ciavatta and Palombari worked at I = 3M, so their results cannot be directly compared with other results at lower I to determine which species and constants are likely to be

avored. Although the predominant species is uncertain, whichever species is predominant has been found to have a violet-pink color which has been reported by several investigators. Its absorption maximum is at 484 nm with a molar absorptivity of 110 l/mol cm.

Most recently, Kostka et al. have examined the reduction of Mn(III) complexes by microbes(13) using lactate and formate as electron donors. They also examined the reduction by inorganic species such as Fe(II) and sulfide. Unlike previous studies in which Mn(III) was formed, either from Mn(VII) or electrochemical oxidation, Kostka et al. used the dissolution of Mn(III) solids by $P_2O_7^{4-}$ to form the Mn(III) complex. They did not examine the kinetics, chemical dependences, or thermodynamics of the dissolution reaction.

4.1.2 Citrate

Citrate forms another relatively well studied Mn(III) complex. It was first used by Duke in 1947(14). He used it in an analytical method in studying Mn(III) oxalate complexes. The citrate, being a stronger complexing agent than oxalate, bound any Mn(III) present and was inert enough to allow analysis. Duke reported a maximum absorption at 430nm with a molar absorptivity of 340 l/mol cm.

Carrell and Glusker(15-16) examined the structure of both crystalline and solution phase Mn(III) citrate complexes. They found the citrate acts as a tridentate ligand.

A few kinetic studies have been done with citrate complexes. Several such studies were conducted by Milad et al. in the 70s(17-19). The earliest of these studies involved measuring the oxidation of Mn(II) by oxygen in a citrate medium. They found the formation of the Mn(III) citrate complex. The reaction was carried out at a pH of about 11, although this was only an initial pH and they reported pH drops of several pH units. Therefore, although they report a rate expression, it was certainly affected by the large change in pH. Another study by the same group reported the

reduction of the Mn(III) citrate complex through reaction with the citrate. They found it to be first order in Mn and autocatalytic. They also report a first order dependence on initial pH but made no attempt to control this variable. A third study by this group examined the reduction of Mn(III) by H₂O₂ in the presence of citrate. They found the reaction to be first order in both Mn and peroxide. Both citrate and Mn(II) retarded the reaction. Barek and Berka(20) examined the reaction of Mn(III)SO₄ complexes with citrate and oxalate, and found mineralization of the citrate. A study by Loll and Bollag(21) found an enzyme-like material in soil that apparently consisted of Mn and citrate.

4.1.3 Ethylenediaminetetraacetate (EDTA)

EDTA is the least well studied of the three ligands used in this study. Yet its complex has the largest stability constant. The standard reduction potential of Mn(III) in an EDTA medium drops to 0.82V versus the S.H.E.(10). The log of the complexation constant is 24.75. Yoshino et al.(22) synthesized the Mn(III)EDTA compound and reported its absorptivity to be 267 l/mol cm at 500nm. They found a pK_a for the complex of 5.3.

Macartney and Thompson(23) report self exchange rates for Mn-EDTA complexes, the transfer of electrons between the Mn(II) and Mn(III) EDTA complexes. They found a self exchange constant of 0.7 M⁻¹s⁻¹. Bose et al.(24) have found that when reacting MnO₄⁻ with EDTA an intermediate was formed which appeared to be a Mn(III) complex with either EDTA or one of its degradation products. Gangopadhyay et al.(25) also found that Mn(III)CDTA complexes can oxidize EDTA. Thus although EDTA forms the most thermodynamically stable Mn(III) complex studied here, it is also susceptible to oxidation by Mn(III).

4.1.4 This Study

This study has examined the kinetic inertness of the Mn(III) complexes of the three above mentioned ligands. These ligands were chosen because they were

reported to have distinct molar absorptivities and therefore could be followed relatively easily using UV-visible spectrophotometry. These ligands were also chosen for their differing chemical properties and their reported presence in natural environments.

Pyrophosphate has been found along with other polyphosphates in lake sediments and is also involved in biological processes. It is interesting not only because it forms a weak complex with Mn(III), but also because it has no redox chemistry itself. Therefore the possibility of internal redox reactions is eliminated. Although the weakest binding of the ligands, absence of redox reactions make it more likely to persist once formed.

EDTA is a commonly used industrial chelator and is thus now found in many natural waters. It is a very strong chelator and thus forms the most thermodynamically stable of the Mn(III) complexes among these ligands studied. It does, however, have the possibility of undergoing redox transformations. The fact that it is capable of binding all 6 coordination sites of Mn³⁺ may also lead to interesting chemistry.

Citrate is a common biological product and is produced in natural systems. It is also a strong complexing agent of Mn(III) although not as strong as EDTA. It too has the ability to participate in redox reactions. It is only a tridentate ligand and therefore may have different behavior from EDTA. Another interesting feature of citrate is that, unlike pyrophosphate and EDTA, oxidation of Mn(II) is reported to be relatively rapid in the presence of citrate(17).

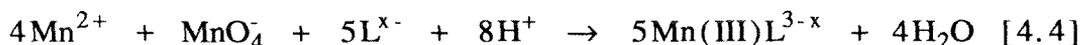
4.2.0 Experimental

All Mn(III) complexes were synthesized using reagent grade chemicals with no further purification. The ligands used were Na₄P₂O₇·10H₂O by Malinckrodt, Na₃C₆H₅O₇·2H₂O by Fisher, and Na₂C₁₀H₁₄N₂O₈·2H₂O by J. T. Baker. The Mn(II) salt used was in most cases a Mn(NO₃)₂ solution by Aldrich. In cases where NO₃⁻

was undesirable $\text{Mn}(\text{ClO}_4)_2 \cdot 6\text{H}_2\text{O}$ by G. Frederick Smith was used. The permanganate used was a 0.0203 M KMnO_4 solution by Aldrich.

4.2.1 Complex preparation

The Mn(III) complexes were formed with ligand L using the manganous-permanganate reaction.



First a Mn(II) salt, either $\text{Mn}(\text{NO}_3)_2$ or $\text{Mn}(\text{ClO}_4)_2$, was dissolved along with the sodium salt of the ligand in distilled, deionized water. After the salts dissolved, the pH was adjusted using either nitric or perchloric acid and sodium hydroxide. In most cases the excess ligand was also used as the pH buffer; for experiments with low excess ligand another buffer was used. The citrate ligand concentration studies used a carbon dioxide buffer made with 0.05M NaHCO_3 and nitric acid. The experiment examining the oxidation Mn^{2+} in the presence of citrate used a 0.1M N-tris[Hydroxymethyl]methyl-2-aminoethane sulfonic acid (TES) buffer for the pH 7.5 run and a 0.1M tris(hydroxymethyl)aminomethane (TRIS) buffer for the pH 8.0 run. After the pH was adjusted to the desired level, sufficient MnO_4^- was added to give a Mn(II):Mn(VII) ratio of 4:1. In general the reaction quickly proceeded from the purple color of the permanganate to the color of the desired Mn(III) complex in a matter of a few minutes.

4.2.2 Experimental Monitoring

The presence of an Mn(III) complex was monitored spectrophotometrically. The absorbances were monitored periodically at the peak wavelength using a Shimadzu UV-1201 spectrophotometer. The absorptivities of Mn(III)pyrophosphate and Mn(III)CIT were verified to be independent of pH. EDTA, on the other hand, has two identified complexes with differing spectra as reported by Yoshino et al.

Therefore below pH 5.3 the Mn(III)EDTA complex was monitored for at 488nm. Above pH 5.3 the complex was monitored for at 450nm. The absorptivity of each Mn(III)EDTA complex was found to be independent of pH, once the effect of the two complexes were taken into account.

All reactions were carried out in polyethylene bottles or Pyrex flasks which were open to laboratory air and at laboratory temperatures, about 20-22°C. For experiments where the effect of the exclusion of oxygen was examined, the Mn(II)-ligand solution was made and adjusted to the proper pH, and was then bubbled with N₂ for at least an hour before the permanganate was added. After addition of the permanganate the container was sealed with parafilm. While this does not guarantee a zero oxygen concentration it gives a much lower oxygen value than air saturation and should be sufficient to observe the effects of oxygen on the reactions involved.

4.3 Results and Discussion

4.3.1 Pyrophosphate

4.3.1.1 Effect of pH

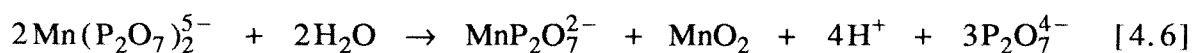
Figure 4.1 shows the fraction of Mn bound in the Mn(III)pyrophosphate complex versus time for several pHs. The fraction bound is calculated by dividing the measured absorbance by the calculated absorbance if all the Mn were present as the Mn(III) complex. Fractions above 1.0 are either because of the precipitation of solids or unreacted permanganate. From pH 7 to 9 the complex is lost only very slowly over a period of about 3 months. Above pH 9 fairly rapid precipitation of solids occurs, which could be a result of rapid oxidation of Mn(III) or disproportionation. First order fits are shown for each of the pH curves.

There are two effects of pH. One is a change of the rate constant for disappearance of the Mn(III)P₂O₇ species and the other is the initial amount of Mn(III) formed. The initial amounts formed and the rate constants, as calculated from the curve fit, are included in Table 4.2. The initial amount formed and the rate of

loss of Mn(III) complex seem to follow a similar trend. The initial amount formed is generally smaller when the rate constant is faster. This would seem to indicate that the reduction in initial amount formed is simply a result of the loss of complex being faster relative to the formation rate. For both the rate constant and the initial amount of complex formed, a maximum in stability is found at pH 7.3. At pH 7.3 there is the highest initial amount of complex formed and the smallest rate constant, leading to the most inert conditions. This may result from the singly protonated ligand being the predominant species, as proposed by Ciavatta and Palombari(11), yielding a neutral complex in solution according to the following reaction



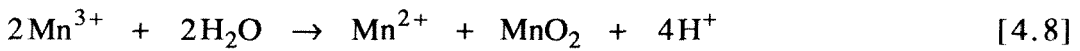
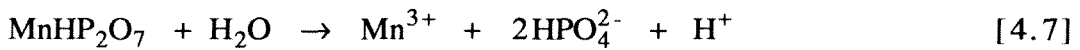
If this is true then the complex formation would be most stable between pH 7 and 8 where the singly protonated pyrophosphate species is predominant. Another possibility is that the complex formed is the $\text{Mn}(\text{P}_2\text{O}_7)_2^{5-}$ species as suggested by Gordienko et al. (12). According to the equilibrium constants given by them the complex does indeed have a maximum thermodynamic stability near pH 7.3 as shown in Figure 4.2, which is a plot of ΔG of the disproportionation reaction given by 4.6



versus pH. The equilibrium constants used for the calculation were those of Gordienko et al.(12). To make the calculations solution conditions must be assumed. It was assumed that the ratio of P_2O_7 :Mn was 50:1 and the Mn(III):Mn(II) ratio was 10:1. The constants were used as given, not adjusting for I or T. The calculations show that the $\text{Mn}(\text{P}_2\text{O}_7)_2^{5-}$ complex is predominant at all pHs above 1 and is

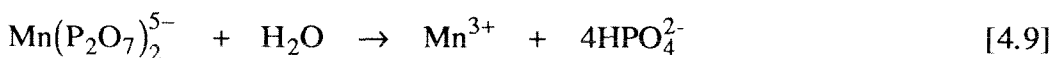
thermodynamically stable between pH 1 and 11.5 with a maximum stability around pH 7.

If the complex is indeed thermodynamically stable as suggested by Figure 4.2 the slow loss of the complex is possibly caused by slow hydrolysis of the pyrophosphate over time, leading to dissociation of the complex and subsequent disproportionation as shown in reactions 4.7 and 4.8

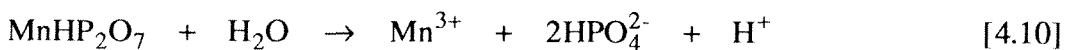


Clesceri and Lee(26) studied the hydrolysis of pyrophosphate and found a rate constant of $6 \times 10^{-5} \text{ min}^{-1}$. This is actually faster than the observed loss of Mn(III) complex. Therefore the hydrolysis of pyrophosphate can account for the loss of Mn(III) complex. Although no solids were observed forming in solution it is possible the amount of Mn disproportionated is so small that the product solids may still be colloidal and not visible. If there is no solids formation then the only other sink for Mn(III)P₂O₇ is reduction to Mn(II) by some trace contaminant.

Some insight may be gained into which complex is formed by examining the proposed mechanism and calculating the theoretical dependence on pH for each complex and then comparing that to the actual behavior. If Mn(P₂O₇)₂⁵⁻ is the major species then the rate limiting step for complex loss is given by:



If MnHP₂O₇ is the major species then the rate limiting step is given by:



The rate expressions for these two mechanisms are not simple and give complicated dependences on hydrogen ion which may explain why there is no clear trend in the data. For equation 4.9 being the rate limiting step, the rate expression can be written as

$$\frac{d[\text{Mn(III)(P}_2\text{O}_7)_2^{5-}]}{dt} = -k_h \cdot [\text{Mn(III)(P}_2\text{O}_7)_2^{5-}] \quad [4.11]$$

where k_h is the hydrolysis rate in s^{-1} . The concentration of the Mn the complex can be expressed in terms of total manganese.

$$\text{Mn}_T = [\text{Mn}^{3+}] + [\text{Mn(P}_2\text{O}_7)_2^{5-}] + [\text{Mn}^{2+}] + [\text{MnO}_2] \quad [4.12]$$

Equation 4.8 allows $[\text{MnO}_2]$ to be expressed as equal to $[\text{Mn}^{2+}]$ yielding

$$\text{Mn}_T = [\text{Mn}^{3+}] + [\text{Mn(P}_2\text{O}_7)_2^{5-}] + 2 \cdot [\text{Mn}^{2+}] \quad [4.13]$$

Using equilibrium expressions for disproportionation and complex formation will yield the expression

$$\text{Mn}_T = \frac{[\text{Mn(P}_2\text{O}_7)_2^{5-}]}{K_c \cdot [\text{P}_2\text{O}_7^{4-}]^2} + [\text{Mn(P}_2\text{O}_7)_2^{5-}] + 2 \frac{K_d \cdot [\text{Mn(P}_2\text{O}_7)_2^{5-}]}{K_c^2 \cdot [\text{P}_2\text{O}_7^{4-}]^4 \cdot [\text{H}^+]^4} \quad [4.14]$$

Solving equation 4.14 for $[\text{Mn(P}_2\text{O}_7)_2^{5-}]$ and substituting into equation 4.11 gives

$$\frac{d[\text{Mn}(\text{P}_2\text{O}_7)_2^{5-}]}{dt} = -k_h \cdot \left(\frac{-\left(1 + \frac{1}{a}\right) \pm \sqrt{\left(1 + \frac{1}{a}\right)^2 + 4 \cdot \frac{2 \cdot K_d \cdot \text{Mn}_T}{a^2 \cdot [\text{H}^+]^4}}}{\frac{4 \cdot K_d}{a^2 \cdot [\text{H}^+]^4}} \right) \quad [4.15]$$

where $a = K_c \cdot [\text{P}_2\text{O}_7^{4-}]^2$, K_c is the equilibrium constant for complex formation in M^{-2} , and K_d is the equilibrium constant for disproportionation in M^3 . This is an extremely complex dependence on hydrogen ion concentration, especially when it is considered the pyrophosphate speciation is also pH dependent. Examining the equation more closely allows determination of the dominant terms in the pH dependence. Above pH 8.4 all of the pyrophosphate is unprotonated and therefore has a concentration on the order of 10^{-2} M. Even at pH 6, $[\text{P}_2\text{O}_7^{4-}]$ is still on the order of 10^{-5} M. Therefore, because K_c is $10^{31.8}$, a is always a large number therefore $1/a \ll 1$ in the entire pH range studied. The second term inside the radical is also small as K_d is on the order of 10^7 . Although this term is small it cannot be eliminated because although the number inside the radical is nearly one so is the first term in the numerator. If both are assumed to be 1 then the only answer becomes zero. Thus above pH 8.4 the dependence on hydrogen ion concentration is complex and can be given by

$$\frac{d[\text{Mn(III)}(\text{P}_2\text{O}_7)_2^{5-}]}{dt} = - \left(-1 + \frac{1}{a} + \sqrt{\left(1 + \frac{1}{a}\right)^2 + \frac{2b \cdot \text{Mn}_T}{[\text{H}^+]^4}} \right) \cdot \left(\frac{[\text{H}^+]^4}{b} \right) \quad [4.16]$$

where

$$b = \frac{4 \cdot K_d}{K_c^2 \cdot [\text{P}_2\text{O}_7]_T^4} \quad [4.17]$$

Although the radical term cannot be eliminated it would be expected that the fourth order term would dominate over the radical term. Between pH 6 and 8.4 the singly protonated pyrophosphate becomes the dominant species and $[P_2O_7^{4-}]$ becomes dependent on the inverse first power of hydrogen ion concentration. This would change equation 4.16 to

$$\frac{d[Mn(III)(P_2O_7)_2^{5-}]}{dt} = - \left(-1 + \frac{[H^+]^2}{a} + \sqrt{\left(1 + \frac{[H^+]^2}{a}\right)^2 + \frac{2b' \cdot Mn_T}{[H^+]^4}} \right) \cdot \left(\frac{1}{b}\right) \quad [4.18]$$

Here $a' = K_c \cdot K_{a4}^2$, where K_{a4} is the fourth acidity constant for pyrophosphate, and

$$b' = \frac{4 \cdot K_d}{K_c^2 \cdot K_{a4}^4 \cdot [P_2O_7]_T^4} \quad [4.19]$$

In this pH domain the zero order pH terms would be expected to dominate.

For equation 4.10 being the rate limiting step, the rate expression can be written as

$$\frac{d[Mn(III)HP_2O_7]}{dt} = -k_h \cdot [Mn(III)HP_2O_7] \quad [4.20]$$

where k_h is the hydrolysis rate in s^{-1} . The concentration of the Mn the complex can be expressed in terms of total manganese.

$$Mn_T = [Mn^{3+}] + [MnHP_2O_7] + 2 \cdot [Mn^{2+}] \quad [4.21]$$

Using equilibrium expressions for disproportionation and complex formation will yield the expression

$$\text{Mn}_T = \frac{[\text{MnHP}_2\text{O}_7]}{K_e \cdot [\text{P}_2\text{O}_7^{4-}]} + [\text{MnHP}_2\text{O}_7] + 2 \frac{K_d \cdot [\text{MnHP}_2\text{O}_7]}{K_e^2 \cdot [\text{P}_2\text{O}_7^{4-}]^2 \cdot [\text{H}^+]^4} \quad [4.22]$$

Solving equation 4.22 for $[\text{MnHP}_2\text{O}_7]$ and substituting into equation 4.20 gives

$$\frac{d[\text{MnHP}_2\text{O}_7]}{dt} = -k_h \cdot \left(\frac{-\left(1 + \frac{1}{a}\right) \pm \sqrt{\left(1 + \frac{1}{a}\right)^2 + 4 \cdot \frac{2 \cdot K_d \cdot \text{Mn}_T}{a^2 \cdot [\text{H}^+]^4}}}{\frac{4 \cdot K_d}{a^2 \cdot [\text{H}^+]^4}} \right) \quad [4.23]$$

where $a = K_e \cdot [\text{HP}_2\text{O}_7^{3-}]$, K_e is the equilibrium constant for complex formation in M^{-1} , and K_d is the equilibrium constant for disproportionation in M^3 . Between pH 6.0 and pH 8.4 all of the pyrophosphate can be assumed to be in the singly protonated form and the pH dependence would be expected to be

$$\frac{d[\text{Mn(III)HP}_2\text{O}_7]}{dt} = - \left(-1 + \frac{1}{c} + \sqrt{\left(1 + \frac{1}{c}\right)^2 + \frac{2d \cdot \text{Mn}_T}{[\text{H}^+]^4}} \right) \cdot \left(\frac{1}{d} \right) \quad [4.24]$$

where

$$c = \frac{4 \cdot K_d}{K_e^2 \cdot [\text{P}_2\text{O}_7]_T^2} \quad [4.25]$$

Here the overall dependence on hydrogen ion is complicated but would appear to be roughly dependent on the negative second power. Above pH 8.4 the $[\text{HP}_2\text{O}_7^{3-}]$ becomes dependent on the first order of $[\text{H}^+]$ and the overall dependence can be written as

$$\frac{d[\text{Mn(III)HP}_2\text{O}_7]}{dt} = \left(-1 + \frac{1}{c' \cdot [\text{H}^+]} + \sqrt{\left(1 + \frac{1}{c' \cdot [\text{H}^+]} \right)^2 + \frac{2d' \cdot \text{Mn}_T}{[\text{H}^+]^4}} \right) \cdot \left(\frac{[\text{H}^+]^2}{d'} \right) \quad [4.26]$$

Here $c' = K_c \cdot K_{a4}^{-1}$ and

$$d' = \frac{4 \cdot K_d \cdot K_{a4}^2}{K_c^2 \cdot [\text{P}_2\text{O}_7]_T^2} \quad [4.27]$$

Most likely the second order term will dominate in equation 4.26. Summarizing, if equation 4.9 is the rate limiting step then the dependence on $[\text{H}^+]$ would be approximately fourth order above pH 8.4 and approximately zero order between pH 6 and pH 8.4. If equation 4.10 is the rate limiting step the $[\text{H}^+]$ dependence would be approximately second order above pH 8.4 and approximately negative second order between pH 6.0 and pH 8.4

The rate constants although somewhat scattered can be examined to see if they fit either of these dependences. The points at 7.8 and 8.0 probably should be excluded because they are close to $\text{p}K_4$ of pyrophosphate so both the unprotonated and singly protonated ligand are important. This would make invalid the assumptions used to derive 4.9 - 4.12. Eliminating those two points would appear to give a dependence on hydrogen ion of close to an order of -3 below pH 8. Above pH 8.4 there is only one point so it is not possible to tell, although it certainly seems to be a smaller dependence than at lower pH. Although none of the above expressions fit the observed data the expression for the MnHP_2O_7 species seems to come the closest. Its second order dependence would seem much closer to the observed data than the zero order dependence required by the $\text{Mn}(\text{P}_2\text{O}_7)_2^{5-}$ species. This would imply that the reactions occurring in this system are given by 4.5, 4.8, and 4.1.

It is interesting to note that considering the pH dependence of the pyrophosphate alone, it would be expected that the shift in pH dependence would occur at the pK_4 of pyrophosphate, which is at 8.4. However; the data shift seems to be at pH 7.3. This could be simply experimental error in one or more points that produces an artificial shift. If it is real then it is due to some other pH dependence other than the pyrophosphate. This would most likely imply a hydrolysis speciation of the Mn(III). This is certainly possible. Only the first pK of Mn(III) is known and it is thought to be about 0. It is possible that Mn(III) has a second or third pK around 7.3.

Overall the dependence on pH is a complicated one due to the protonation of the pyrophosphate as well as the dependence of the disproportionation reaction and possibly the manganese speciation. Although the complicated nature of the pH dependence makes precise interpretation of the results difficult the main effect of pH seems to be one of governing which complex is dominant. It is mostly a thermodynamic effect rather than a kinetic one. The dominant complex seems to be the neutral $MnHP_2O_7$ complex which is lost due to hydrolysis of the pyrophosphate. The complete set of proposed reactions is given in mechanism 4.1.

4.3.1.2 Effect of ligand concentration

Figure 4.3 shows the fraction of Mn bound in the $Mn(III)P_2O_7$ complex versus time. The y axis is calculated by dividing the absorbance of the solution by the absorbance if all of the Mn were bound in the $Mn(III)P_2O_7^-$ species. Numbers above 1.0 indicate either unreacted permanganate or precipitation of solids. At an excess of 10:1 $P_2O_7:Mn$ rapid solids formation is observed and is most likely indicative of disproportionation. At ratios greater than 25:1 the complex appears to be thermodynamically stable.

Although the 10:1 excess ligand run showed solids formation, the other runs showed no visible solids formation. Therefore the values above 1.0 in these cases are

most likely due to unreacted permanganate. There are two possible explanations for the presence of the unreacted permanganate. One is that the reaction of the permanganate with Mn(II) is slow but eventually all the permanganate reacts to form Mn(III). The other is that there is a slight excess of permanganate that never reacts. Although the errors in dispensing permanganate are precise, because the molar absorptivity of permanganate is 100 times higher than the Mn(III) complex it would only take a 0.5% excess to give an adsorption difference of 50%.

One possible way to differentiate between the two possibilities is to examine the nature of the decay of the absorbance. If there is an excess then the decay of the complex should be relatively unaffected, and the decay of the absorbance would represent the decay of the Mn(III) complex. If there is just a slow formation reaction then two effects on absorbance should be seen, one the slow formation of the complex and two the loss of the complex. Such a behavior should fit better to a 2 exponential curve rather than a single exponential. Both single and double exponential curves were fit to the data to see which better described the observed behavior. In all but the highest pyrophosphate concentration the single exponential curve showed the best fit. Therefore it is likely that there is a slight excess of permanganate that remains unreacted during the experiment. It is possible that at high pyrophosphate concentrations there may be some sort of complex formation that may slow down the formation reaction as well, but the dominant effect would seem to be that of a consistent offset throughout the experiment. Therefore all the data was fit using a single exponential and the rate constants obtained are assumed to be representative of the loss of the complex only. If the complex formation is indeed slow then the reported rate constants would represent an upper limit on the value, and the actual loss rate would be slower than reported.

The effect of the ligand appears to exhibit a maximum behavior at a pyrophosphate concentration of 25mM, rather than a consistent increase or decrease

across the range of concentrations used. The rate constants and initial relative concentrations are shown in Table 4.3. The rate constant is the greatest at a $P_2O_7:Mn$ ratio of 50:1. The rate constants are larger if the ratio is larger or smaller than this ratio. The rate constants show considerable variation with respect to ligand concentration. Other than being able to say the maximum stability appears at a ligand:Mn ratio of 50:1 it is difficult to discern a definite dependence on ligand concentration. The faster rates at high concentrations of pyrophosphate can be explained by the hydrolysis pathway noted in equation 4.7. This reaction will proceed faster at high pyrophosphate concentrations, causing the complex to dissociate more quickly. At low pyrophosphate concentrations the rate is faster because of the low complexing ability of the ligand and thus smaller thermodynamic driving force for formation of the complex. Because of the uncertain correlations for both pH and ligand concentration it is difficult to determine which complex is the dominant one. Whichever complex is dominant Mn(III) can be stabilized for months using a sufficient excess of pyrophosphate ligand. The optimal conditions for complex formation are a ligand:Mn ratio of 50:1 and a pH of 7.3, which seem to be set by the stability of the ligand itself as much as by the complex stability.

The rather high kinetic inertness of the pyrophosphate complex is not the result of a large complexation constant; it has the smallest equilibrium constant of the three ligands studied. The stability is instead caused by lack of loss pathways. Because pyrophosphate cannot donate an electron, the only redox mechanism for Mn(III) loss is disproportionation. In the presence of large excesses of pyrophosphate the disproportionation becomes kinetically hindered.

4.3.2 EDTA

4.3.2.1 Effect of pH

Figure 4.4 shows the fraction of Mn bound in the Mn(III)EDTA complex versus time for several pHs and an EDTA:Mn ratio of 50:1. Half lives range from 1 to

15 minutes and are shown in Figure 4.5. Stability is greatest at high or low pH, while the complex is less stable near neutral pH.

The observed stability is probably the result of two different species; a protonated form that is more stable at low pH, and an unprotonated form stable at high pH, as shown in reactions 4.28 and 4.29



Yoshino et al.(22) found that there is a protonated and unprotonated form of the complex and the pK_a of the complex is 5.3, consistent with the findings of this study. First order fits are shown in Figure 4.4 for each of the curves. Table 4.4 shows the fit parameters for each pH. The fitted initial concentration at time zero is less than unity for all of the middle to high pH runs, indicating that 100% yield was not obtained in the formation reaction. This is likely because the complex is thermodynamically unstable toward disproportionation. Even though the Mn(III) complex has a large equilibrium constant and is thermodynamically stable with regard to Mn^{3+} and EDTA, it is not thermodynamically stable with respect to the products of disproportionation. This is verified by calculation, using the complexation constant given by Davies (10). The calculation was done for the disproportionation of the Mn(III)EDTA complex to the Mn(II)EDTA complex and MnO_2 . An EDTA concentration of 0.01 M and a Mn(III):Mn(II + IV) ratio of 10:1 was assumed. It is calculated that the Mn(III)EDTA complex is unstable toward disproportionation at all pH's above 6. Therefore the reason the complex exists at all is most likely because of slow kinetics of disproportionation.

Figure 4.6 shows a plot of the log of the rate constants obtained from the fits of Figure 4.4 versus pH. The graph does not show a simple dependence. However, if

it is taken into account that the pH effects are actually caused by two complexes, then a simple dependence can be found. If it is assumed that the pK of 5.3 given by Yoshino et al. (22) is correct then below 5.3 the singly protonated ligand has the predominant effect and above 5.3 the unprotonated ligand dominates. Looking at the data, it can be reduced to two linear relations one from pH 3.6 to 5.2 and one from pH 5.2 to 9.0. The point at pH 5.2 technically cannot be included solely with the MnEDTA curve or the MnHEDTA curve because it is so close to the pK_a of the complex. Therefore a curve fit was done for the data above 5.3, excluding the 5.2 data point. The resulting curve fit was then used to calculate the contribution from MnEDTA at pH 5.2. Then the contribution that would have been required for the MnHEDTA species was calculated from the observed data and the pK given by Yoshino et. al.(22). The resulting calculated points are shown by the hollow symbols in figure 4.6. The fit for the data below pH 5.2 represents the effect of the Mn(III)HEDTA complex and yields the relation:

$$k_{\text{MnHEDTA}}^* = 10^{-5.29} \cdot [\text{H}^+]^{-0.48} \quad [4.30]$$

Where k* is the pseudo first order constant with units of s⁻¹, defined by the relation

$$\frac{d[\text{MnHEDTA}]}{dt} = -k_{\text{MnHEDTA}}^* \cdot [\text{MnHEDTA}] \quad [4.31]$$

when all other variables are held constant. The pseudo first order rate constant is the product of an intrinsic rate constant times any other variables which effect the rate. A general expression for the pseudo first order rate constant is given by

$$k_{\text{MnHEDTA}}^* = k_{\text{int}} \cdot [\text{H}^+]^x \cdot [\text{EDTA}]^y \dots \quad [4.32]$$

where k_{int} is the intrinsic constant and x and y are the dependences on hydrogen ion concentration and EDTA respectively. Therefore in equation 4.30 $k_{\text{int}} = 10^{-5.29} \text{M}^{0.48} \text{sec}^{-1}$.

The fit for the data above pH 5.2 is the effect of the Mn(III)EDTA^- complex and yields:

$$k_{\text{MnEDTA}}^* = 10^{-0.66} \cdot [\text{H}^+]^{0.29} \quad [4.33]$$

These equations indicate that although pH is important for Mn(III)EDTA stability the dependence on pH is not simple. The reaction comprises two or more reactions, some of which are equilibrium steps and others rate controlling, yielding a noninteger order. As expected, the rate of disappearance of the protonated complex has an inverse correlation with $[\text{H}^+]$. The dependence on pH for the unprotonated ligand is small and may be insignificant. If electron transfer within the complex is the rate limiting step then the dependences should be:

$$\frac{d[\text{Mn(III)EDTA}]}{dt} = - \frac{k_e \cdot K_{a4} \cdot [\text{Mn}^{3+}]_{\text{T}} \cdot [\text{EDTA}]_{\text{T}}}{[\text{H}^+]} \quad [4.34]$$

$$\frac{d[\text{Mn(III)HEDTA}]}{dt} = -k_e \cdot [\text{Mn}^{3+}]_{\text{T}} \cdot [\text{EDTA}]_{\text{T}} \quad [4.35]$$

respectively for the unprotonated and protonated species. k_e is the rate constant for electron transfer. The dependences on hydrogen ion come largely from the fact that within the entire pH range studied HEDTA^{3-} is the predominant EDTA species. Neither equation 4.34 or 4.35 describes the observed dependences very well. Therefore there is something missing from the rate limiting step. It is possible that the Mn has pH speciation as well as the EDTA, but even this would not yield the proper pH dependence. The most likely explanation is that electron transfer within the

complex is not the rate limiting step. Instead there must be some reaction with a pH dependent species that controls the rate.

4.3.2.2 Effect of ligand concentration

Figure 4.7 shows the fraction of Mn bound in the EDTA complex versus time for several EDTA concentrations at pH 6.8. In solutions where there is excess EDTA the complex is reduced rapidly on a time scale of 15 to 30 minutes. If only a stoichiometric amount of EDTA is used then the complex is stable for about 2 days. First order fits are shown for each data set. The values of the fit parameters are given in Table 4.5.

Again it is noted that the initial concentrations from the fit are smaller than they should be. This is an indication of the thermodynamic instability of the complexes toward disproportionation. Figure 4.8 shows the plot of log k versus log [EDTA]. A linear fit of the graph gives the relation

$$k_{\text{MnEDTA}}^* = 10^{-0.69} \cdot [\text{EDTA}^{4-}]^{1.35} \quad [4.36]$$

Combining equations 4.33 and 4.36 gives the expression:

$$\frac{d[\text{Mn(III)EDTA}]}{dt} = -k_{\text{int}} \cdot [\text{H}^+]^{0.29} \cdot [\text{EDTA}^{4-}]^{1.35} \cdot [\text{Mn(III)EDTA}] \quad [4.37]$$

where k_{int} is on the order of $10^{1.4} \text{ sec}^{-1}\text{M}^{-1.64}$. This gives the overall rate expression for Mn(III)EDTA, a similar expression for MnHEDTA cannot be found because no experiments on pH dependence were conducted below pH 6.

At first it might seem counterintuitive that the rate of loss of Mn(III)EDTA complex is dependent on the EDTA concentration. This can be explained if the reaction is not an internal electron transfer but an external transfer with excess ligand. Such a trend was observed by Yoshino et al. (22) in their preparation of the complex.

They noted that if the complex was prepared with an excess of EDTA that the yield was lower and some of the Mn(III) was reduced. This is also consistent with the pH dependence observations noted previously. It appears that at least part of the missing pH dependence is due to reaction of the Mn(III)EDTA complex with another EDTA molecule. The rate limiting step would then become electron transfer from the Mn(III)EDTA complex to the solution EDTA molecule as shown:

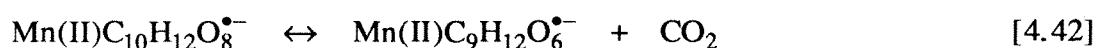
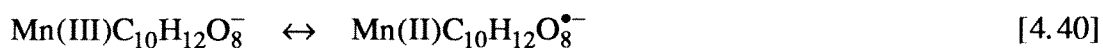


This would yield a rate expression of the form:

$$\frac{d[\text{Mn(III)EDTA}^-]}{dt} = -\frac{k_e \cdot [\text{Mn}^{3+}]_T \cdot [\text{EDTA}]_T^2}{[\text{H}^+]} \quad [4.39]$$

This still does not yield a dependence in agreement with equation 4.37. The most likely explanation for the discrepancy is that both the internal and external electron transfer mechanisms are operative. The sum of equations 4.39 and 4.35 would yield a result that would appear to be between first and second order in EDTA which is in line with the observations. The hydrogen ion dependence is still unexplained by the combination of the two mechanisms. This could be explained by either pH speciation of the Mn or by reaction of the complex with a species other than the predominant HEDTA species. Most likely the complex can react with any form of EDTA, and the overall pH dependence is a sum of the different dependences. The observed dependence being between zero and first order would imply that the reaction is fastest with the doubly and triply protonated EDTA species. A mechanism that would be consistent with all the above observations is that the Mn(III) forms a complex with the EDTA. The complex can then undergo a reversible electron transfer in which the

electron continues to move from the Mn(III) to one of the carboxyl oxygen until one of two things happens. Either the complex transfers the electron to a solution EDTA molecule, probably through hydrogen atom abstraction, or the molecule rearranges to decarboxylate giving off CO₂ and a radical species. The transfer to the external EDTA would be much faster than the rearrangement. This mechanism is shown in equations 4.40 to 4.42 and is shown in more detail in mechanism 4.2.



Equation 4.41 represents the rate limiting step, although if there is not sufficient excess EDTA present, then 4.42 can become rate limiting.

4.3.2.3 Effect of light and ionic strength

Figure 4.9 shows results of experiments conducted with and without light. It is seen laboratory light has little effect on the Mn(III)EDTA complexes, unlike other metal EDTA complexes.

If the mechanism in equations 4.40 to 4.42 is correct then the rate limiting step of electron transfer to the solution EDTA is rate limiting. Since EDTA can bind all six of the octohedral sites of the Mn atom, the electron transfer is most likely outer sphere. The fact that EDTA forms stable compound with other metals with high reduction potentials, such as Fe(III) and Co(III)(26, 27), suggests that EDTA complexes are very stable and require external electron donors or acceptors to undergo rapid redox reactions. If the mechanism is an outer sphere mechanism it should be dependent on ionic strength. Figure 4.10 shows the decomposition of Mn(III)EDTA at 2 different ionic strengths. The rate constants are $1.44 \pm 0.03 \times 10^{-4}$

s^{-1} at an I of 5M and $1.30 \pm 0.06 \times 10^{-4} s^{-1}$ at an I of 0.5M. It appears then that there is a slight ionic strength effect in the proper direction, the reaction being slower at lower ionic strength. Reaction 4.41 produces an unstable EDTA radical. This radical most likely reacts with oxygen, another EDTA, or another complex to give further degradation. Such radical reactions are known to give fractional dependences, as were found in this study. Bose et al. found that the oxidation of EDTA by MnO_4^- gave off CO_2 and ethylenediamineN,N',N' triacetic acid(24). Ayoko et. al found the oxidation of EDTA by Fe(III) gave off CO_2 , ethylenediamine, and formaldehyde among the products (28).

4.3.3 Citrate

4.3.3.1 Effect of pH

Figure 4.11 shows the fraction of Mn bound in the Mn(III)citrate complexes versus time for several pHs. The complex loss is much more rapid at pH 6 than at pH 10. A very interesting additional behavior was noted; the reoxidation of Mn and the reformation of the complex after initial loss. At pHs above 9 the complex was seen to return to its original concentration in just a day or two, while at pH 6 the return took weeks to months.

The reappearance of the Mn(III) complex obviously indicates a second reaction. Because of the second reaction a simple curve fit cannot be done to obtain information on the pH dependence of the initial reaction. To obtain information on the pH dependence of this initial reaction first order fits were used on the initial points only. Points which showed a higher value than the previous one were considered to be influenced by the reoxidation and therefore disregarded from the fit. Parameters from these fits are shown in Table 4.6. The rate of reaction shows an inverse relationship to pH. Figure 4.12 shows a plot of $\log k$ versus pH. The pH dependence can be seen to be very weak. It is given by the expression

$$k_{\text{MnCIT}}^* = k_{\text{MnCIT}} \cdot [\text{H}^+]^{0.18} \quad [4.43]$$

This is very close to being independent of hydrogen ion concentration. Indeed if internal electron transfer within the Mn(III)CIT complex is the rate limiting step then a zero order dependence on hydrogen ion concentration would be expected, as given by the relationship

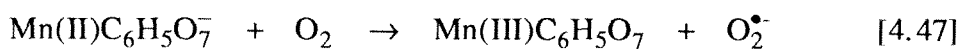
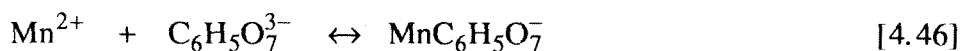
$$\frac{d[\text{Mn(III)CIT}]}{dt} = -k_e \cdot [\text{Mn}^{3+}]_T \cdot [\text{CIT}]_T \quad [4.44]$$

The slight dependence may be due to experimental error or to a slight contribution from either protonated citrate species or to hydroxyl complexes of Mn.

4.3.3.2 effect of oxygen on reformation of the Mn(III) complex

To further investigate the unusual behavior of the Mn(III) complex, i.e., being reformed after its reduction, experiments were repeated in solutions that had been N₂ sparged. Similar pHs were used as in the previous air exposed experiments. The experiments with N₂ sparging were conducted in the same way as the air exposed experiments except that the bottles were sealed with parafilm as explained in section 4.2.2. The results are given in Figure 4.13.

The nitrogen sparged solutions showed no reoxidation of the complex after initial loss. This indicates that O₂ is involved in the reoxidation of Mn(II) to Mn(III) as in reactions 4.45 - 4.47



The radical species generated in reaction 4.45 will then react further; most likely resulting in decarboxylation of the citrate and release of CO₂. The superoxide molecule formed in equation 4.47 is also available to oxidize another Mn(II) or a citrate molecule.

If the no oxygen runs in Figure 4.13 are fit to simple first order fits, rate constants for solely the loss of Mn(III)CIT can be found. The pH 9.1 data, however; does not fit well to a single exponential. The data fit much better to two processes, an initial fast decay followed by a slower decay. This was confirmed by fitting the pH 9.1 data to a double exponential. This yielded a much better fit raising r^2 from 0.79 to 0.99. The rate constants were determined to be $1.2 \pm 0.2 \times 10^{-4} \text{ s}^{-1}$ for the faster process and $4.2 \pm 0.6 \times 10^{-7} \text{ s}^{-1}$ for the slower process. Doing the same for the pH 7.4 data gives $8.3 \pm 5 \times 10^{-4} \text{ s}^{-1}$ and $4.4 \pm 0.5 \times 10^{-5} \text{ s}^{-1}$ for the fast and slow process respectively. This clearly shows that the degradation is made up of at least two processes, one of which does not seem to be present in the experiments with oxygen. One likely possibility for this step is that in an oxygen system the radicals formed by reaction 4.45 are quickly consumed by oxygen. In the absence of oxygen their presence may slow down the reaction, possibly by reacting with Mn(II) to reform the Mn(III) complex. If the hydrogen ion dependence of the initial decay is examined it is found to be about 0.5 order in hydrogen ion concentration. While this may be caused by the error in doing a two point fit, it is likely indicative that even the initial decay is not a simple one step process, but is most likely the decay of two different species, possibly the unprotonated and singly protonated species.

In order to verify the mechanism experiments were done to examine the oxidation of Mn(II) in the presence of citrate. Figure 4.14 shows the calculated concentration of Mn(III)CIT, based on absorbance at 430 nm, versus time of two Mn(II) solutions in the presence of citrate. The solutions were exposed to normal laboratory air. The concentration of Mn(III)CIT based on the peak at 430 nm, does

increase on the time scale of a few weeks. Oxidation at that pH in the absence of ligands would occur on a time scale of years as demonstrated in Chapter 3 of this work as well as by others. Therefore the autoxidation of Mn(II) is more rapid in the presence of citrate than in the absence of ligands.

It is interesting to note that the lower pH data in Figure 4.13 can be fit fairly well with a simple first order decay and a first order appearance term. This indicates that the behavior can be explained by two independent processes, the reduction of the Mn(III)CIT complex and the oxidation of the Mn(II)CIT complex. At low pH there is a large enough difference in the rate of reduction and oxidation that the two processes can be modelled as independent of each other. At higher pH the rates are much closer to each other and the interdependence of the reactions must be taken into account.

4.3.3.3 effect of ligand concentration

Figure 4.15 shows the dependence of Mn(III)-citrate complex stability on the citrate concentration. These experiments were all done with bicarbonate buffers. Because of slow degassing of CO₂ over time the pH in these solutions rose from 6.8 to about 9 over the course of the experiment. All four experiments experienced the same pH rise. Although the pH rise most likely facilitated precipitation of both MnCO₃ and oxidized Mn solids, all 4 solutions experienced the same conditions so that differences noticed are because of citrate concentration differences. The complexity of the reaction makes analysis for rate dependence on citrate difficult. Only the first two days data were used for the first order fits. Results of these fits are given in Table 4.7.

Figure 4.16 shows a plot of log k versus log[CIT]. The dependence is distinct but small, described by the expression:

$$k_{\text{MnCIT}}^* = k_{\text{MnCIT}} \cdot [\text{CIT}]^{-0.13} \quad [4.48]$$

Where k_{MnCIT} is on the order of $1 \times 10^{-4} \text{ M}^{0.13} \cdot \text{s}^{-1}$. Although it could be argued that the dependence on citrate is negligible that would not make sense mechanistically. If the rate limiting step is the transfer of an electron within the Mn(III)CIT complex, then the dependence on citrate would be expected to be first order as shown in equation 4.44. The most likely explanation for the slight negative dependence is that although only the first two points were taken the reoxidation step was most likely still obscuring the results. The reoxidation should have an inverse first order dependence on the citrate concentration. Therefore the two effects together would sum to a dependence that appeared close to zero.

Both the Mn(III) citrate complex reduction and reoxidation are affected by the ligand:Mn ratio. The complex is more stable at higher citrate concentrations with little complex loss at a citrate:Mn ratio of 50:1. The complex also is reoxidized faster with higher citrate concentration. The experiments with less than a 50:1 excess of citrate all produced solids that interfered with spectrophotometric measurements. No data are included in Figure 4.15 for periods after precipitation of solids was noticed. The onset of precipitation was quicker in solutions with lower citrate concentrations. The nature of the solids formed also varied. At a 2:1 excess of citrate the solids formed contained very little oxidized Mn and appeared to be MnCO_3 . The solids in solutions with a 5:1 or 10:1 excess were brownish in color and turned leuco crystal violet dye purple, revealing the presence of oxidized manganese. This indicates that in very low excess of citrate the Mn(III) is reduced to Mn(II) at the expense of a citrate but the remaining citrate is not enough to allow reoxidation so the Mn(II) precipitates as either MnCO_3 or Mn(OH)_2 . At higher excesses, but still lower than a 50:1 excess, Mn(III) is reduced and begins to reoxidize. At some point, however, the remaining citrate is not sufficient to stabilize the Mn(III), which either disproportionates, continues oxidation to a Mn(IV)oxide, or precipitates out as Mn(III) solids. Above a 50:1 excess of citrate

the complex appears to be reoxidized completely and remain over a period of a few months.

The overall results of the citrate complex system indicate a cycle, the reactions of which are shown in mechanism 4.3. The Mn(III)citrate undergoes an electron transfer which reduces the Mn(III) to Mn(II). The electron transfer is most likely internal as there is no evidence of added stability at lower citrate concentrations as would be expected for an external electron transfer. The Mn(II) can then be complexed by excess citrate and in the presence of sufficient oxygen can be reoxidized to the Mn(III) complex. The overall result should lead to a catalytic destruction of citrate.

4.4.0 Conclusions

This study has shown that Mn(III) can be stabilized kinetically for periods of days to months in neutral to alkaline pH. The two factors which affect the inertness of these complexes are the complexing strength of the ligand, and the ability of the ligand to participate in redox reactions. Differences in pH and ligand concentrations can speed up or slow down loss of the Mn(III) complex.

4.4.1 Pyrophosphate

The Mn(III)pyrophosphate complex is the most kinetically inert of the complexes studied. Its inertness is caused by a lack of redox pathways. The complex is favored by pH around 7.3 and a ligand:Mn ratio of 50:1. The complex may be either MnHP_2O_7 as proposed by Ciavatta et al. or $\text{Mn}(\text{P}_2\text{O}_7)_2^{5-}$ as proposed by Gordienko et al.. The data do not allow a distinction between the two. The complex is kinetically inert with regard to disproportionation and is lost very slowly over a

period of several months. The complex most likely decomposes because of loss of pyrophosphate due to hydrolysis.

4.4.2 EDTA

Mn(III)EDTA complexes, although they have the largest formation equilibrium constants, are the shortest lived in aqueous systems. The complexes appear to be unable to undergo internal electron transfer but readily accept electrons from external donors. The oxidation of free EDTA by the Mn(III) complex is very rapid in solution. The rate law for the reduction of the Mn(III)EDTA⁻ complex at pH > 6 is given by:

$$\frac{d[\text{Mn(III)EDTA}]}{dt} = -k_{\text{int}} \cdot [\text{H}^+]^{0.29} \cdot [\text{EDTA}^{4-}]^{1.35} \cdot [\text{Mn(III)EDTA}] \quad [4.37]$$

4.4.3 Citrate

Mn(III)citrate complexes are intermediate between the other two complexes in terms of equilibrium constants and rates of loss. They exhibit a complex behavior, however, that distinguishes them from the other Mn(III) complexes studied. Mn(III) citrate complexes appear able to undergo internal electron transfer resulting in the one electron oxidation of citrate. Unlike the other two ligands, citrate is able to promote reoxidation of Mn(II) back to Mn(III). The reduction coupled with the reoxidation leads to a cycle that gives catalytic destruction of citrate.

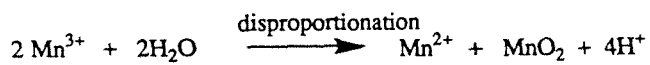
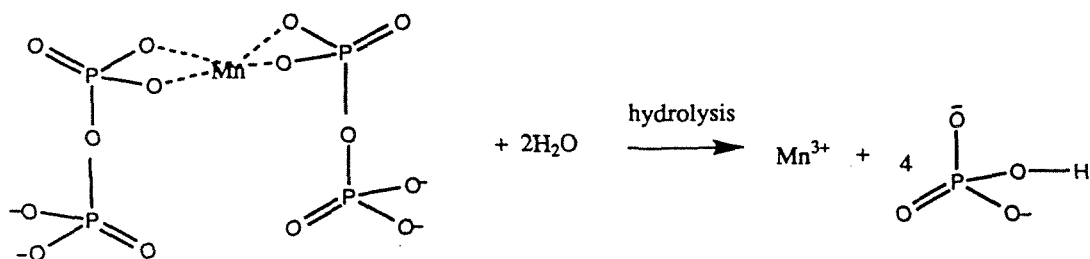
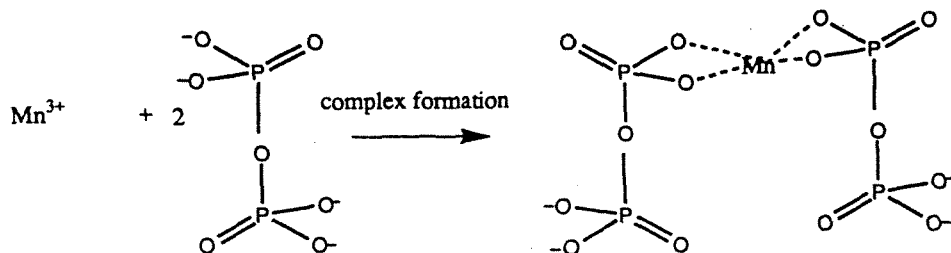
References

- (1) *CRC Handbook of Chemistry and Physics*; 71 ed.; Lide, D. R., Ed.; CRC Press: Boca Raton, 1974.
- (2) Hupfer, M.; Gachter, R.; Ruegger, H. *Limnology and Oceanography* **1995**, *40*, 610 - 617.
- (3) Powell, R. T.; Oskin, T.; Ganapathisubramanian, N. *Journal of Physical Chemistry* **1989**, *93*, 2718 - 2721.

- (4) Cabelli, D. E.; Bielski, B. H. J. *Journal of Physical Chemistry* **1984**, *88*, 3111 - 3115.
- (5) Bhat, I. K.; Sherigara, B. S.; Pinto, I. *Transition Metal Chemistry* **1993**, *16*, 163 - 166.
- (6) Kenten, R. H.; Mann, P. J. G. *Biochemical Journal* **1952**, *50*, 360 - 369.
- (7) Kenten, R. H.; Mann, P. J. G. *Biochemical Journal* **1955**, *61*, 279 - 286.
- (8) Archibald, F. S.; Fridovich, I. *Archives of Biochemistry and Biophysics* **1982**, *214*, 452 - 463.
- (9) Aitken, M. D.; Irvine, R. L. *Archives of Biochemistry and Biophysics* **1990**, *276*, 405 - 414.
- (10) Davies, G. *Coordination Chemistry Reviews* **1969**, *4*, 199 - 224.
- (11) Ciavatta, L.; Palombari, R. *Gazzeta Chimica Italiana* **1983**, *113*, 557 - 562.
- (12) Gordienko, V. I.; Sidorenko, V. I.; Mikhailyuk, Y. I. *Russian Journal of Inorganic Chemistry* **1970**, *15*, 1241.
- (13) Kostka, J. E.; Luther, G. W.; Neelson, K. H. *Geochimica et Cosmochimica Acta* **1995**, *59*, 885 - 894.
- (14) Duke, F. R. *Journal of the American Chemical Society* **1947**, *69*, 2885 - 2888.
- (15) Carrell, H. L.; Glusker, J. P. *Acta Crystallographica* **1973**, *B29*, 638 - 640.
- (16) Glusker, J. P.; Carrell, H. L. *Journal of Molecular Structure* **1973**, *15*, 151 - 160.
- (17) Guindy, N. M.; Basily, E. K.; Milad, N. E. *Journal of Applied Chemistry and Biotechnology* **1974**, *24*, 407 - 413.
- (18) Guindy, N. M.; Daoud, J. A.; Milad, N. E. *Egyptian Journal of Chemistry* **1977**, *20*, 131 - 139.
- (19) Milad, N. E.; Guindy, N. M.; Helmy, F. M. *Egyptian Journal of Chemistry* **1971**, *14*, 571 - 580.

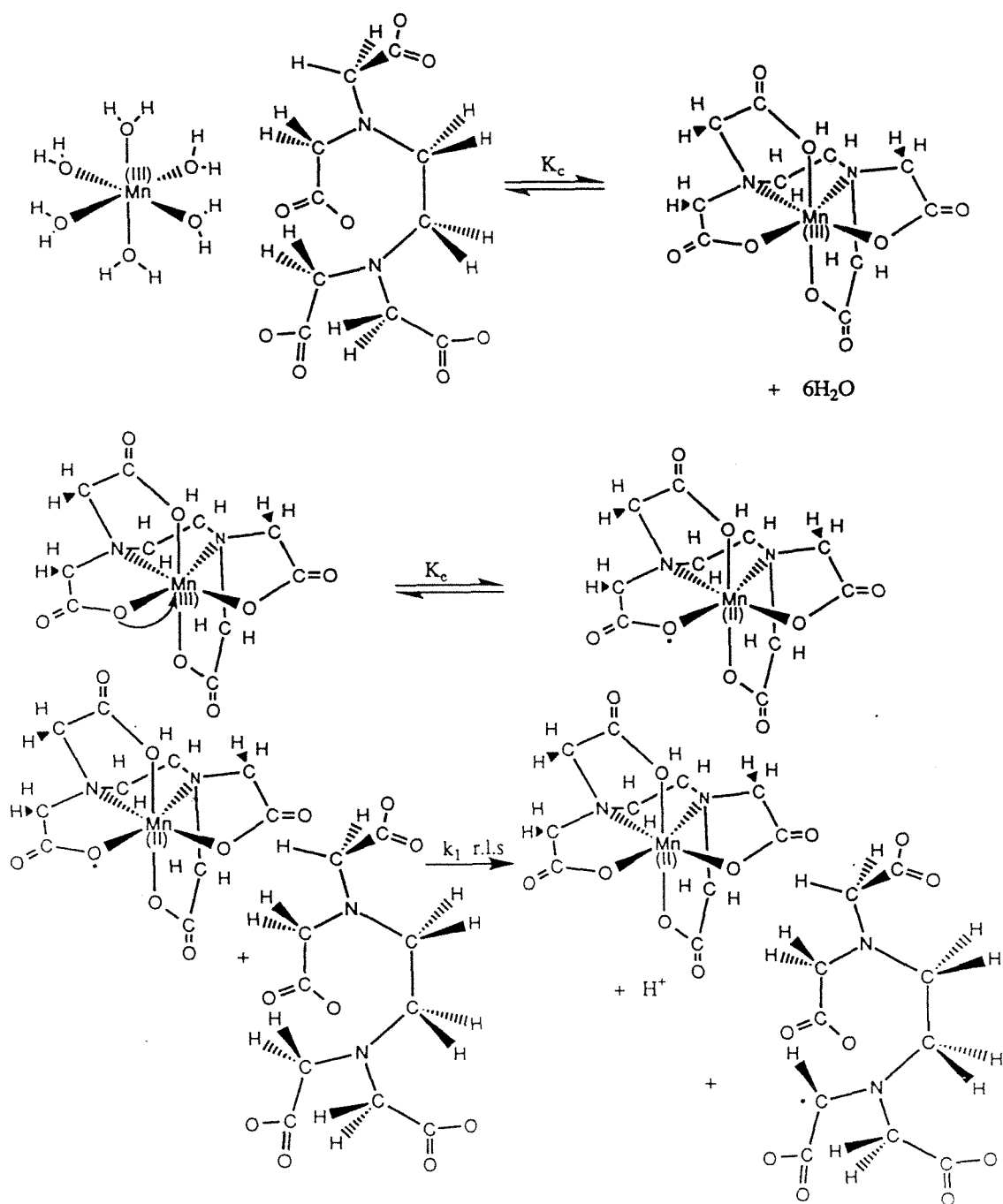
- (20) Barek, J.; Berka, A.; Civivosa, D. *Collection of Czechoslovakian Chemical Communications* **1984**, *49*, 954 - 962.
- (21) Loll, M. J.; Bollag, J. M. *Soil Biology and Biochemistry* **1985**, *17*, 115 - 117.
- (22) Yoshino, Y.; Ouchi, A.; Tsunada, Y.; Kujima, M. *Canadian Journal of Chemistry* **1962**, *40*, 775 - 783.
- (23) Macartney, D. H.; Thompson, D. W. *Inorganic Chemistry* **28**, 2195 - 2199.
- (24) Bose, R. H.; Keane, C.; Xidis, A.; Reed, D. W.; Li, R.; Tu, H.; Hanket, P. L. *Inorganic Chemistry* **1991**, *30*, 2638 - 2642.
- (25) Gangopadhyay, S.; Ali, M.; Scha, S. K.; Banerjee, P. *Journal of the Chemical Society : Dalton Transactions* **1991**, 2729 - 2734.
- (26) Clesceri, N. L.; Lee, G. F. *International Journal of Air and Water Pollution* **1965**, *9*, 743 - 751.
- (27) Jardine, P. M.; Jacobs, G. K.; O'Dell, J. D. *Soil Science Society of America Journal* **1993**, *57*, 954-962.
- (28) Ayoko, G. A.; Iyon, J. F.; Mamman, S. *Transition Metal Chemistry* **1994**, *19*, 151 - 153.

Mechanism 4.1: Mn(III)-Pyrophosphate

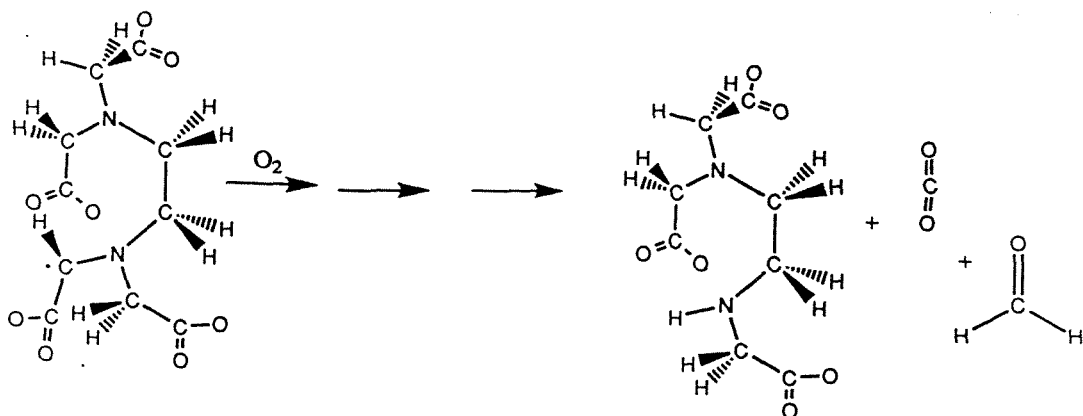


Mechanism 4.2

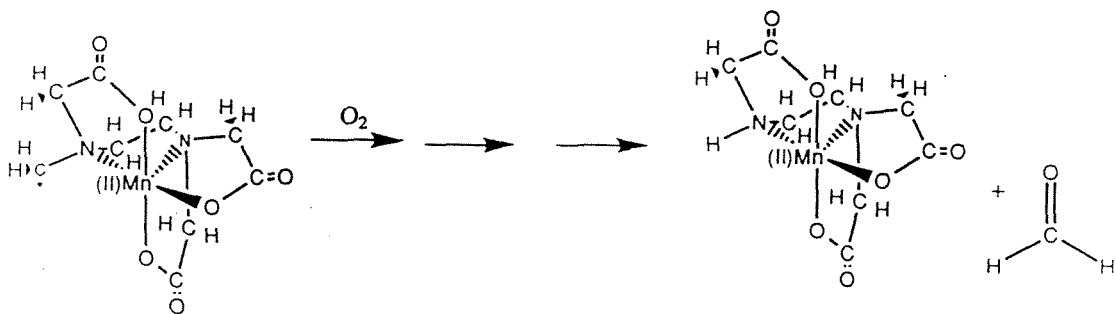
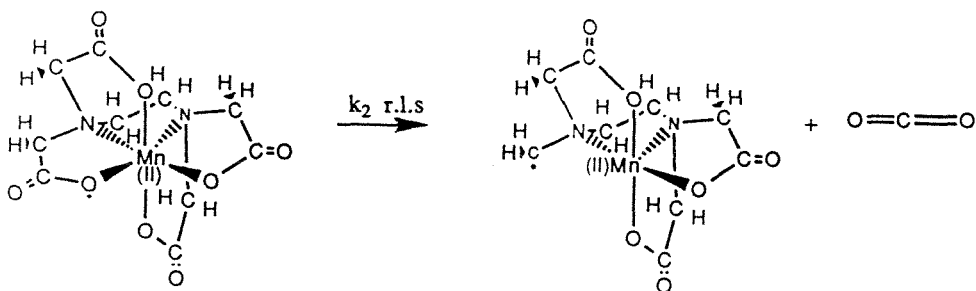
Mn(III)EDTA Proposed Reaction Mechanism



Mechanism 4.2 (continued)



If no excess EDTA



Mechanism 4.3

Proposed Mn(III) citrate reaction scheme

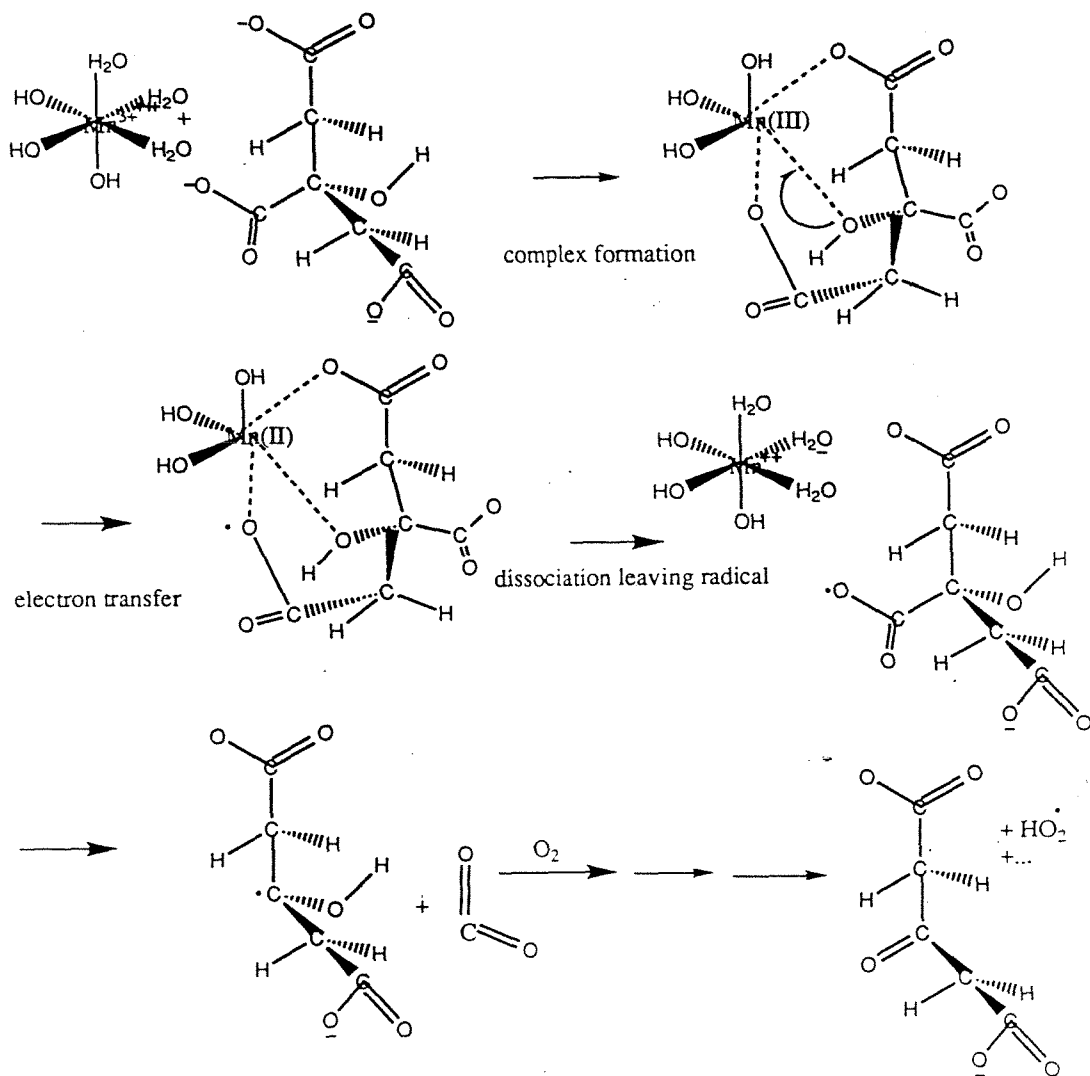


Table 4.1
Some Properties of Ligands Used in This Study

	Pyrophosphate	Citrate	EDTA
ϵ ($M^{-1}cm^{-1}$) ^a	96	210	257
λ_{max}	484	430	480
log K	4.8 ^b	14? ^c	24.75 ^d
log k_{ox} (min^{-1})	-7.22 ^e	-3.51 ^f	-8.0 ^e
E° (V)	1.01 ^g	?	0.82 ^h

^a ϵ is the molar absorptivity of the complex, λ_{max} is the wavelength of maximum absorbance, log K is the equilibrium constant of the ligand with Mn(III), log k_{ox} is the rate constant for the autoxidation of Mn(II) in the presence of the ligand, and E° is the standard reduction potential of Mn(III)/Mn(II) in the presence of the ligand.

^b for the compound $MnH_2P_2O_7$

^c estimated from analogy to Fe citrate complexes

^d for the compound $MnEDTA^-$ G. Davies (1969)

^e H. Bilinski and J. J. Morgan (1969)

^f N.E. Milad, N.M. Guindy, and F.M. Helmy (1971)

^g pH = 7.1

^h pH = 5.5

Table 4.2
 First Order Fit Parameters for Mn(III)P₂O₇ Disappearance
 [P₂O₇] = 25mM

pH	k(s ⁻¹)	C ₀ /C _T	r ²
6.94	1.9 ± 0.2 x 10 ⁻⁷	0.727 ± 0.007	.98
7.3	1.53 ± 0.08 x 10 ⁻⁸	0.984 ± 0.002	.92
8.04	1.2 ± 0.3 x 10 ⁻⁷	0.68 ± 0.01	.85
8.98	2.9 ± 0.2 x 10 ⁻⁸	0.634 ± 0.002	.93

Table 4.3
 First Order Fit Parameters for Mn(III)P₂O₇ Disappearance
 pH = 7.8

[L] (mM)	k(s ⁻¹)	C ₀ /C _T	r ²
5	3.1 ± 0.6 x 10 ⁻⁵	1.21 ± 0.01	.66
12.5	2.81 ± 0.08 x 10 ⁻⁷	1.293 ± 0.008	.99
25	3.6 ± 0.3 x 10 ⁻⁸	1.025 ± 0.006	.87
50	3.9 ± 0.3 x 10 ⁻⁷	1.31 ± 0.03	.95
100	1.4 ± 0.2 x 10 ⁻⁷	0.94 ± 0.02	.85

Table 4.4
Reaction First Order Fit Parameters for Mn(III)EDTA Disappearance
[EDTA] = 25mM

pH	$k(s^{-1})$	$C(0)/C_t$	r^2
3.6	$1.7 \pm 0.5 \times 10^{-4}$	$.62 \pm .04$.92
4.1	$9.0 \pm 1 \times 10^{-4}$	$1.12 \pm .06$.99
5.2	$3.4 \pm 0.1 \times 10^{-3}$	$1.24 \pm .03$.999
6.0	$3.8 \pm 0.2 \times 10^{-3}$	$0.39 \pm .01$.999
6.5	$3.7 \pm 0.3 \times 10^{-3}$	$0.59 \pm .03$.996
6.9	$2.1 \pm 0.1 \times 10^{-3}$	$0.62 \pm .01$.998
7.3	$1.4 \pm 0.05 \times 10^{-3}$	$0.57 \pm .01$.998
7.7	$1.08 \pm 0.02 \times 10^{-3}$	$0.648 \pm .005$.999
9.5	$3.8 \pm 0.07 \times 10^{-4}$	$0.689 \pm .004$.999

Table 4.5
Reaction First Order Fit Parameters for Mn(III)EDTA disappearance
pH 6.8

[EDTA] (mM)	$k(s^{-1})$	$C(0)/C_t$	r^2
25	$1.160 \pm 0.005 \times 10^{-3}$	$0.563 \pm .002$.9999
5	$1.7 \pm 0.1 \times 10^{-4}$	$0.607 \pm .007$.997
2.5	$8.0 \pm 0.8 \times 10^{-5}$	$0.625 \pm .007$.970
0.5	$5.7 \pm 0.5 \times 10^{-6}$	$0.78 \pm .02$.977

Table 4.6
 First Order Fit Parameters for Mn(III)CIT Disappearance
 [CIT] = 0.2M

pH	k (s ⁻¹)	C(0)/Ct	r ²
6.1	1.6 ± 0.2 x 10 ⁻⁵	1.00 ± .05	.99
6.8	6.4 ± 0.8 x 10 ⁻⁶	0.96 ± .07	.97
8.5	3.6 ± 1. x 10 ⁻⁶	1.03 ± .08	.97
9.2	1.86 x 10 ⁻⁶	1.0	-
9.8	1.92 x 10 ⁻⁶	1.0	-

Table 4.7
 First Order Fit Parameters for Mn(III)CIT Disappearance
 pH₀ = 6.0

[CIT] (mM)	k (s ⁻¹)	C(0)/Ct	r ²
25	7.78 x 10 ⁻⁶	.85	-
5	9.72 x 10 ⁻⁶	.46	-
2.5	9.17 x 10 ⁻⁶	.4	-
1	1.25 x 10 ⁻⁵	.56	-

Figure 4.1a

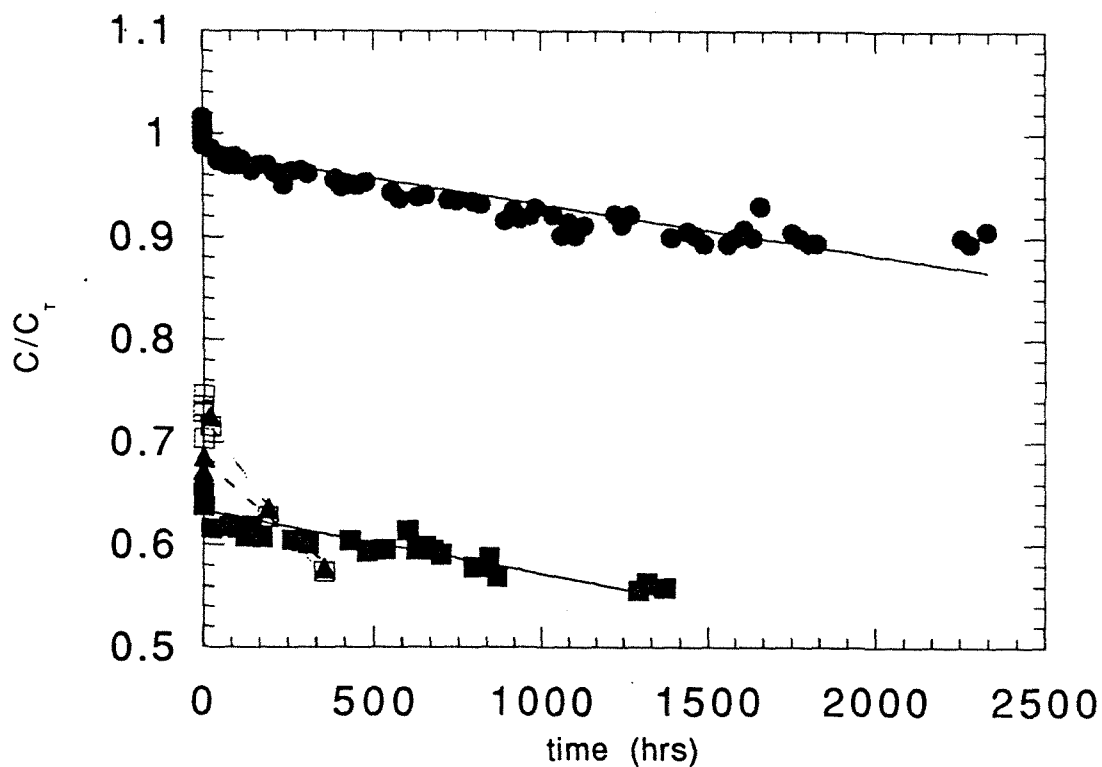


Figure 4.1 Disappearance of $\text{Mn(III)P}_2\text{O}_7$ complex - dependence on pH. Plot of calculated concentration of $\text{Mn(III)P}_2\text{O}_7$ divided by total Mn (C/C_T) versus time. Three different pHs are shown: \square - 6.94, \bullet - 7.33, \blacktriangle - 8.04, and \blacksquare - 8.98. Points above 1.0 are due to either unreacted MnO_4^- or to solids formation. Excess ligand acted as the pH buffer. Total Mn was 0.5mM and total P_2O_7 was 25mM. The lines are first order fits. Part b shows a blow up of the lower left corner of part a.

Figure 4.1b

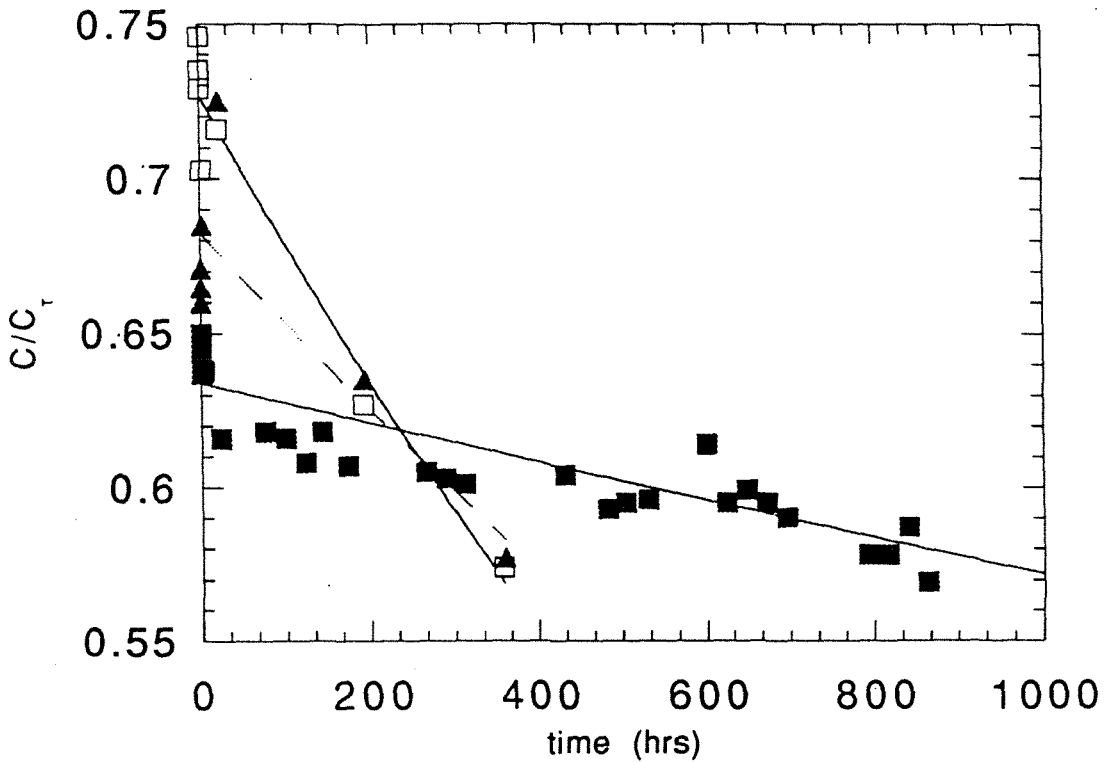


Figure 4.1 Disappearance of $Mn(III)P_2O_7$ complex - dependence on pH. Plot of calculated concentration of $Mn(III)P_2O_7$ divided by total Mn (C/C_T) versus time. Three different pHs are shown: \square - 6.94, \bullet - 7.33, \blacktriangle - 8.04, and \blacksquare - 8.98. Points above 1.0 are due to either unreacted MnO_4^- or to solids formation. Excess ligand acted as the pH buffer. Total Mn was 0.5mM and total P_2O_7 was 25mM. The lines are first order fits. Part b shows a blow up of the lower left corner of part a.

Figure 4.2

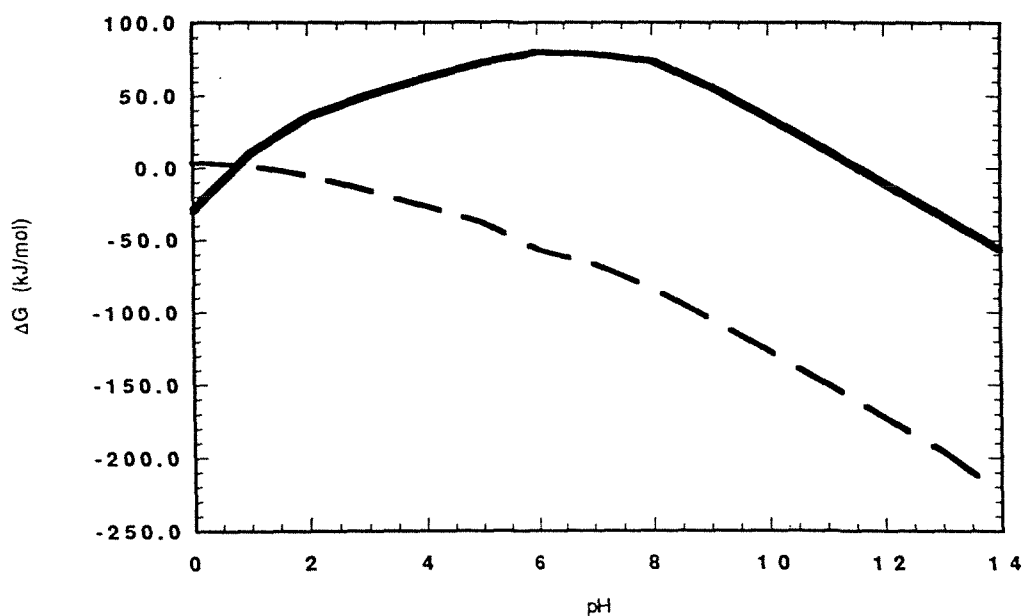


Figure 4.2 ΔG of disproportionation of Mn(III) P_2O_7 complexes. Plot of ΔG of disproportionation of Mn(III) P_2O_7 versus pH. The solid line is for the complex $Mn(P_2O_7)_2^{5-}$ and the dotted line is for the complex $MnP_2O_7^-$. A Mn: P_2O_7 ratio of 1:50 was assumed. A ratio of Mn(III):Mn(II) = 10 was assumed. Solution conditions are $T = 25^\circ C$ and $I = 0.3M$. The equilibrium constants of Gordienko et. al. (12) were used.

Figure 4.3

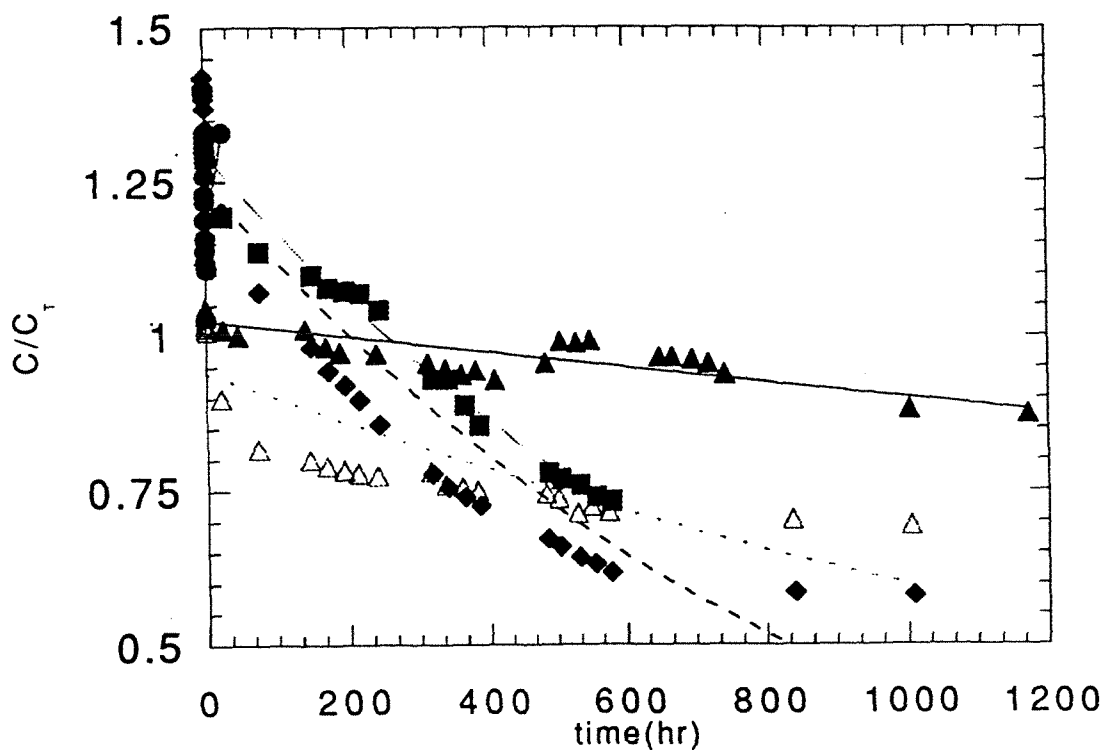


Figure 4.3 Disappearance of $\text{Mn(III)P}_2\text{O}_7$ complex - dependence on ligand. Plot of calculated concentration of $\text{Mn(III)P}_2\text{O}_7$ divided by total Mn (C/C_T) versus time. Five different ligand concentrations are shown: ● - 5mM, ■ - 12.5mM, ▲ - 25mM, ◆ - 50mM, and Δ - 100mM. Points above 1.0 are due to either unreacted MnO_4^- or solids formation. Excess ligand acted as pH buffer. Total Mn was 0.5mM and the pH was 7.8. The lines shown are first order fits.

Figure 4.4

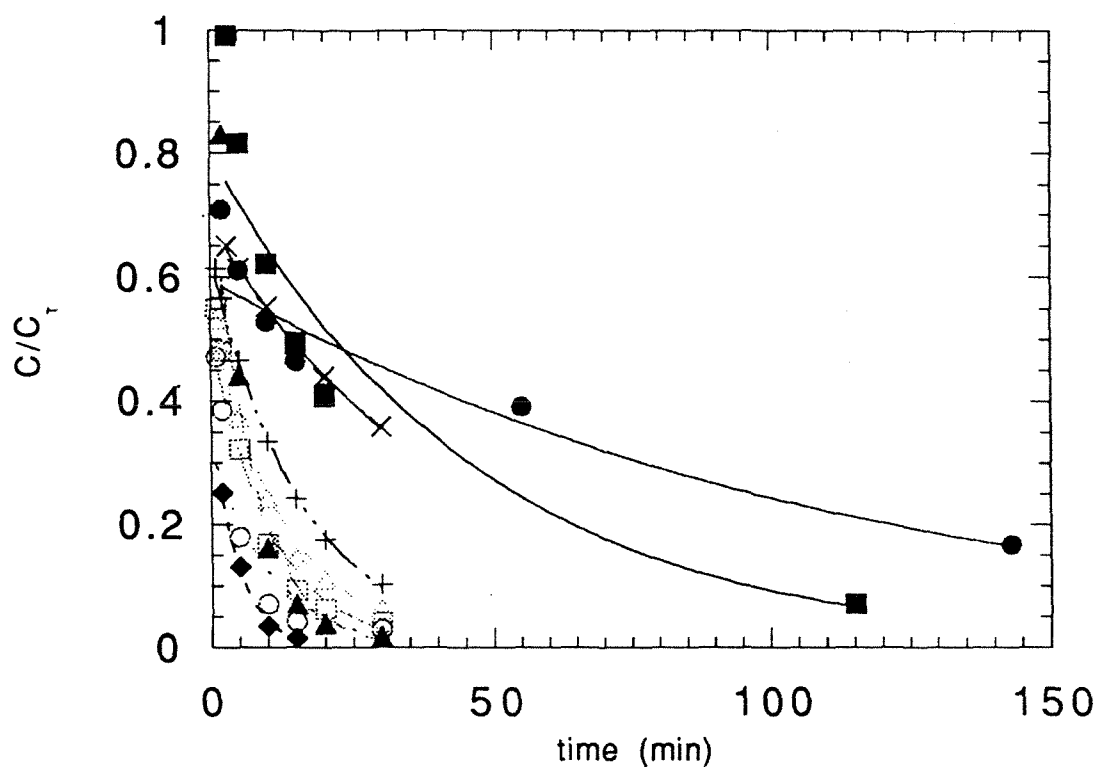


Figure 4.4 Disappearance of Mn(III)EDTA complex - dependence on pH. Plot of calculated concentration of Mn(III)EDTA divided by total Mn (C/C_T) versus time. Nine pHs are shown: ● - 3.6, ■ - 4.1, ▲ - 5.2, ◆ - 6.0, ○ - 6.5, □ - 6.9, △ - 7.3, + - 7.7, x - 9.5. Excess EDTA was used as a pH buffer. Total Mn was 0.5mM and total EDTA was 25mM. Lines shown are first order fits.

Figure 4.5

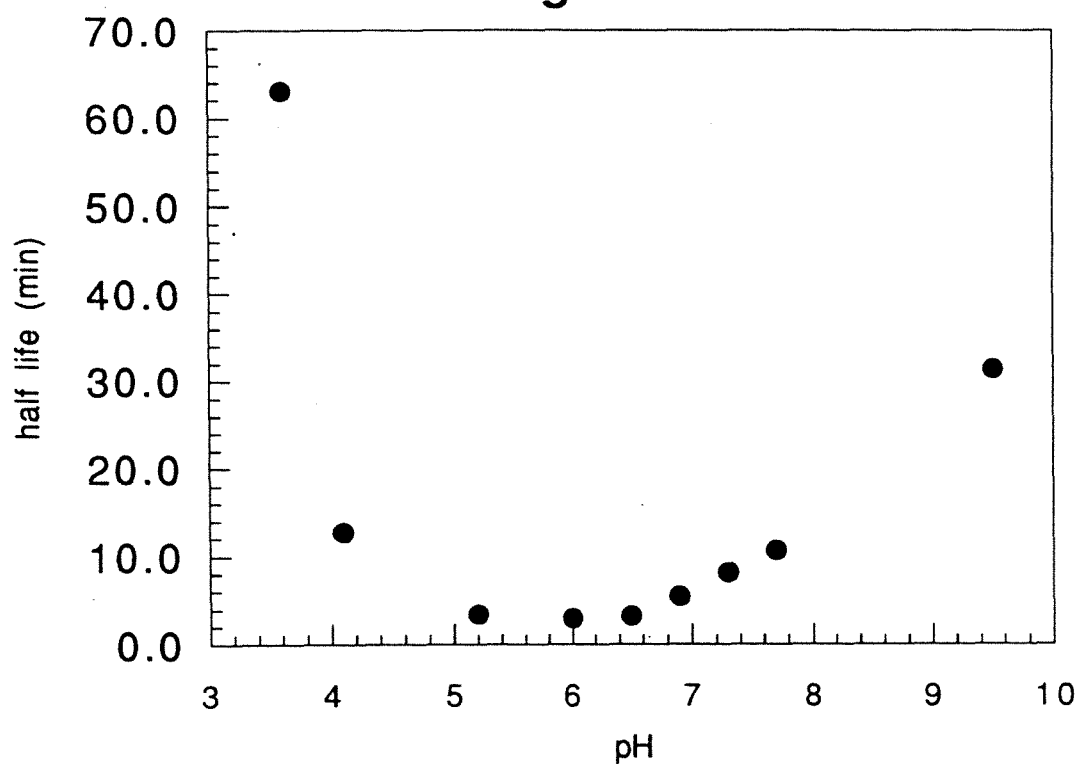


Figure 4.5 Half life for Mn(III)EDTA complex disappearance. Plot of half life of the Mn(III)EDTA complex versus pH. Half lives were taken from figure 4.4. The plot shows two distinct species with a transition near pH 5. Conditions were total Mn = 0.5mM and total EDTA = 25mM.

Figure 4.6

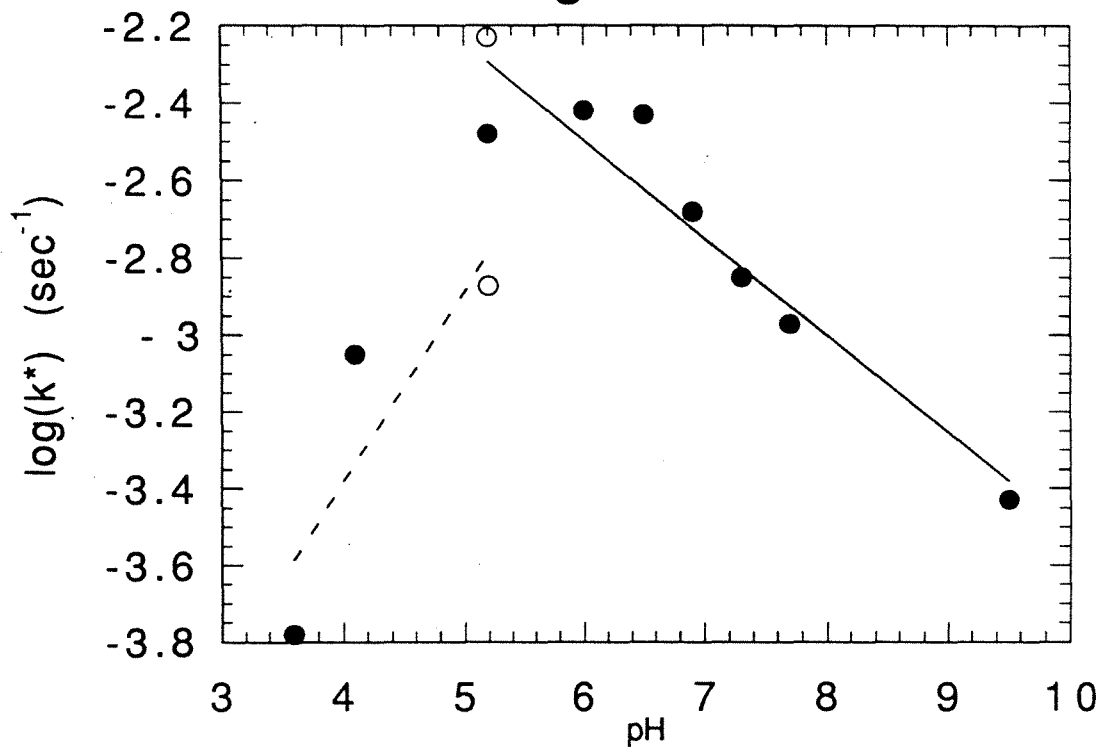


Figure 4.6 Rate constants for Mn(III)EDTA complex disappearance. Plot of $\log(k)$ for the loss of Mn(III)EDTA versus pH. $\log(k)$ s were obtained from first order fits of figure 4.4. Conditions are the same as for figure 4.4. Two linear fits are shown one for the MnHEDTA complex and one for the MnEDTA complex.

Figure 4.7a

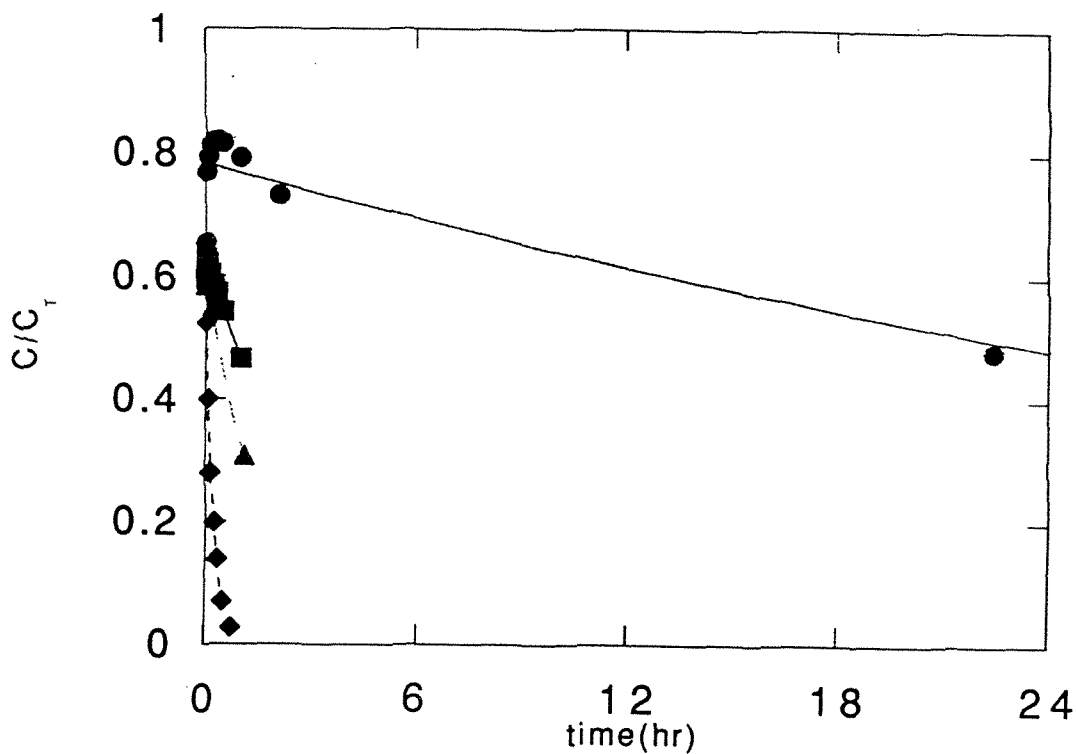


Figure 4.7 Disappearance of Mn(III)EDTA complex - dependence on ligand. Plot of calculated concentration of Mn(III)EDTA divided by total Mn (C/C_T) versus time. Four different ligand concentrations are shown: ● - 0.5mM, ■ - 2.5mM, ▲ - 5mM, and ◆ - 25mM. TES was used as a pH buffer. Total Mn was 0.5mM and the pH was 6.8. First order fits are shown. Part b shows in more detail the first hour of reaction.

Figure 4.7b

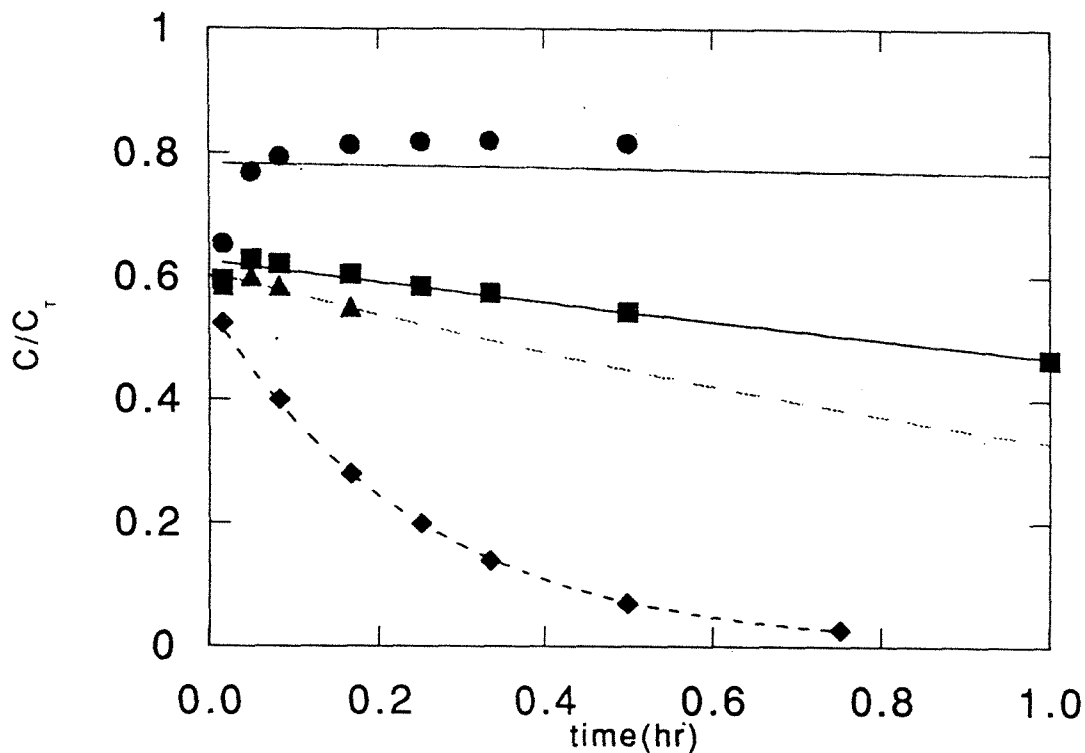


Figure 4.7 Disappearance of Mn(III)EDTA complex - dependence on ligand. Plot of calculated concentration of Mn(III)EDTA divided by total Mn (C/C_T) versus time. Four different ligand concentrations are shown: ● - 0.5mM, ■ - 2.5mM, ▲ - 5mM, and ◆ - 25mM. TES was used as a pH buffer. Total Mn was 0.5mM and the pH was 6.8. First order fits are shown. Part b shows in more detail the first hour of reaction.

Figure 4.8

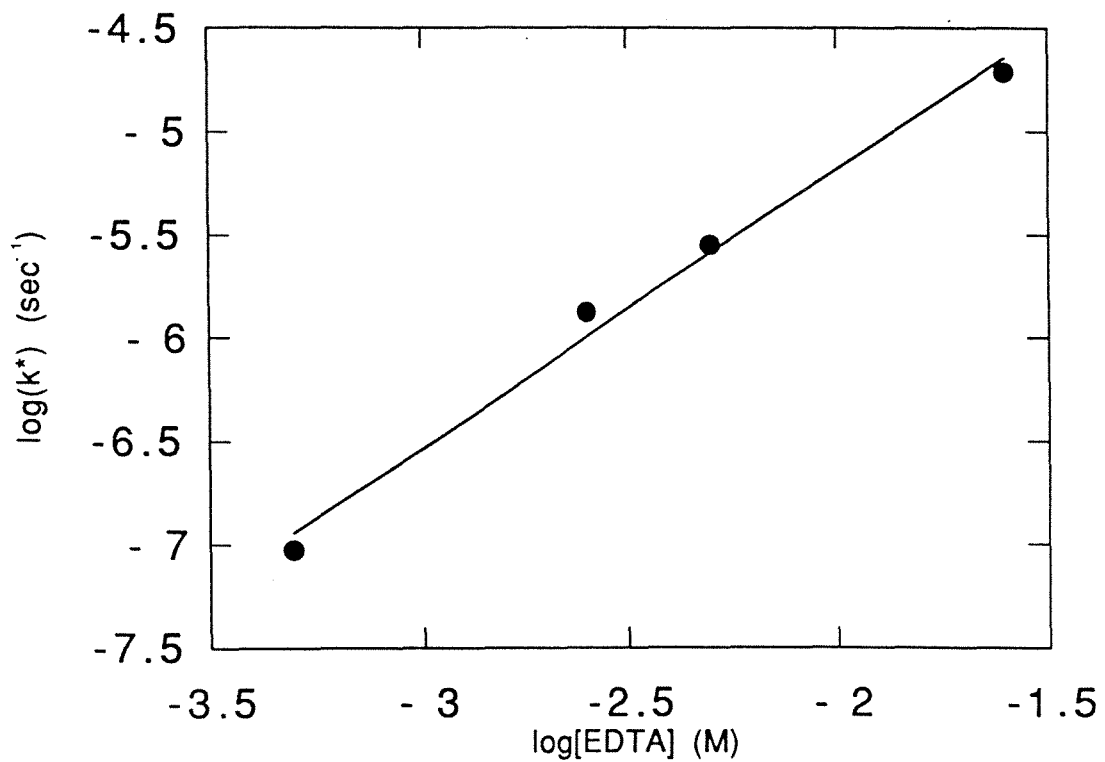


Figure 4.8 Rate constants for Mn(III)EDTA complex Disappearance. Plot of $-\log(k)$ for the Mn(III)EDTA loss reaction versus $-\log[\text{EDTA}]$. $\log(k)$ s were obtained from first order fits of Figure 4.7. Conditions are the same as in that figure. A linear fit is shown.

Figure 4.9

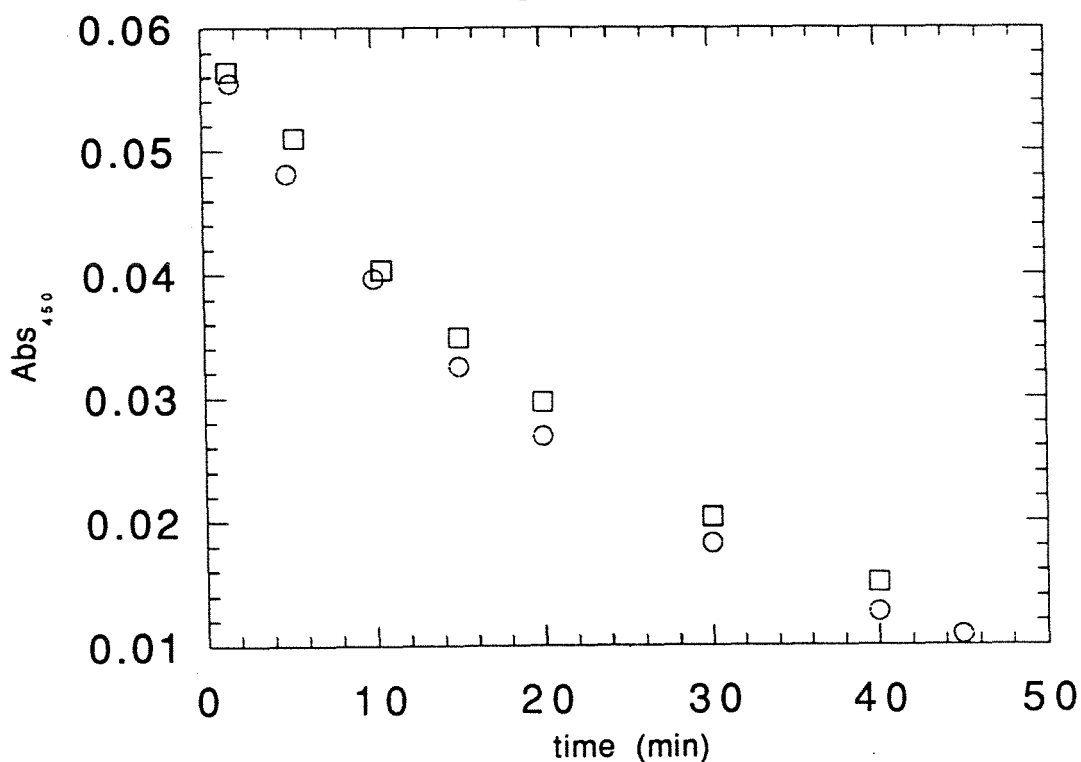


Figure 4.9 Disappearance of Mn(III)EDTA complex - dependence on light. Plot of calculated concentration of Mn(III)EDTA divided by total Mn (C/C_T) versus time. Effect of light is shown. Os were in the light and □s were in the dark. Dark sample was wrapped in tin foil and stored in a dark cupboard. Light sample was exposed to normal laboratory light. Total Mn was 0.5mM, total EDTA was 25mM, and pH was 8.8.

Figure 4.10

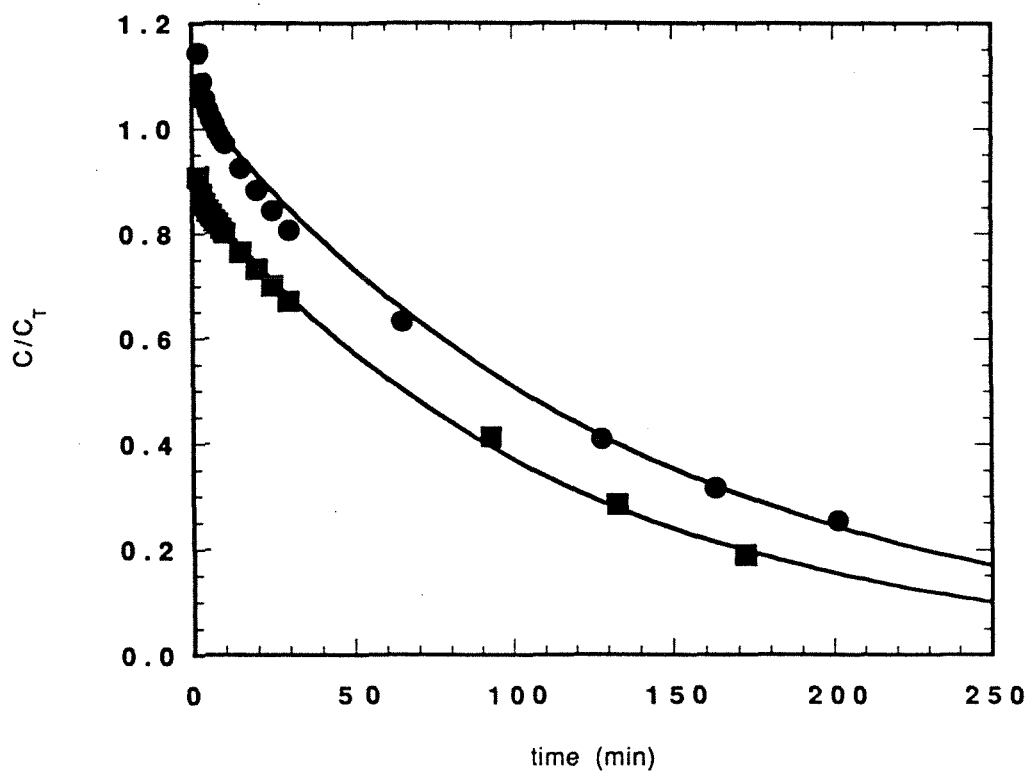


Figure 4.10 Disappearance of Mn(III)EDTA complex - dependence on I. Plot of calculated concentration of Mn(III)EDTA divided by total Mn (C/C_T) versus time. Effect of ionic strength is shown. ●s are for $I = 0.5M$ and ■s are for $I = 5M$. Ionic strength was adjusted using $NaClO_4$. Total Mn was $0.5mM$, total EDTA was $25mM$ and pH was 8.0 .

Figure 4.11a

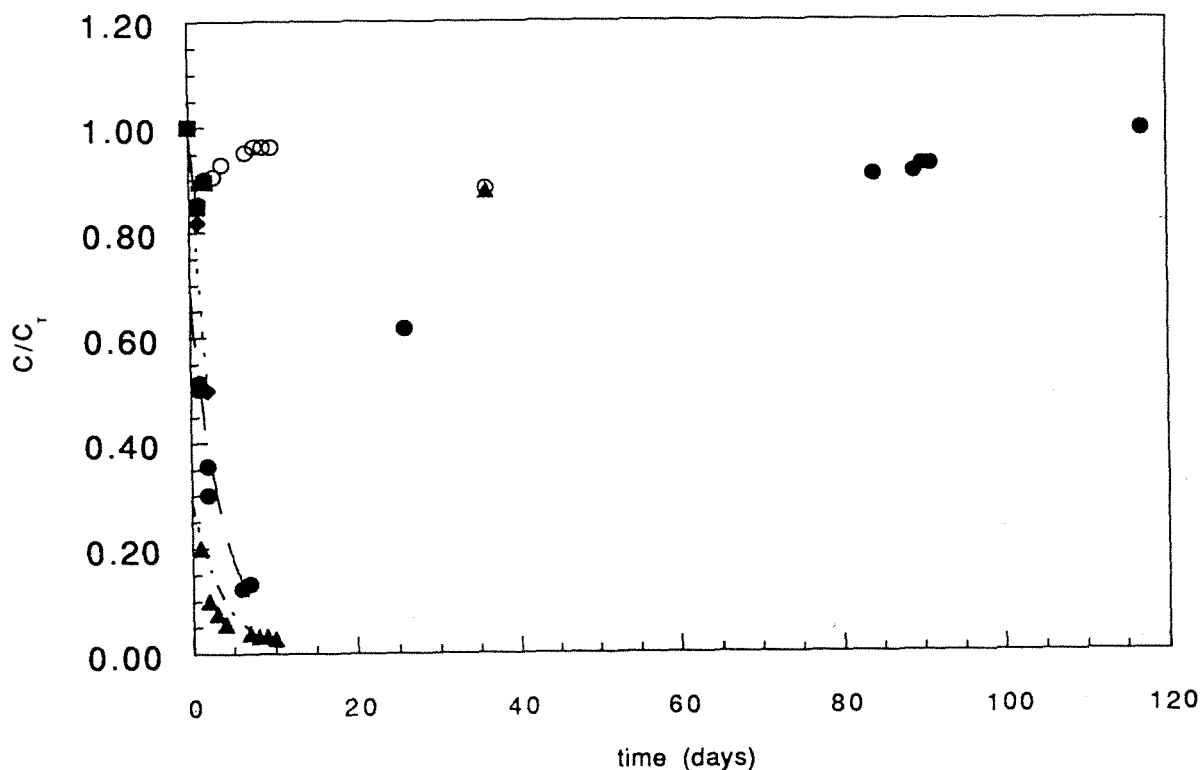


Figure 4.11 Disappearance of Mn(III)CIT complex - dependence on pH. Plot of calculated concentration of Mn(III)CIT divided by total Mn (C/C_T) versus time. Five pHs are shown: \blacktriangle - 6.1, \bullet - 6.8, \blacklozenge - 8.5, \circ - 9.2, and \blacksquare - 9.8. Total Mn was 1mM and total citrate was 200mM. All solutions were in contact with the atmosphere. Excess ligand was used as the pH buffer. First order fits were drawn using points up until increases in absorbance were noted. This ends up being a day for pHs above 8 and a week for pHs below 8. Part b shows more detail of the first week.

Figure 4.11b

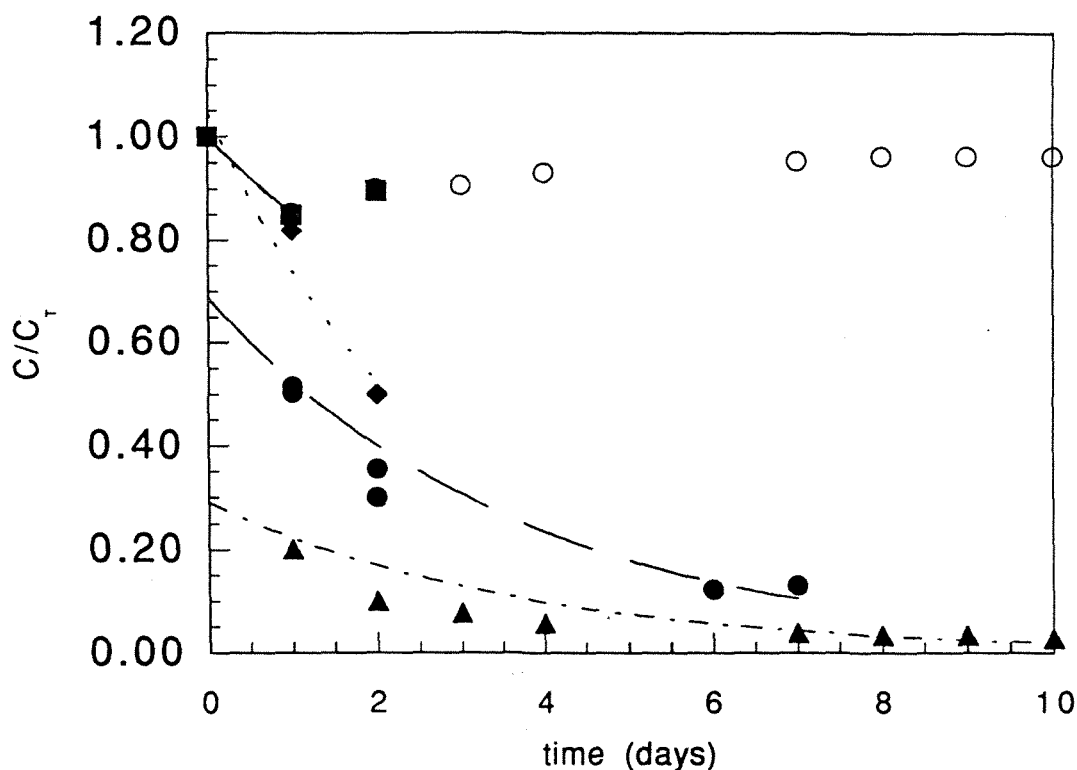


Figure 4.11 Disappearance of Mn(III)CIT complex - dependence on pH. Plot of calculated concentration of Mn(III)CIT divided by total Mn (C/C_T) versus time. Five pHs are shown: ▲ - 6.1, ● - 6.8, ◆ - 8.5, ○ - 9.2, and ■ - 9.8. Total Mn was 1mM and total citrate was 200mM. All solutions were in contact with the atmosphere. Excess ligand was used as the pH buffer. First order fits were drawn using points up until increases in absorbance were noted. This ends up being a day for pHs above 8 and a week for pHs below 8. Part b shows more detail of the first week.

Figure 4.12

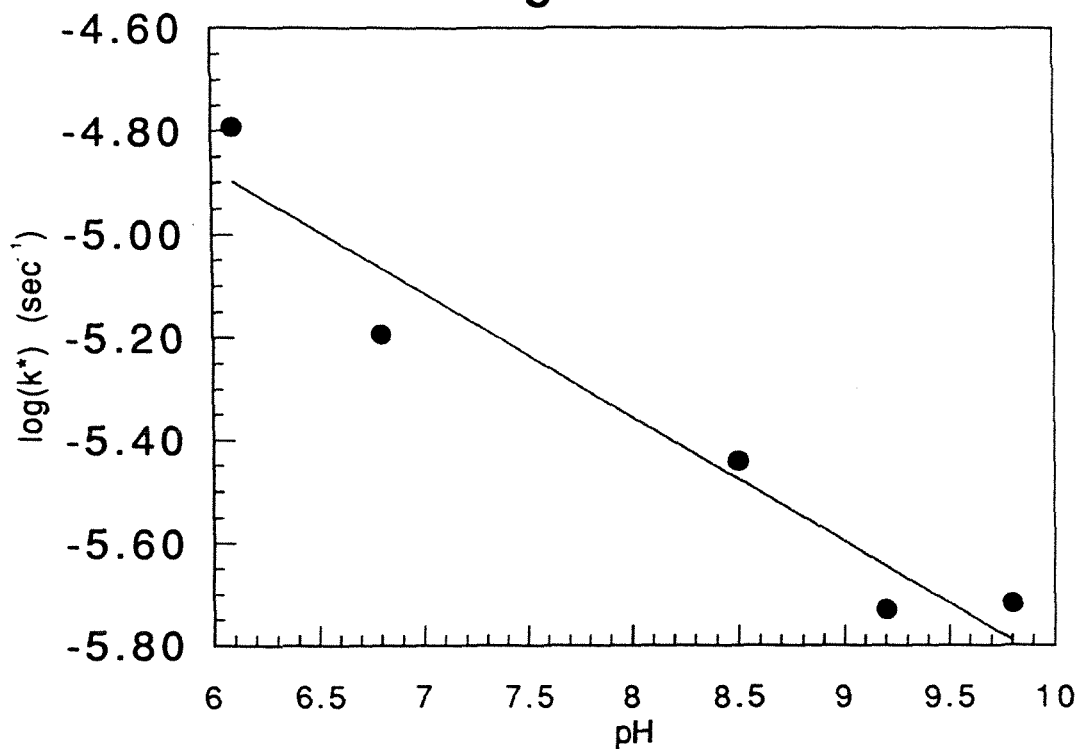


Figure 4.12 Rate constants for Disappearance of Mn(III)CIT complex. Plot of $-\log(k)$ for the loss of Mn(III)CIT versus pH. $\log(k)$ s were obtained from first order fits of the initial rate in Figure 4.11. Conditions are the same as in that figure. A linear fit is shown.

Figure 4.13a

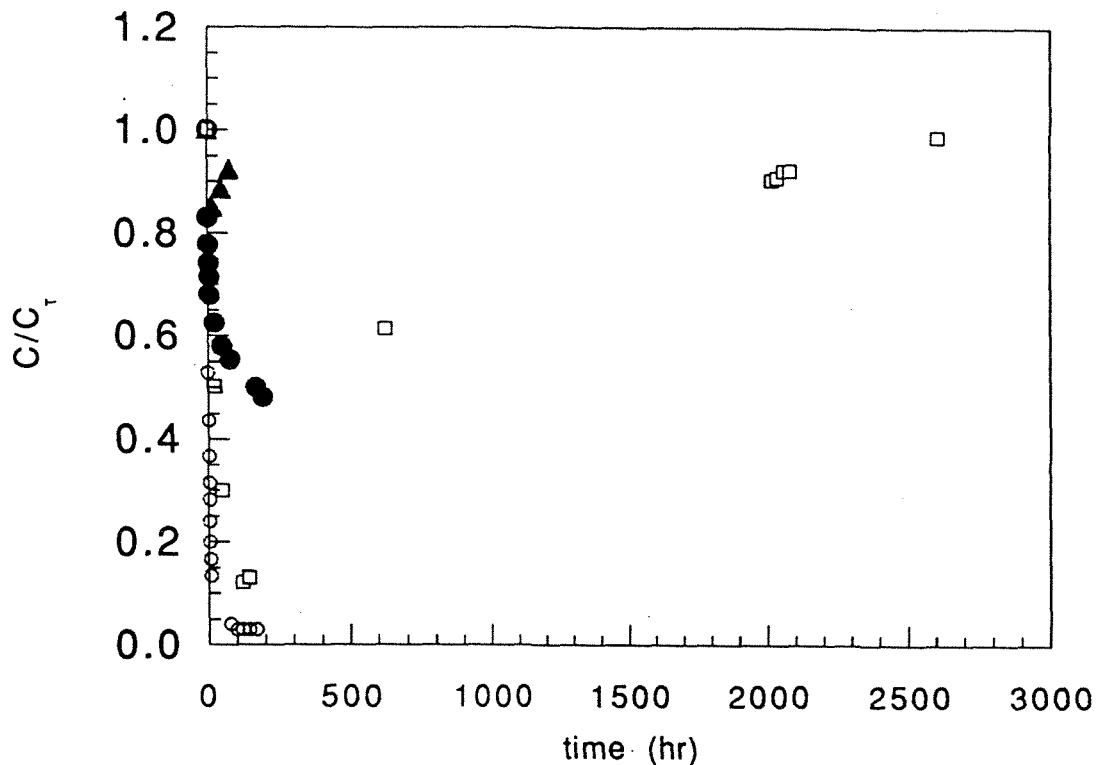


Figure 4.13 Disappearance of Mn(III)CIT complex - dependence on oxygen. Plot of calculated concentration of Mn(III)CIT divided by total Mn (C/C_T) versus time. Two sets of pHs are shown, each with an air saturated run and an oxygen depleted run. ●s represent pH 9.1 with oxygen absent. ▲s represent pH 9.2 with oxygen present. ○s represent pH 7.4 with oxygen absent. □s represent pH 6.8 with oxygen present. Total Mn is 0.5mM and total citrate is 25mM. Oxygen depleted samples were bubbled with N_2 for an hour before the run began and kept in a parafilm sealed spectrophotometric cell. Part b shows more detail of the first week of reaction.

Figure 4.13b

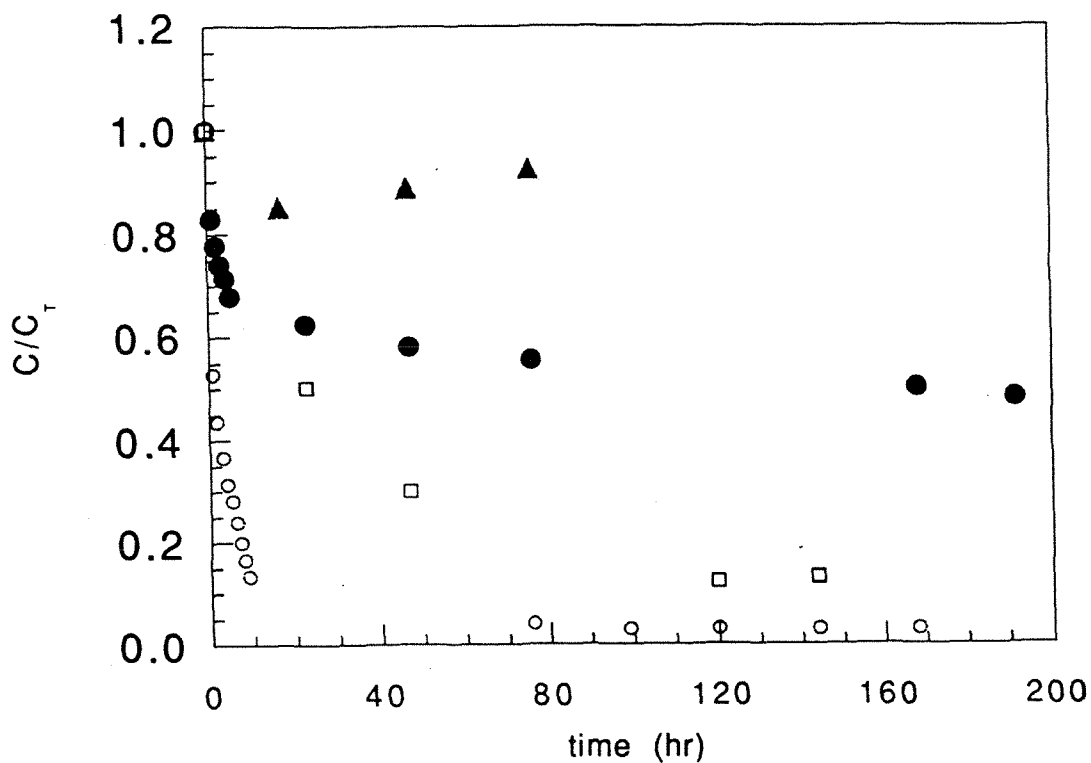


Figure 4.13 Disappearance of Mn(III)CIT complex - dependence on oxygen. Plot of calculated concentration of Mn(III)CIT divided by total Mn (C/C_T) versus time. Two sets of pHs are shown, each with an air saturated run and an oxygen depleted run. ●s represent pH 9.1 with oxygen absent. ▲s represent pH 9.2 with oxygen present. ○s represent pH 7.4 with oxygen absent. □s represent pH 6.8 with oxygen present. Total Mn is 0.5mM and total citrate is 25mM. Oxygen depleted samples were bubbled with N₂ for an hour before the run began and kept in a parafilm sealed spectrophotometric cell. Part b shows more detail of the first week of reaction.

Figure 4.14

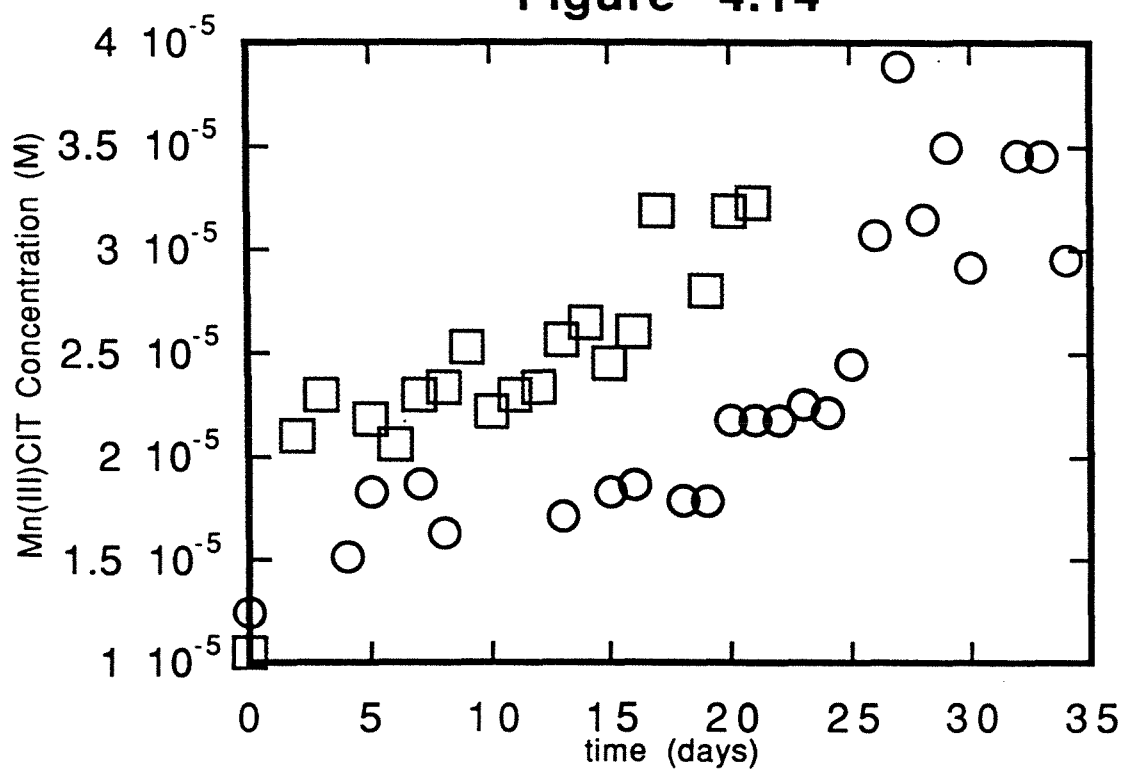


Figure 4.14 Oxidation of Mn(II) in the presence of citrate. Plot of calculated concentration of Mn(III)CIT versus times. Data show appearance of Mn(III)CIT from Mn(II) solution at two pHs: □s for pH 8 and○.s for pH 7.5. Total Mn is 0.5mM and total citrate is 25mM. The samples are exposed to laboratory air.

Figure 4.15a

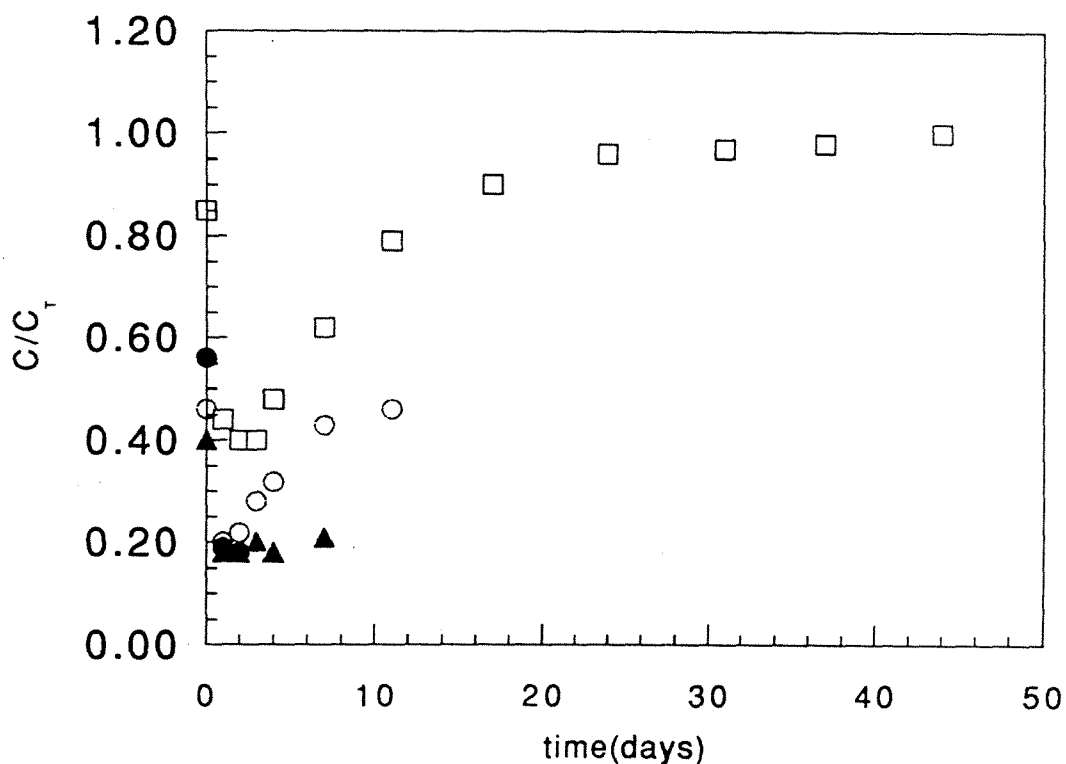


Figure 4.15 Disappearance of Mn(III)CIT complex - dependence on ligand. Plot of calculated concentration of Mn(III)CIT divided by total Mn (C/C_T) versus time. Four ligand concentrations are shown: ● - 1.0mM, ▲ - 2.5mM, ○ - 5mM, and □ - 25mM. Total Mn was 0.5mM. Bicarbonate buffers were used to control pH. Initial pH was 6.0. Degassing of CO_2 led to a steady but uniform pH rise in all 4 samples. First order fits are shown using the first two days of data. Part b shows the first 2 days in closer detail.

Figure 4.15b

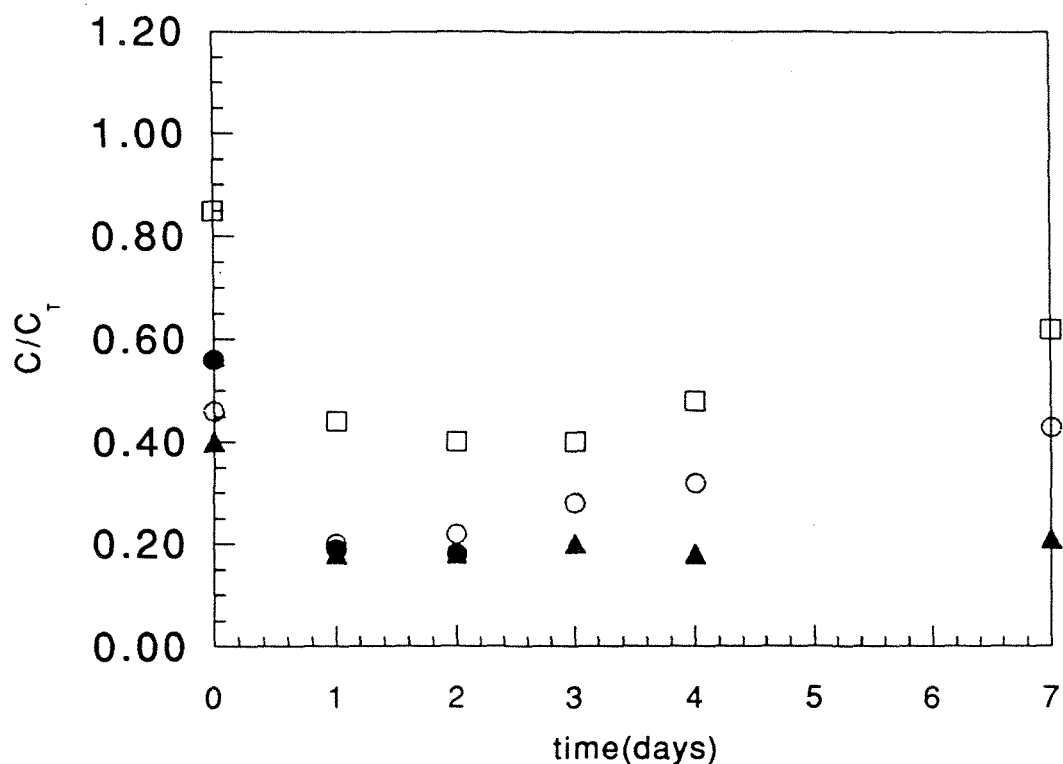


Figure 4.15 Disappearance of Mn(III)CIT complex - dependence on ligand. Plot of calculated concentration of Mn(III)CIT divided by total Mn (C/C_T) versus time. Four ligand concentrations are shown: ● - 1.0mM, ▲ - 2.5mM, ○ - 5mM, and □ - 25mM. Total Mn was 0.5mM. Bicarbonate buffers were used to control pH. Initial pH was 6.0. Degassing of CO_2 led to a steady but uniform pH rise in all 4 samples. First order fits are shown using the first two days of data. Part b shows the first 2 days in closer detail.

Figure 4.16

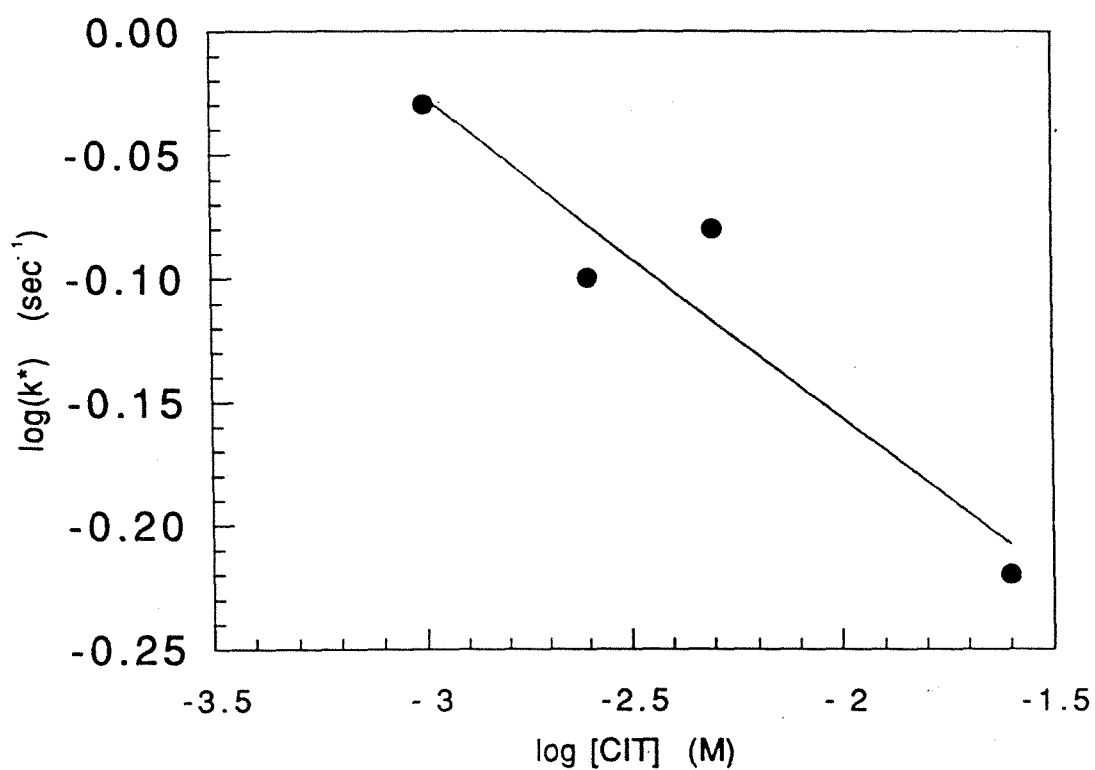


Figure 4.16 Rate constants for disappearance of Mn(III)CIT complexes. Plot of $-\log(k)$ for the Mn(III)CIT initial loss versus $-\log[CIT]$. $\log(k)$ s were obtained from first order fits of the initial rates of Figure 4.15. A linear fit is shown.

MnOOH DISSOLUTION BY LIGANDS

5.1 Introduction

Having established that Mn(III) complexes can be kinetically long lived species in pH ranges prevalent in natural waters, it is necessary to consider possible sources of Mn(III) present in such systems. In considering sources of Mn(III) complexes there are three possibilities: oxidation of Mn(II), dissolution of solid phase Mn(III), or reduction of Mn(IV) solids. All of these processes would require the presence of significant amounts of stabilizing ligands.

Oxidation of Mn(II) would have to be considered a primary source of Mn(III), as Mn(II) is the most abundant form of Mn in many natural waters. In order for the oxidation of Mn(II) to produce Mn(III) complexes, significant amounts of ligand need to be present upon oxidation of the Mn(II). This appears unlikely in open water columns and only appears likely in sediments, soils, and other areas of high biological activity. Although the presence of stabilizing ligands, such as citrate, has been found to accelerate the oxidation of Mn(II)(1), the rates are still slow and are unlikely to contribute significantly to formation of Mn(III) complexes. The most likely environment for production of Mn(III) complexes in natural systems would be in areas of high biological activity. Such biological processes are likely to be a significant source of Mn(III) complexes in natural systems if they do indeed exist. Production of Mn(III) complexes by biological processes has been well-studied (2-8) and will not be addressed further in this study.

The dissolution of Mn(III) solids can be seen as also related to the oxidation of Mn(II), since Mn(III)-containing solids have been found to be the product of Mn(II) oxidation in most biotic and abiotic oxidation processes. The Mn(III) solids are then an intermediate stage between Mn(II) and Mn(III)L. This path may be of interest because it allows the oxidation of Mn(II) to occur away from sources of the stabilizing ligands. For example, Mn(II) could be oxidized to Mn(III)-containing

particles in the water column. The particles could then sink to the sediments where there are much higher concentrations of ligands such as polyphosphates and organics. Such a process is outlined in Figure 5.1. This pathway of Mn(III) formation has received little study and is the one investigated in this chapter.

Reduction of Mn(IV) in the presence of stabilizing ligands is the third possibility for formation of Mn(III) complexes. This is an interesting possibility, although studies to date that have examined reduction of Mn(IV) oxides by organics have found no evidence of Mn(III) intermediates(9). Several studies have shown that some organic ligands can stabilize Mn(IV)(10-18) but the issue of formation from solid phase Mn(IV) has not been addressed. This question will not be addressed by this study and remains an open one.

5.1.1 Mn(III) solid phases

Evidence for the existence of long lived Mn(III)-containing phases has been accumulating in the last twenty years. Kessick and Morgan (19) found MnOOH to be the primary product of their laboratory oxidation experiments, using formula weight and average oxidation state to make the determination. Stumm and Giovanoli (20) also found MnOOH as the product of Mn(II) oxidation. They identified the product as γ -MnOOH and postulated a Mn_3O_4 intermediate. They suggested that in natural systems these particles would be difficult to detect because they would form very small colloidal particles. Such particles would be ideal candidates for dissolution reactions because the high surface area to mass ratio would allow more ligand to bind at the surface. Hem (21-24) reported a series of experiments examining the products of Mn(II) oxidation. He found that the oxidation goes through a series of Mn(III)-containing mineral phases before eventually forming MnO_2 . The mineral phases that were predominant were dependent on temperature and the anions present. β -MnOOH was the Mn(III) phase formed most commonly. This was the initial mineral phase produced at temperatures near 0°C. At higher temperatures, Mn_3O_4 was found to

form intermediately before MnOOH. α - and γ -MnOOH were produced if sulfate was present in the solution. Murray et. al. (25) examined the oxidation of Mn(II) at pH 9 and 25°C. They found that the reaction proceeded through Mn₃O₄ and β -MnOOH intermediates before arriving at a long lived γ -MnOOH product. They also examined the surface of the intermediates using spectroscopic and microscopic techniques and found that in the hausmanite phase Mn(III) was predominant at the surface. This is significant as Mn(III) would then be readily available for surface reactions such as dissolution. Junta et. al. (26) also used spectroscopic and microscopic techniques to examine Mn(II) oxidation on oxide surfaces. They found that all the oxidation products contained Mn(III) with β -MnOOH being the predominant phase. All of these studies show that Mn(III) solid phases are products of the oxidation of Mn(II). β -MnOOH seems to be the predominant phase, while γ -MnOOH and Mn₃O₄ could also form in significant amounts.

5.1.2 MnOOH reactions

Little work has been done to characterize the types of reactions that MnOOH and other Mn(III)-containing minerals might undergo in natural systems. Johnson and Xyla (27) synthesized Mn oxides in the laboratory and examined the oxidation of Cr(III) by the Mn oxides. They found the oxide MnOOH to be the one that oxidized Cr(III) most rapidly. They also found that organic compounds slowed down the reaction. They reported a rate law and stoichiometry for the reaction. Xyla et. al. (28) examined the dissolution of MnOOH in the presence of oxalate. They found that light had no effect on the reaction, unlike the behavior of Fe oxides. They reported dissolution of the MnOOH to produce Mn(II) in solution, i.e. a reductive dissolution. Kostka et. al. (29) used dissolution of MnOOH by pyrophosphate to synthesize Mn(III) pyrophosphate complexes. They do not report details of the reaction. These few studies by Kostka and Xyla show that MnOOH can be dissolved both reductively and nonreductively. However, they leave unresolved many specifics of these

processes. The types of ligands which can dissolve MnOOH and the effects of chemical variables such as pH need to be examined in order to better understand the reactions of Mn(III) solids in aqueous systems.

5.1.3 This Study

This study has examined the dissolution of a Mn(III)-containing oxide in the presence of the ligands discussed in Chapter 4, i.e. pyrophosphate, EDTA, and citrate. MnOOH was chosen as the oxide to use because it is the most prevalent oxide produced by oxidation of Mn(II) under natural conditions. Both the oxidation state of the remaining solid and that of the dissolved species were monitored to determine the extent of dissolution that occurred and whether dissolution occurring was reductive or nonreductive.

5.2 Experimental

5.2.1 Solids preparation

The solids were prepared by the method used by Johnson and Xyla(27): 0.06 moles of MnSO₄ was added to 1.0 l of water. The pH was then raised by adding 300 ml of a 0.2M NH₃ solution. Then 20.4 ml of 30% H₂O₂ were slowly added dropwise. The suspension was then heated to 90°C for one hour and aged for two weeks. The suspension was then oven dried at 60°C, crushed and stored in polyethylene tubes before use.

5.2.2 Solids characterization

Three 0.1g samples of the solids were analyzed using the iodine titration method to determine oxidation state. The formaldoxime method was also used to determine total Mn and from that a formula weight. The results of these analyses are given in Table 5.1. The results give the average oxidation state as 3.0, indicating that the synthesis was successful and the solids are largely Mn(III). The formula weight was found to be 100 ± 3 g/mole Mn. This is consistent with a MnOOH oxy-hydroxo solid with one water of hydration. Although these results indicate that the solids are

Mn(III) solids and appear to be MnOOH, the data do not definitively tell that other phases are not present or the mineral structures. Therefore X-ray diffraction patterns were taken for the solids.

The X-ray diffraction patterns are shown in Figure 5.2. Various Mn oxide standard diffraction patterns are shown in Figure 5.3 - 5.5. The lack of a strong line at around 57° rules out the possibility of any MnO₂ phases as shown in Figure 5.3. Figure 5.4 shows standards for several Mn(III)-containing minerals other than MnOOH. Absence of the peak at 22° rules out bixbyite. Hausmanite; however, shows a good match for all the peaks except for the ones at 24° and 49° . This makes it likely that hausmanite is one of the phases present. The peaks at 24° and 49° indicate another phase. The oxidation state analysis also gives an average oxidation state of 3.0. If hausmanite were the major phase the oxidation state should be closer to 2.67 not 3.0. Therefore hausmanite cannot be the major mineral phase present. Having ruled out Mn(IV) solids that means that the major phase must be a pure Mn(III) phase, most likely MnOOH.

Figure 5.5 shows the standards for the various MnOOH phases. Manganite and groutite are eliminated because they do not have a peak at 24° . Feitknechtite does; however, match the peak and is the other phase present. Therefore the synthesis was fairly successful and produced a solid phase that is largely feitknechtite (β -MnOOH) with some contamination of hausmanite. The X-ray diffraction method does not allow determination of the percentages of each phase. The iodine titration results allow a cap to be put on the amount of hausmanite. No more than 10-20% of the solids could be hausmanite and still allow for the oxidation state obtained.

The pH_{zpc} was determined using the particle velocity measurements described in Chapter 2. The pH_{zpc} was determined to be 6.2 ± 0.2 . This agrees well with the 6.1 reported by Xyla et. al. for γ -MnOOH (28).

5.2.3 Experimental procedure

The dissolution experiments in this chapter were carried out in a two-liter glass reactor. Prior to the start of the experiment the reactor was filled with 1.5 liters of deionized distilled water. Enough ligand was added to bring the concentration to the desired level for the experiment. When the ligand had dissolved pH was adjusted to the desired pH using concentrated perchloric acid or sodium hydroxide. Once the pH was stable, the powdered solids were added to the vessel and the reaction was begun. Solids were kept suspended using a magnetic stir bar.

Generally 25 ml of sample were withdrawn using a glass pipette. If a large extent of dissolution had occurred then larger samples were taken. The sample was filtered through a 0.05 μ m nucleopore polycarbonate filter. Once the filtering was complete an aliquot of filtrate was withdrawn and measured spectrophotometrically for absorbance of Mn(III) complexes. A second aliquot was measured for total Mn using the formaldoxime method described in Chapter 2. The solids were analyzed for their average oxidation state using the iodine titration method described in Chapter 2.

5.3 Results and Discussion

5.3.1 Pyrophosphate

5.3.1.1 Effect of pH

Figures 5.6 and 5.7 show the results for the dissolution of MnOOH solid by pyrophosphate at two different pHs. Figure 5.6 shows the appearance of solution species versus time. Solid symbols represent the Mn(III)P₂O₇ complex. Open symbols represent total dissolved Mn. Although some of the values for Mn(III)P₂O₇ are larger than total Mn, the points are well within experimental error of each other. Therefore all the dissolved Mn is believed to be present as the Mn(III) complex. In a time of one day nearly all the solids were dissolved.

The lines shown are first-order fits to the data. The fit was of the form:

$$[\text{Mn}] = [\text{Mn}]_0 \cdot (1 - \exp(-k^* \cdot t)) \quad [5.1]$$

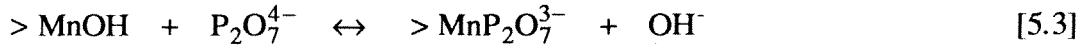
The rate is twice as fast at pH 6.5 as it is at 7. The rate constants are: $k = 3.0 \pm 0.2 \times 10^{-5} \text{ s}^{-1}$ at pH 7, and $k = 5.0 \pm 0.8 \times 10^{-5} \text{ s}^{-1}$ at pH 6.5. A run at pH 8, shown in Figures 5.9 and 5.10, showed a slower rate than either of the lower pH runs, although not directly comparable because of different solids and ligand concentrations. It is apparent that the reaction proceeds faster at lower pH.

If it is assumed that the solids concentration and pyrophosphate concentration do not have a large effect on the rate, then the pH 8 run can be compared with the two other pH runs to evaluate the quantitative effect of pH on reaction rate. This assumption is plausible if the total pyrophosphate is large enough that the surface is saturated with pyrophosphate at all solids concentrations. The pH 8 run has a $\text{P}_2\text{O}_7:\text{Mn}$ ratio of 50:1 and is almost certainly saturated. The pH 6.5 and 7.0 runs have $\text{P}_2\text{O}_7:\text{Mn}$ ratios of 10:1. It does not seem unreasonable to assume that this is sufficient to give saturation of the surface. Therefore the comparison will be made assuming that in all 3 cases the surface is saturated with pyrophosphate. Figure 5.8 shows a plot of $\log k^*$ versus pH for the 3 different pH runs. k^* is the pseudo-first order rate constant. A linear fit gives the relation:

$$k^* = k \cdot [\text{H}^+]^{0.46} \quad [5.2]$$

where $k = 10^{-1.27} \text{ M}^{-0.46} \text{ s}^{-1}$ and is the intrinsic rate constant assuming that all concentrations other than $[\text{H}^+]$ are constant. The non-integer power of $[\text{H}^+]$ suggests a complex dependence of the rate on pH. The simplest mechanism possible for the dissolution is the binding of the pyrophosphate at a surface site and the subsequent release into solution as shown in equations 5.3 and 5.4:

(not all equations balanced with respect to charge)



If equation 5.4 is the rate limiting step then the rate expression can be given by

$$\frac{d[> \text{MnP}_2\text{O}_7]}{dt} = -k_d \cdot [> \text{MnP}_2\text{O}_7] \quad [5.5]$$

where k_d is the rate constant for dissolution in s^{-1} . Equation 5.5 can be written in terms of the equilibrium of equation 5.3 giving

$$\frac{d[> \text{MnP}_2\text{O}_7]}{dt} = -\frac{k_d \cdot K_a \cdot [> \text{MnOH}] \cdot [\text{P}_2\text{O}_7^{4-}]}{[\text{OH}^-]} \quad [5.6]$$

where K_a is the adsorption constant for pyrophosphate and is unitless. Further expressing equation 5.6 in terms of the acid base equilibria of the surface sites and the pyrophosphate in the pH range of 6.2 to 8.4 would yield

$$\frac{d[> \text{MnP}_2\text{O}_7]}{dt} = -\frac{k_d \cdot K_a \cdot [> \text{MnOH}] \cdot [\text{P}_2\text{O}_7^{4-}]_T \cdot K_{a4} \cdot K_{sa1} \cdot [\text{H}^+]}{K_w \cdot \left([\text{H}^+]^2 + K_{sa1} \cdot [\text{H}^+] + K_{sa1} \cdot K_{sa2} \right)} \quad [5.7]$$

where K_{sa} 's are the acidity constants for the surface sites in M, K_w is the ion product of water in M^2 , and $[>]_T$ is the total concentration of surface sites in M. The pH behavior will depend on the acidity constants of the surface. If the neutral and negative surface sites are both significant this could yield a dependence on hydrogen ion that appeared to be to the one-half power. The expression would also change

somewhat as the reaction proceeded to near completion and $[>]_T$ was no longer a constant term. Most likely then the observed results can be explained by reactions 5.3 and 5.4.

Figure 5.7 shows the average oxidation state of the solids for two different pHs. Overall there is little evident trend in the data. There may be a slight rise in oxidation state, but this is barely larger than the error bars. If there is a slight rise in oxidation state it could be because of disproportionation of Mn(III) in solution giving rise to precipitation of some MnO₂. Overall, the oxidation state data verify that the dissolution is a nonreductive process. There is no lowering of the oxidation state so it is unlikely that reductive dissolution is occurring, a conclusion verified by measurement of solution species. Any rise in oxidation state is caused either by a slow oxidation of the solids by oxygen or precipitation of MnO₂ from the solution phase.

5.3.1.2 Effect of solids concentration

Figure 5.9 shows the appearance of solution phase Mn from MnOOH dissolution versus time for two different solids concentrations. Closed symbols represent the Mn(III)P₂O₇ complex and the open symbols represent total dissolved Mn. In most cases the points are within experimental error of each other. It does seem that for the 1g/l run there is slightly more dissolved Mn than accounted for by the Mn(III) complex. This may result from either excess Mn(II) left over from the synthesis or from the dissolution of hausmanite, Mn₃O₄. For both solids concentrations about 90% of the solids are dissolved in the first 2 to 3 days, followed by a much slower dissolution rate.

Lines shown are first order fits to the data, using the expression in equation 5.1. The reaction rate constants are the same within experimental error for both solids concentrations. The rate constant for the 1g/l run is $1.00 \pm 0.1 \times 10^{-5} \text{ s}^{-1}$, and the rate

constant for the 0.2g/l run is $1.03 \pm 0.1 \times 10^{-5} \text{ s}^{-1}$. This shows that solids concentration has little effect on the rate constant in the range studied.

Although it may seem surprising at first that the rate is independent of solids concentration, it is really to be expected. Although surface reactions are usually written in terms of moles per surface area and found to be first order in surface area, this assumes that total surface area is a constant. When significant dissolution occurs then surface area is not a constant and the rate constant required to fit the data becomes independent of the mass of solids as can be seen in the following derivation. If the rate of dissolution of the solid is written as:

$$\frac{d[\text{MnL}]}{dt} = k_1 \cdot m_s \cdot a \cdot \langle \text{MnL} \rangle \quad [5.8]$$

where k_1 is the rate constant of dissolution in s^{-1} , m_s is the concentration of solids in g/l, a is the surface area of solids in m^2/g , and $\langle \text{MnL} \rangle$ is the concentration of surface sites occupied by the ligand in mol/m^2 , then the rate can be written in terms of surface sites according to the equilibrium constant for ligand adsorption reaction as shown in reaction 5.3.

$$\frac{d[\text{MnL}]}{dt} = \frac{k_1 \cdot K_a \cdot a \cdot m_s \cdot [\text{L}] \cdot \langle \text{MnOH} \rangle}{[\text{OH}^-]} \quad [5.9]$$

where K_a is the equilibrium expression for adsorption. This can be rewritten in terms of total ligand and total surface sites using α_L and α_s the fraction of ligand in the unprotonated form and the fraction of surface sites in the >MnOH species respectively.

$$\frac{d[\text{MnL}]}{dt} = \frac{k_1 \cdot K_a \cdot a \cdot m_s \cdot [\text{L}]_T \cdot \langle \text{>} \rangle_T \cdot \alpha_L \cdot \alpha_s}{[\text{OH}^-]} \quad [5.10]$$

If most of the solids remained as solids and $\langle \rangle_T$ could be taken as a constant then 5.10 would describe the dependence and would depend directly on m_s . However, this is not the case. Instead m_s is proportional to the amount of solids present

$$m_s = \beta \cdot [\text{Mn}]_{\text{solid}} \quad [5.11]$$

This can be related to total Mn by

$$\text{Mn}_T = [\text{Mn}]_{\text{aq}} + [\text{Mn}]_{\text{solid}} \quad [5.12]$$

where $[\text{Mn}]_{\text{aq}}$ is the total amount of dissolved Mn in M and $[\text{Mn}]_{\text{solid}}$ is the total concentration of solids in M. Substituting into equation 5.10 gives

$$\frac{d[\text{MnL}]}{dt} = \frac{k_1 \cdot K_e \cdot a \cdot [\text{L}]_T \cdot \langle \rangle_T \cdot \alpha_L \cdot \alpha_s}{\beta \cdot [\text{OH}^-]} \cdot ([\text{Mn}]_T - [\text{Mn}]_{\text{aq}}) \quad [5.13]$$

defining k'' as

$$k'' = \frac{k_1 \cdot K_e \cdot a \cdot [\text{L}]_T \cdot \langle \rangle_T \cdot \alpha_L \cdot \alpha_s}{\beta \cdot [\text{OH}^-]} \quad [5.14]$$

yields

$$\frac{d[\text{MnL}]}{dt} = k'' \cdot ([\text{Mn}]_T - [\text{Mn}]_{\text{aq}}) \quad [5.15]$$

This is the same form that was used to fit the dissolution data. Therefore the rate constant k'' , which is equivalent to the k^* of equation 5.1, is independent of mass

concentration of solids. There is a dependence on surface area; however, it is a specific surface area which can be assumed to be the same for the same mineral.

To check this analysis the initial rates can be examined at a point when less dissolution has taken place and the assumption of constant surface sites is better. If the first two points are taken in the data of Figure 5.9 and fit with a simple zero order fit, as suggested by equation 5.10, the resulting rate constants do indeed show a dependence on the solids concentration. The rate constants calculated are $0.0052 \text{ M}\cdot\text{s}^{-1}$ for the 1 g/l run and $0.00060 \text{ M}\cdot\text{s}^{-1}$ for the 0.2 g/l run. The dependence turns out to be to the approximately 1.4 power if it is assumed that the formula weights of the solids in both experiments were 100 g/mol. This would give solution concentrations of 1mM and 0.2 mM respectively.

However; examining the data for the 0.2 g/l experiment shows that the dissolution levels out at 0.1mM. At this point there were no detectable solids remaining. This result is the same regardless of whether the Mn(III) complex, total dissolved Mn, or solids concentration is examined. All three lines of evidence point to a total Mn concentration in the system of 0.1 mM. Either half of the Mn in the system has gone into an undetectable form or there was an error in weighing the solids. The first possibility seems unlikely, as it would be difficult to imagine how that quantity of Mn could be lost. The second possibility is much more likely. If it is considered that the 1 g/l experiment was conducted within a few days of synthesizing the solid, while the 0.2 g/l experiment was conducted over a month later, a possible explanation arises. It is possible that while the initial analysis showed one water of hydration this was not an equilibrium value. The solids may have adsorbed additional water between the two experiments. While it might seem difficult to believe this could result in a doubling of the formula weight, this actually would only require an additional five waters of hydration. This would mean that the solid formula weight rose from 100 g/(mol Mn) initially to 200 g/(mol Mn) for the second experiment. In fact if all of the

other dissolution experiments are examined the total Mn concentrations found in them correspond to 1 mol of Mn per 200 g of solid added. Therefore it will be assumed that the formula weight of the solid was 200 g/(mol Mn) for all but the 1 g/l MnOOH-P₂O₇ experiment.

Taking this factor into account the dependence on the solid concentrations of the initial zero order dissolution rates is to the 0.94 order of solids concentration, which is within experimental error of the first order dependence predicted by equation 5.10. This result demonstrates that the rate constant for complete or near complete dissolution is independent of the concentration of solids, while the initial rate is dependent on solids concentration.

5.3.1.3 Effect of Ligand

Another interesting thing to note is that the pH 6.5 and 7.0 runs shown in Figure 5.6 are at a ratio of ligand:Mn of 10:1. In Chapter 4 this ratio was inadequate for stabilization of the Mn(III)P₂O₇ complexes synthesized from MnO₄⁻ and Mn(II). Therefore it appears that the dissolution method is able to produce kinetically inert Mn(III) complexes at lower ligand excesses. The seeming added stability must be kinetic as the product is the same. It may be because of Mn(IV) or Mn(V) intermediates that may be involved in the reduction of Mn(VII). The energy barrier for these intermediates to form MnO₂ solids may be smaller than that for forming Mn(III) complexes. Thus the Mn(VII) reaction would require more ligand to make the loss of an extra electron to form Mn(III) energetically favorable. Mn(III)-containing solids do not need to undergo any redox reactions and therefore may require less ligand to stabilize the Mn(III) complexes.

5.3.1.4 Oxidation State

Figure 5.10 shows the average oxidation state of the solids versus time. Again there appears to be a slight upward trend of the oxidation state but it is difficult to

distinguish it from random scatter. Interestingly, in the 1g/l run there was an initial dip in the oxidation state of the solids. It is a significant drop and is more than can be explained by error in measuring volume or in knowing the concentration of the standards. The oxidation state levels out around an average oxidation state of 2.6 which is about the oxidation state of hausmanite. The most likely explanation for this drop in oxidation state is the selective dissolution of MnOOH in preference to the hausmanite phase. This would seem likely, given the observation by Murray et. al. (25) that in mixed phases MnOOH dominates the surface and Mn₃O₄ is in the interior. The effect is probably not noticed in the experiments described previously in this chapter because they were much more rapid so that the interior layers of the particles were being dissolved more rapidly and thus not remaining isolated from the solution for significant periods of time.

These data are all consistent with reactions 5.3 and 5.4 giving the release of the unprotonated species into solution. This is also consistent with the observations of the solution phase reaction.

5.3.2 EDTA

Figures 5.11 and 5.12 show the concentration of solids and solution species versus time for dissolution of MnOOH by EDTA at two different pHs. In both cases only total Mn is shown as no Mn(III)EDTA complexes were detected in solution.

In these two experiments both excess of EDTA and pH were varied. Although this does not allow a clear interpretation of the effect of either variable it allows insight into both with fewer experiments. In both cases the dissolution is rapid and complete.

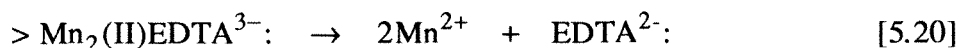
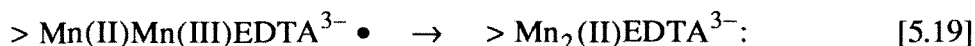
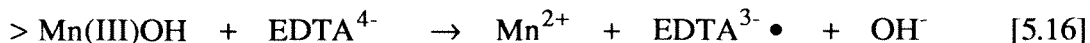
The reaction is much faster at lower pH and higher EDTA excess than at higher pH and lower EDTA excess. Rate constants were found using a first order rate expression to fit the solids concentration and the expression in equation 5.1 to fit total

Mn. The first order rate constant for pH 8.0 is $6.83 \pm 0.05 \times 10^{-5} \text{ s}^{-1}$, and the rate constant at pH 7.0 is $1.8 \pm 0.8 \times 10^{-4} \text{ s}^{-1}$. These results are consistent with both the solution phase EDTA experiments and the pyrophosphate dissolution experiments. The rates of both Mn(III)EDTA reduction and dissolution of MnOOH have been found to be faster at lower pH. Mn(III)EDTA reduction has also been found to be faster at higher EDTA concentration. Most likely; however, the pH is the dominant effect since EDTA is in such large excess that the surface is probably saturated in both cases.

Because the fit rate constant is independent of solids as explained in section 5.3.1.2, if the ligand has no effect on the rate constant then the change in rate constant can be considered wholly the result of pH changes. This would occur if the surface sites are saturated with ligand, which is likely. Considering this the case, the dependence of the rate constant on $[\text{H}^+]$ is approximately 0.4 order. This is very close to the result observed for pyrophosphate and is most likely the result of acid base chemistry of the surface.

It is interesting that the dissolution in the presence of EDTA is an entirely reductive process, unlike that with the other ligands. This is not entirely surprising as the reduction of the Mn(III)EDTA complexes was found to be quite rapid in solution. Yet here, there was no evidence of even a transient Mn(III) solution species. This could be because of the inability of the EDTA to bind more than 2 coordination positions at the surface, whereas the solution species would require 5 to 6 coordination positions to be occupied. Therefore on the surface the EDTA has at least four coordination positions free which could bind other redox active species and thus facilitate further electron transfer. This would allow the reduction to proceed even more quickly than in solution where there are no free coordination positions.

The reduction process could either be a surface binding of EDTA followed by reduction or it could be an outer sphere reduction reaction. The following candidate reactions are proposed (where not all species are balanced with respect to charge):



The EDTA radicals would further react, giving off CO_2 and then reacting with oxygen to produce formaldehyde. The mechanism given by reactions 5.17 - 5.20 would be favored, given what is known about EDTA adsorption onto surfaces and reduction of solids(30-32). Although the solution reaction is outer sphere, it is the electron transfer away from the EDTA that is the rate limiting outer sphere reaction in solution. In solution because all 4 oxygen plus both nitrogens are coordinated to the metal any electron transfer must either be between the single Mn atom and the EDTA or it must be outer sphere. On the surface this limitation does not exist. EDTA is known to form bi and tetra nuclear complexes with iron(33,34). This should be possible on manganese as well. Xyla et. al. found that there were an average of 5 OH^- sites per nm^2 on $\gamma\text{-MnOOH}$, close enough allow multinuclear binding. Therefore a second inner sphere electron transfer can take place thus eliminating the need for an outersphere transfer. Therefore the reduction is most likely occurring through surface binding. The pH data would also support reactions 5.17 - 5.20 as the mechanism. This proposed mechanism is shown in more detail in mechanism 5.1. Reaction 5.16 is a simple outersphere electron transfer and should produce a simple first order

dependence on pH. The observed data are much more consistent with an inner sphere adsorption of the ligand.

The same experiments with MnOOH and EDTA have recently been reproduced by Tian and Stone at the Johns Hopkins University (35). They used capillary electrophoresis to identify the products of the reaction. They observed (in addition to unreacted free EDTA) an Mn(II)-EDTA species, EDTriA (ethylenediaminetriacetate), an Mn(II)EDTriA complex species, and an unidentified product peak. They saw no evidence of Mn(III)EDTA product, in agreement with the results presented here.

There are few data on the oxidation state of the solids because the solids dissolved so fast that it was difficult to collect enough sample to analyze. There did seem to be a slight drop in the average oxidation state of the solids from 3.0 to about 2.8. This would agree with the mechanism in equations 5.17 to 5.20 where the average oxidation state could be lowered if reaction 5.20 proceeded slowly.

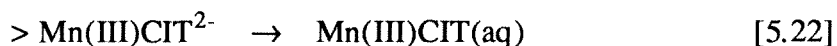
5.3.3 Citrate

Figures 5.13 and 5.14 show the solution phase species concentrations versus time for dissolution of MnOOH by citrate. Two different pHs and ligand concentrations are shown. Diamond shaped symbols are for total Mn and circles are for the Mn(III) citrate complex. Again citrate shows a complex and intermediate behavior between EDTA and pyrophosphate.

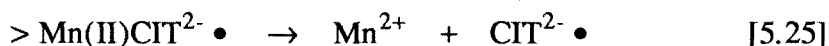
The pH 7.8 run shown in Figure 5.13 did not in fact have a constant pH. In all the other experiments described in this chapter the ligand concentration was sufficient to maintain a constant pH within ± 0.1 pH units. In this experiment; however, the pH rose quickly to 9.0 within the first day and then fell back to 8.5 by the end of the experiment.

In the pH 7.8 run the first two days show a nonreductive dissolution, similar to that exhibited by pyrophosphate, where all the dissolved Mn released is present as the

Mn(III) complex. After about 50 hours the concentration of Mn(III) complex levels off and then begins to drop. The total Mn concentration continues to rise slowly. There are two possible explanations for this behavior. One is that the dissolution step is entirely nonreductive and that as the Mn(III) complex is released to solution it then begins to be reduced in solution. This mechanism can be represented by the reactions (not all species balanced with respect to charge):



The other explanation is that the dissolution changes mechanisms, starting with a nonreductive dissolution and then changing to a reductive dissolution. The preliminary nonreductive dissolution would proceed according to reactions 5.21 to 5.23. Then the following reactions would become predominant in place of reaction 5.23.



In both cases the citrate radical would undergo further decomposition. Such a mechanism has been found in the dissolution of hematite by EDTA in a study by Torres et. al. (30). In the case of EDTA this change in mechanism was found to be caused by the build up of Fe(II) in solution(36-37). The Fe(II) then formed a bridging complex with the EDTA and a surface Fe(III). Electron transfer occurs through the ligand reducing the surface Fe(III) and producing a solution Fe(III) complex. This mechanism could not be ruled out for Mn and citrate but would seem unlikely. A

bridging complex with citrate would most likely be much weaker than with EDTA. Also if electron transfer occurred across a bridging ligand then the total amount of Mn(III)CIT in solution would remain relatively constant requiring reaction 5.23 to be the rate limiting step for loss of Mn(III). This is possible but seems unlikely. What would seem more likely is that the citrate radicals produced in reaction 5.23 go on to react with a surface Mn(III) reducing it to Mn(II). This process would not occur to a significant extent until the reaction had been proceeding a while but once sufficient radicals built up the reduction of Mn(III) by the radicals would be quicker than nonreductive dissolution.

Another interesting observation is that the pH 7.8 citrate dissolution experiment is the only one in which a significant portion of the solids remained undissolved. Only about 1.2 mM of the total 2.5 mM Mn present were dissolved. Although the total Mn in solution is continuing to climb at the end of the experiment it would appear to take a long time for total dissolution. If indeed all the dissolution is nonreductive then it would seem that some sort of equilibrium is being approached. If the dissolution changes mechanisms after the most reactive surface sites are consumed, then it could be that the reduction is just very slow at the higher pH.

The pH 6.3 run is similar in behavior to the pH 7.8 run but is different in the degree and speed of reaction. The pH was constant unlike the pH 7.8 case. The dissolution of the solid is nearly complete in this run, unlike the result at pH 7.8. This could either be because of a shift in the equilibrium, if the nonreductive dissolution is the only important process, or because of a faster reductive pathway, if that becomes an important process.

In the pH 6.3 run much less Mn(III) citrate complex is produced. Again there are two possibilities. One is that all the dissolution occurs by a nonreductive mechanism, according to reactions 5.21 to 5.23, but the reduction of the aqueous complex is much more rapid at pH 6.3. The other possibility is that the initial

dissolution is nonreductive but is then taken over by a reductive process, described by reactions 5.24 and 5.25. If this is this case then it would seem to imply that the reductive process is much more favored by low pH than is the nonreductive process.

The foregoing data for citrate, taken together, seem to indicate that a two step process is most likely. If one process were controlling then the behavior would be expected to be simpler. At higher pH the nonreductive dissolution occurs first releasing Mn(III)CIT and raising the pH by producing OH⁻. Then, after about a day, the reductive mechanism takes over, perhaps initiated by solution reduction of the Mn(III)CIT complexes by internal electron transfer yielding radicals which then react with the solids to initiate a reduction reaction according to equation 5.26 (where not all species balanced with respect to charge):



The citrate would then further react with oxygen to give off CO₂ and produce a ketone. As Mn²⁺ is formed the pH is lowered due to hydrolysis of the metal. In the lower pH run the reductive pathway appears to predominate much earlier on, probably due to a quicker reduction of the Mn(III)CIT complexes in solution leading to further radical generation.

The total rate constant of the MnOOH dissolution reaction increases from $7.8 \pm 1 \times 10^{-6} \text{ s}^{-1}$ at pH 7.8 to $5.0 \pm 2 \times 10^{-4} \text{ s}^{-1}$ at pH 6.3. This shows that the reaction rate is strongly dependent on pH. This would be expected as the pH_{ZPC} of the solid at pH 6.3 is approached and the repulsive forces between the solid and ligand become less intense.

If the dissolution rate is not dependent on ligand concentration, as a consequence of saturation of the surface sites, then the difference in rates can be attributed wholly to pH changes. Considering this to be the case gives a dependence

of the rate on $[H^+]$ of the order of 1.2. This is different than the 0.4 to 0.5 observed for pyrophosphate and EDTA. If reaction 5.26 becomes rate controlling this could explain the difference. If reaction 5.26 occurs as an outersphere transfer as shown it would give a first order dependence on hydrogen ion and not the fractional order observed due to adsorption.

Figure 5.15 shows the average oxidation state of the remaining solids at pH 7.8. There is a slight drop in average oxidation state as the reaction proceeds. This would support a surface reduction as shown in reactions 5.20 and 5.21. The evidence suggests a mechanism given by equations 5.21 to 5.23 in the early stages with equations 5.24 to 5.26 becoming important as the reaction proceeds. The overall mechanism is shown in mechanism 5.2.

5.4 Conclusions

Overall, it has been shown that MnOOH solids can be a source of aqueous phase Mn(III) complexes. Dissolution of the solids is faster at low pH. The pathway of dissolution of MnOOH solids, whether reductive or nonreductive, depends on the ligand used and the pH of the solution.

5.4.1 Pyrophosphate

Pyrophosphate has been found to nonreductively dissolve MnOOH solids to form aqueous phase Mn(III) pyrophosphate complexes. The rate constant is $3.0 \pm 0.2 \times 10^{-5} \text{ s}^{-1}$ at pH 7, and $5.0 \pm 0.8 \times 10^{-5} \text{ s}^{-1}$ at pH 6.5. The reaction rate is proportional to the 0.4 power of the hydrogen ion concentration. The reaction is independent of solids concentration for ligand:Mn ratios greater than 10:1. At pH 8.0 the reaction rate constant was $1.00 \pm 0.1 \times 10^{-5} \text{ s}^{-1}$. The reaction appears to be surface controlled.

5.4.2 EDTA

EDTA has been found to reductively dissolve MnOOH solids. No evidence was found for existence of Mn(III)EDTA solution phase product species. The reaction

is faster at lower pH. At pH 8.0 the rate constant was $6.83 \pm 0.05 \times 10^{-5} \text{ s}^{-1}$, and at pH 7.0 the rate constant was $1.8 \pm 0.8 \times 10^{-4} \text{ s}^{-1}$. The dependence on $[\text{H}^+]$ is approximately 0.4 order. This is most likely the result of multiple electron transfer occurring at the surface.

5.4.3 Citrate

Citrate has been found to show a complicated behavior in the dissolution of MnOOH solids. There is first a rapid nonreductive dissolution producing Mn(III)citrate complexes, followed by a period of increased production of aqueous Mn(II) and loss of solution phase Mn(III). The rate constant at pH 7.8 is $7.8 \pm 1 \times 10^{-6} \text{ s}^{-1}$. The rate constant is $5.0 \pm 2 \times 10^{-4} \text{ s}^{-1}$ at pH 6.3. The dependence on $[\text{H}^+]$ is close to first order, which implies a simple reaction step, possibly an outer sphere reduction process. This process is most likely the reduction of surface Mn(III) by radicals produced by reduction of solution Mn(III) complexes.

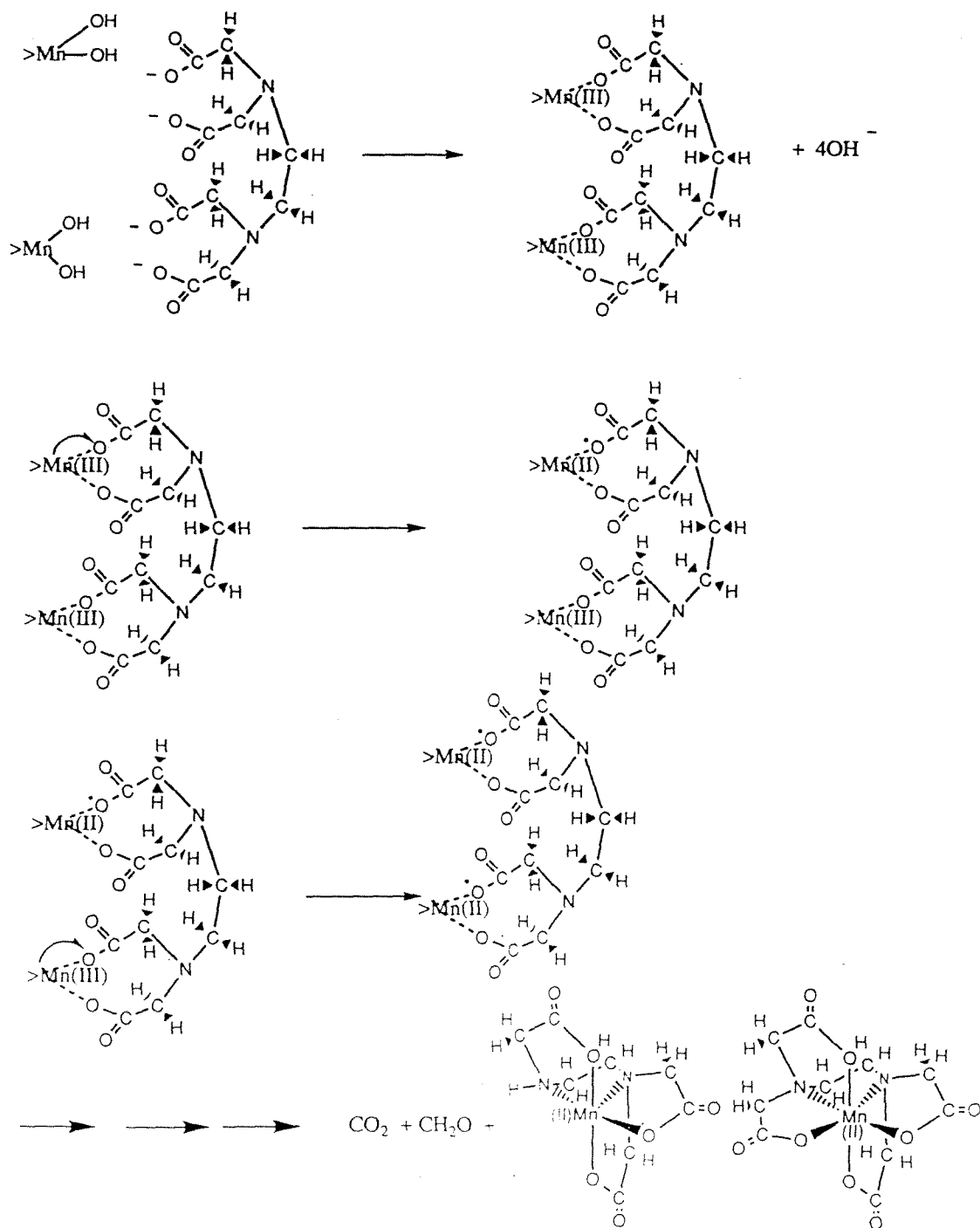
References

- (1) Milad, N. E.; Guindy, N. M.; Helmy, F. M. *Egyptian Journal of Chemistry* **1971**, *14*, 571 - 580.
- (2) Loll, M. J.; Bollag, J. M. *Soil Biology and Biochemistry* **1985**, *17*, 115 - 117.
- (3) Aitken, M. D.; Irvine, R. L. *Archives of Biochemistry and Biophysics* **1990**, *276*, 405 - 414.
- (4) Archibald, F. S.; Fridovich, I. *Archives of Biochemistry and Biophysics* **1982**, *214*, 452 - 463.
- (5) Vites, J. C.; Lynam, M. M. *Coordination Chemistry Reviews* **1994**, *131*, 95 -126.
- (6) Brudwig, G. W.; Crabtree, R. H. *Progress in Inorganic Chemistry* **1989**, *37*, 99 - 142.
- (7) Manchanda, R.; Thorpe, H. H.; Brudvig, G. W.; Crabtree, R. H. *Inorganic Chemistry* **1991**, *30*, 494 - 497.

- (8) Thorpe, H. H.; Sarneski, J. E.; Kulawiec, R. J.; Brudvig, G. W.; Crabtree, R. H.; Papaefthymiou, G. G. *Inorganic Chemistry* **1991**, *30*, 1153 - 1155.
- (9) Stone, A. T. PhD Thesis, California Institute of Technology, 1983.
- (10) Hage, R. *Nature* **369**, 637 - 639.
- (11) Vites, J. C.; Lynam, M. M. *Coordination Chemistry Reviews* **1994**, *131*, 95 -126.
- (12) Brudwig, G. W.; Crabtree, R. H. *Progress in Inorganic Chemistry* **1989**, *37*, 99 - 142.
- (13) Manchanda, R.; Thorpe, H. H.; Brudvig, G. W.; Crabtree, R. H. *Inorganic Chemistry* **1991**, *30*, 494 - 497.
- (14) Thorpe, H. H.; Sarneski, J. E.; Kulawiec, R. J.; Brudvig, G. W.; Crabtree, R. H.; Papaefthymiou, G. G. *Inorganic Chemistry* **1991**, *30*, 1153 - 1155.
- (15) Magers, K. D.; Smith, C. G.; Sawyer, D. T. *Inorganic Chemistry* **1978**, *17*, 515 - 523.
- (16) Richens, D. T.; Smith, C. G.; Sawyer, D. T. *Inorganic Chemistry* **1979**, *18*, 706 - 712.
- (17) Magers, K. D.; Smith, C. G.; Sawyer, D. T. *Inorganic Chemistry* **1980**, *19*, 492 - 496.
- (18) Yamaguchi, K. S.; Sawyer, D. T. *Israeli Journal of Chemistry* **1985**, *25*, 164 - 176.
- (19) Kessick, M. A.; Morgan, J. J. *Environmental Science and Technology* **1975**, *9*, 157 - 159.
- (20) Stumm, W.; Giovanoli, R. *Chimia* **1976**, *30*, 423 -426.
- (21) Hem, J. D.; Roberson, C. E.; Fournier, R. B. *Water Resources Research* **1982**, *18*, 563 - 570.
- (22) Hem, J. D.; Lind, C. J. *Geochimica et Cosmochimica Acta* **1983**, *47*, 2037 - 2046.

- (23) Hem, J. D. *Geochimica et Cosmochimica Acta* **1981**, 47, 1369 - 1374.
- (24) Hem, J. D. *Chemical Geology* **1978**, 21, 199 - 218.
- (25) Murray, J. W.; Dillard, J. G.; Giovanoli, R.; Moers, H.; Stumm, W. *Geochimica et Cosmochimica Acta* **1985**, 49, 463 - 470.
- (26) Junta, J. L.; Hochella, M. F. J. *Geochimica et Cosmochimica Acta* **1994**, 58, 4985 - 4999.
- (27) Johnson, C. A.; Xyla, A. G. *Geochimica et Cosmochimica Acta* **1991**, 55, 2861 - 2866.
- (28) Xyla, A. G.; Sulzberger, B.; Luther, G. W.; Hering, J. G.; Capellen, P. V.; Stumm, W. *Langmuir* 8, 95 - 103.
- (29) Kostka, J. E.; Luther, G. W.; Nealson, K. H. *Geochimica et Cosmochimica Acta* **1995**, 59, 885 - 894.
- (30) Torres, R.; Blesa, M. A.; Matijevic, E. *Journal of Colloid and Interface Science* **1989**, 131, 567 - 579.
- (31) Jardine, P. M.; Jacobs, G. K.; O'Dell, J. D. *Soil Science Society of America Journal* **1993**, 57, 954-962.
- (32) Gangopadhyay, S.; Ali, M.; Saha, S. K.; Banerjee, P. *Journal of the Chemical Society : Dalton Transactions* **1991**, 2729 - 2734.
- (33) Bondietti, G.; Sinniger, J.; Stumm, W. *Colloids and Surfaces A* **1993**, 79, 157 - 167.
- (34) Borggaard, O. K. *Clays and Clay Minerals* **1991**, 39, 324 - 328.
- (35) Tian and Stone personal communication 1995
- (36) Litter, M. I.; Blesa, M. A. *Canadian Journal of Chemistry* **1992**, 70, 2502 - 2510.
- (37) Karametaxas, G.; Hug, S. J.; Sulzberger, B. *Environmental Science and Technology* **1995**, 29, 2992 - 3000.

Mechanism 5.1
Proposed MnOOH-EDTA reaction scheme



Mechanism 5.2

Proposed MnOOH-citrate reaction scheme

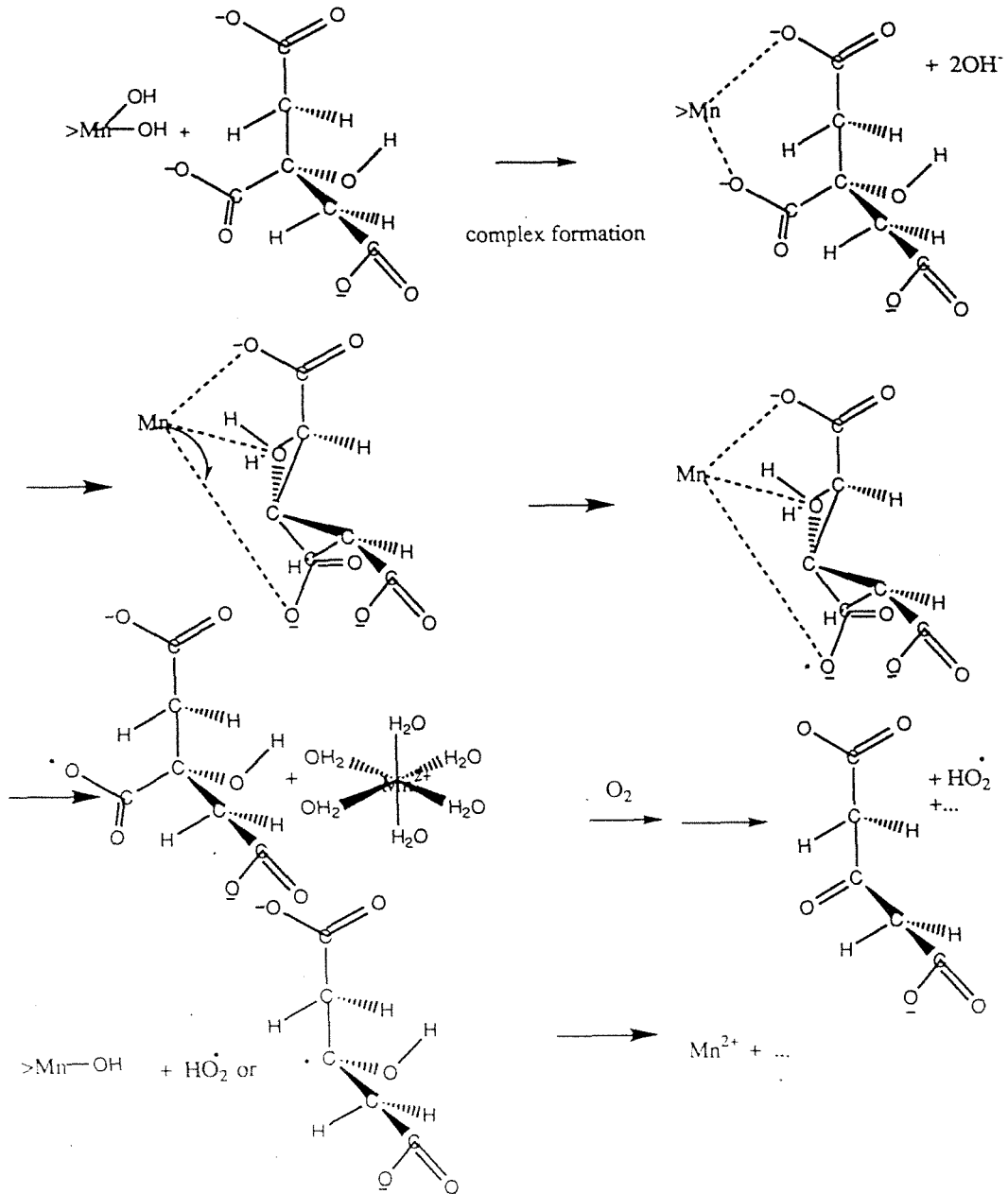


Table 5.1
Redox Characterization of Synthesized Mn Solids

Sample	Total Manganese (mM)	Oxidized Manganese (meq/l)	Molecular Weight (g)	Formula
1	5.21	5.24	97.8	MnO _{1.503}
2	4.70	4.82	100.1	MnO _{1.512}
3	4.72	4.74	103.5	MnO _{1.502}
Avg			100 ± 3	MnO _{1.506 ± .006}

Figure 5.1
Proposed Cycle for Formation
and Loss of Mn(III) Complexes

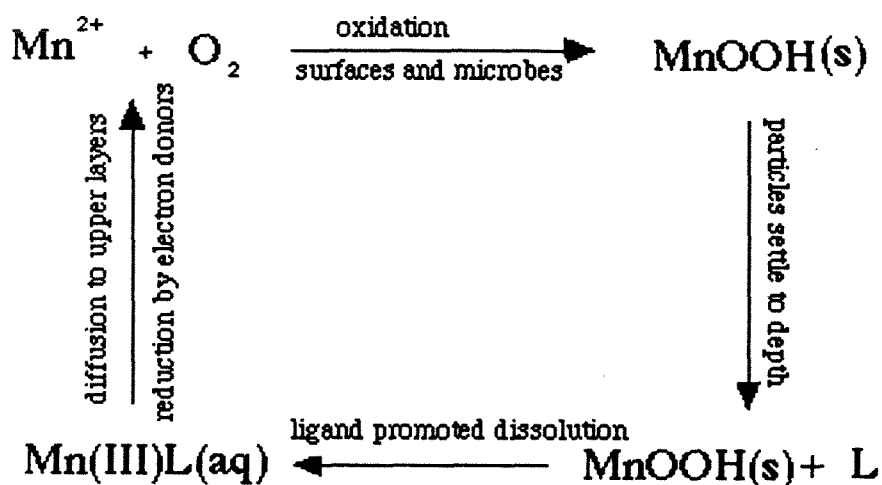
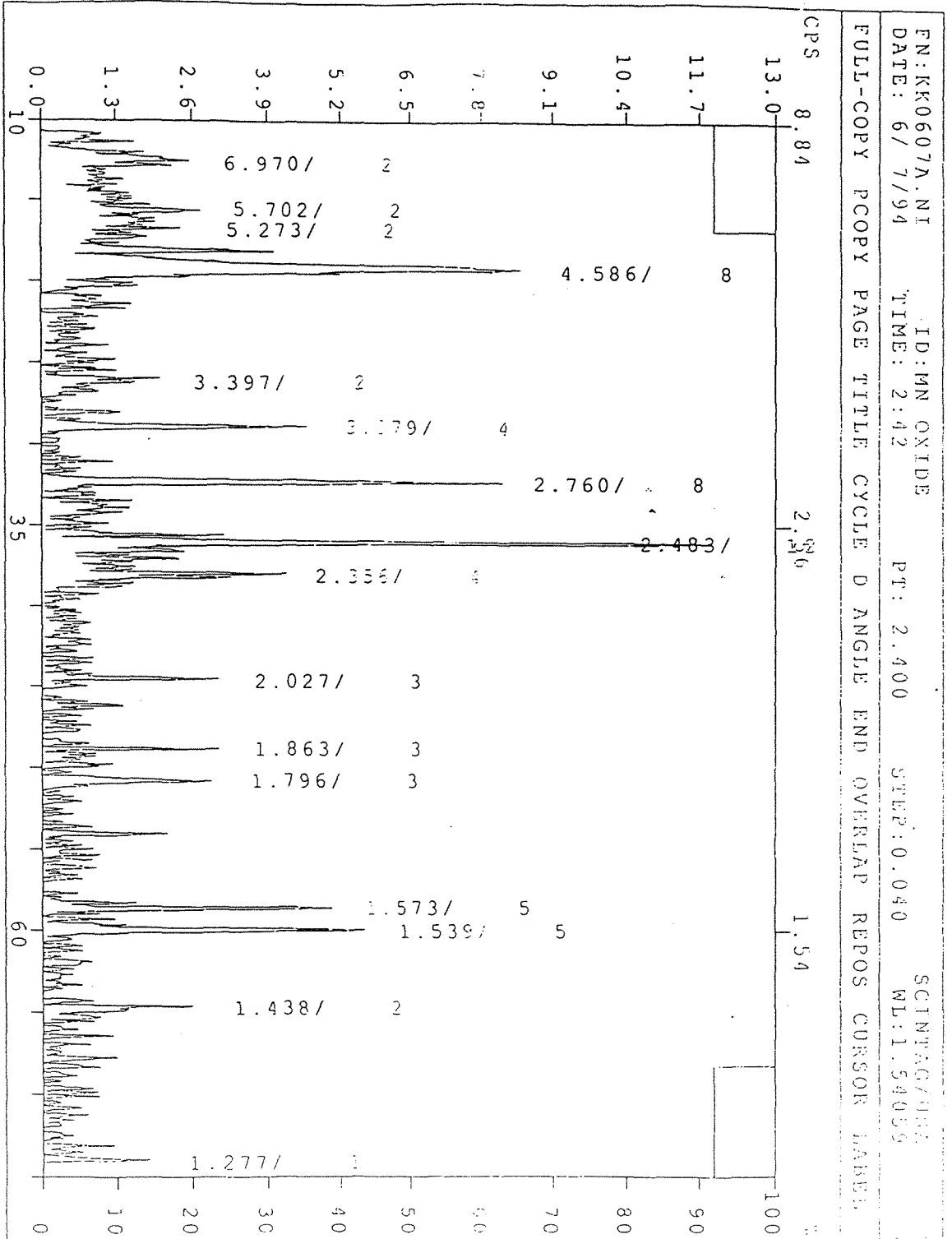


Figure 5.1 Proposed cycle for formation and loss of Mn(III) complexes. Schematic diagram of a possible reaction cycle involving the production of aqueous Mn(III) complexes. L is any Mn(III) stabilizing ligand.

Figure 5.2



FN:KK0607A.NI
DATE: 6/ 7/94

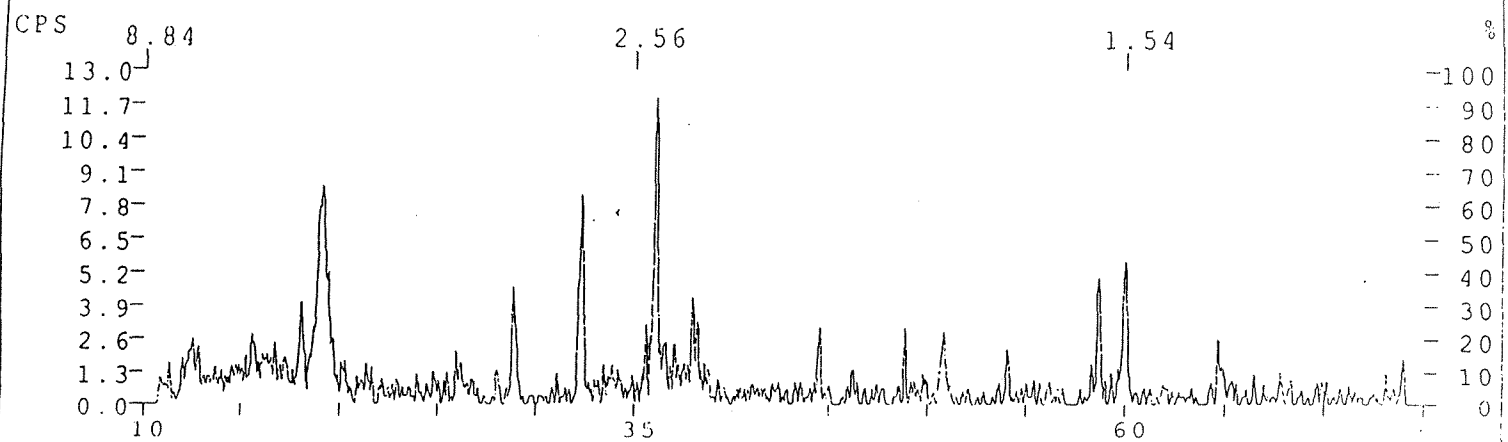
ID:MN OXIDE
TIME: 2:42

PT: 2.400

STEP:0.040

SCINTAG/USA
WL:1.54059

COPY CONTINUE NEXT-CARD END OVERLAP



MANGANESE OXIDE / AKHTENSKITE, SYN

30,820

MN O2

MANGANESE OXIDE / PYROLUSITE, SYN

24,735

MN O2

MANGANESE OXIDE

14,644

MN O2

Figure 5.3

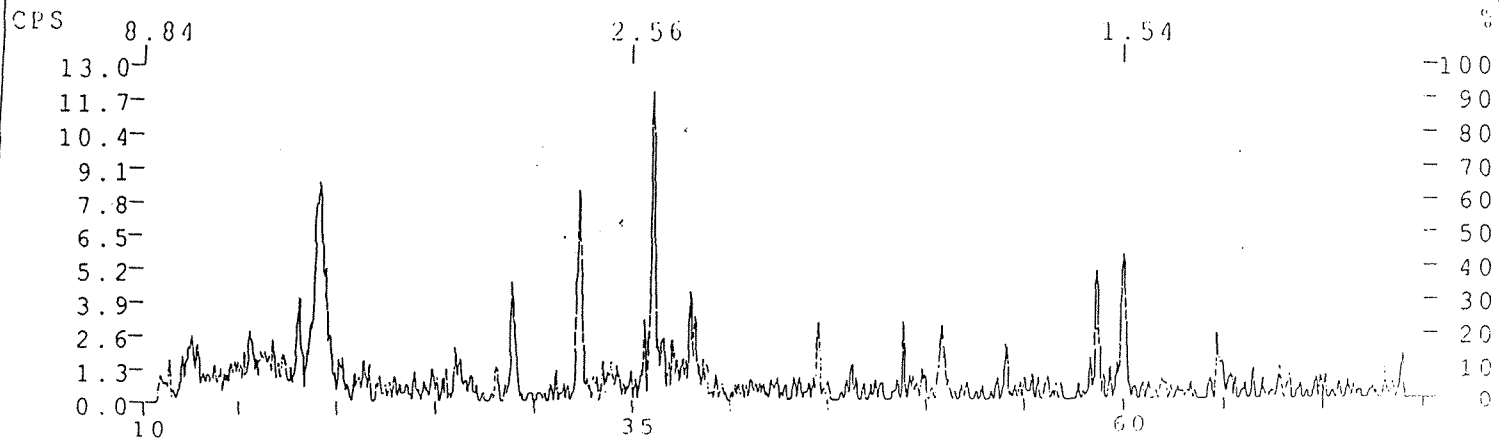
FN:KK0607A.NI
DATE: 6/ 7/94

ID:MN OXIDE
TIME: 2:42

PT: 2.400
STEP:0.040

SCINTAG/USA
WL:1.54059

COPY CONTINUE NEXT-CARD END OVERLAP



MANGANESE OXIDE / BIXBYITE-PCAB, SYN

24,508

MN2 O3

MANGANESE OXIDE / HAUSMANNITE, SYN

24,734

MN3 O4

MANGANESE OXIDE / BIXBYITE-IA3, SYN

31,825

MN2 O3

Figure 5.4

FN:KK0607A.NI
DATE: 6/ 7/94

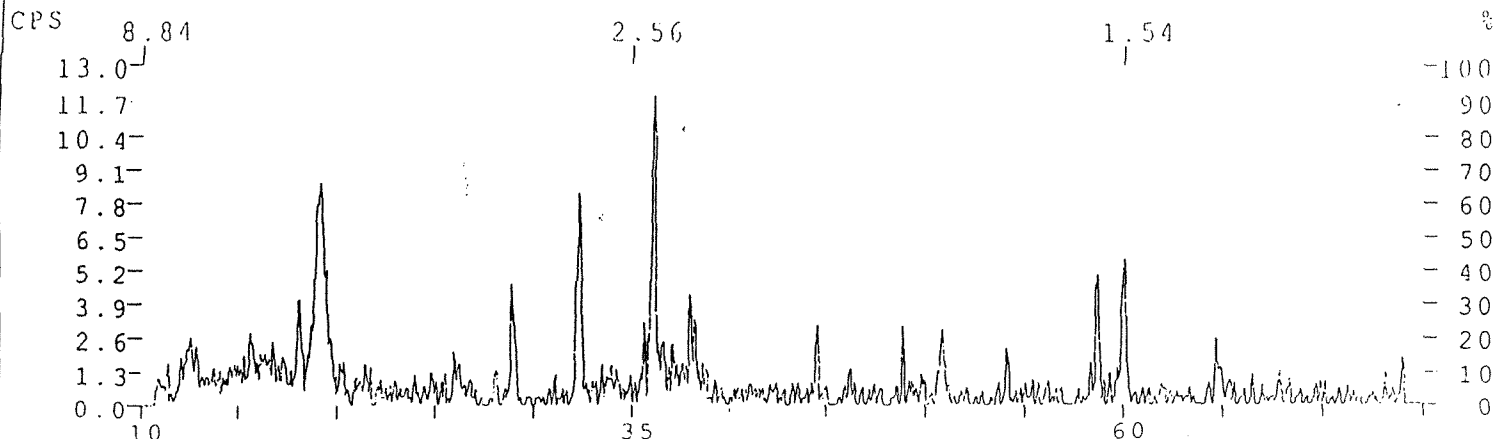
ID:MN OXIDE
TIME: 2:42

PT: 2.400

STEP:0.040

SCINTAG/USA
WL:1.54059

COPY CONTINUE NEXT-CARD END OVERLAP



MANGANESE OXIDE HYDROXIDE / GROUTITE

24,713

MN O O H

MANGANESE OXIDE HYDROXIDE / MANGANITE, SYN

18,805

MN O O H

MANGANESE OXIDE HYDROXIDE / FEITKNECHTITE, SYN

18,804

MN O (O H)

Figure 5.5

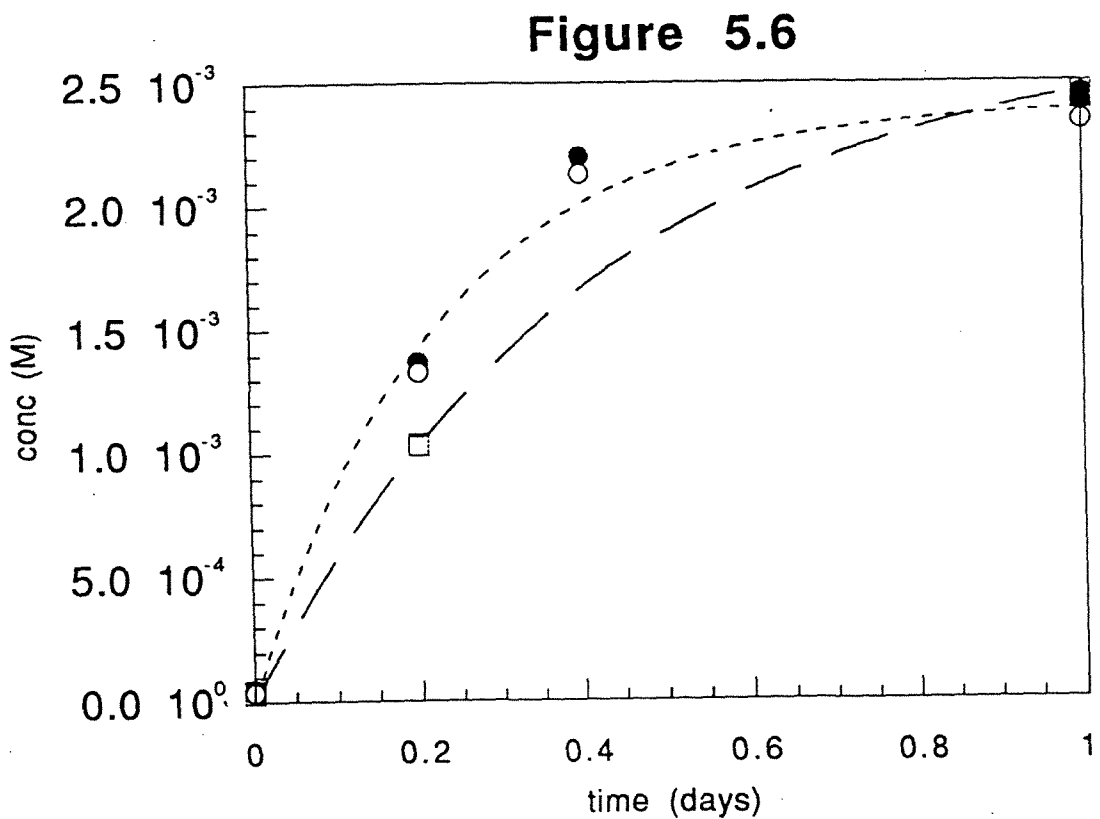


Figure 5.6 Dissolution of MnOOH by P₂O₇ - dependence on pH. Plot of concentration of total Mn and Mn(III)P₂O₇ versus time for the dissolution of MnOOH solid by P₂O₇. Two different pHs are shown, 7.0 and 6.5. Both total dissolved Mn and Mn(III)P₂O₇ are shown. The symbols are: ● - Mn(III)P₂O₇ pH 6.5, ○ - Mn_t pH 6.5, ■ - Mn(III)P₂O₇ pH 7.0, □ - Mn_t pH 7.0. The solids concentration is 0.5g/l and the pyrophosphate concentration is 0.05M. Lines are first order fits to the data.

Figure 5.7

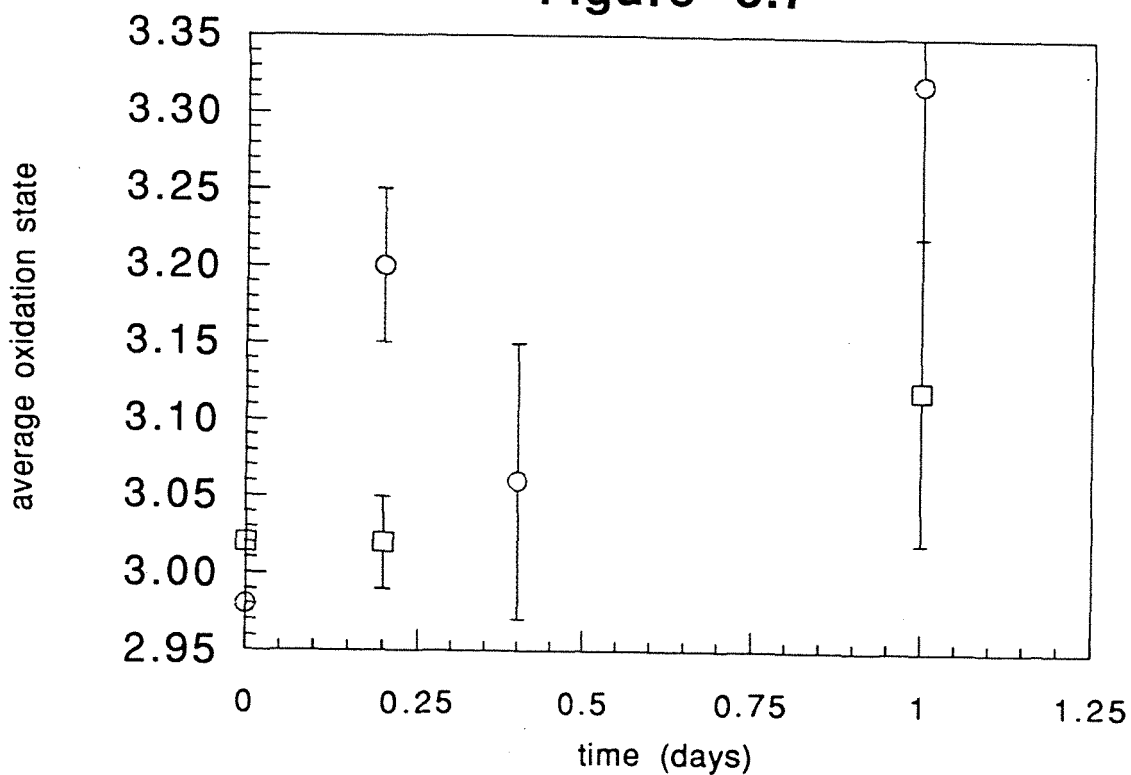


Figure 5.7 Dissolution of MnOOH by P_2O_7 - solids oxidation state. Plot of the average oxidation state of the solids versus time for the dissolution of MnOOH solids by P_2O_7 . Results from two different pHs are shown: \circ - 6.5, and \square - 7.0. The solids concentration is 0.5g/l and the pyrophosphate concentration is 0.05M.

Figure 5.8

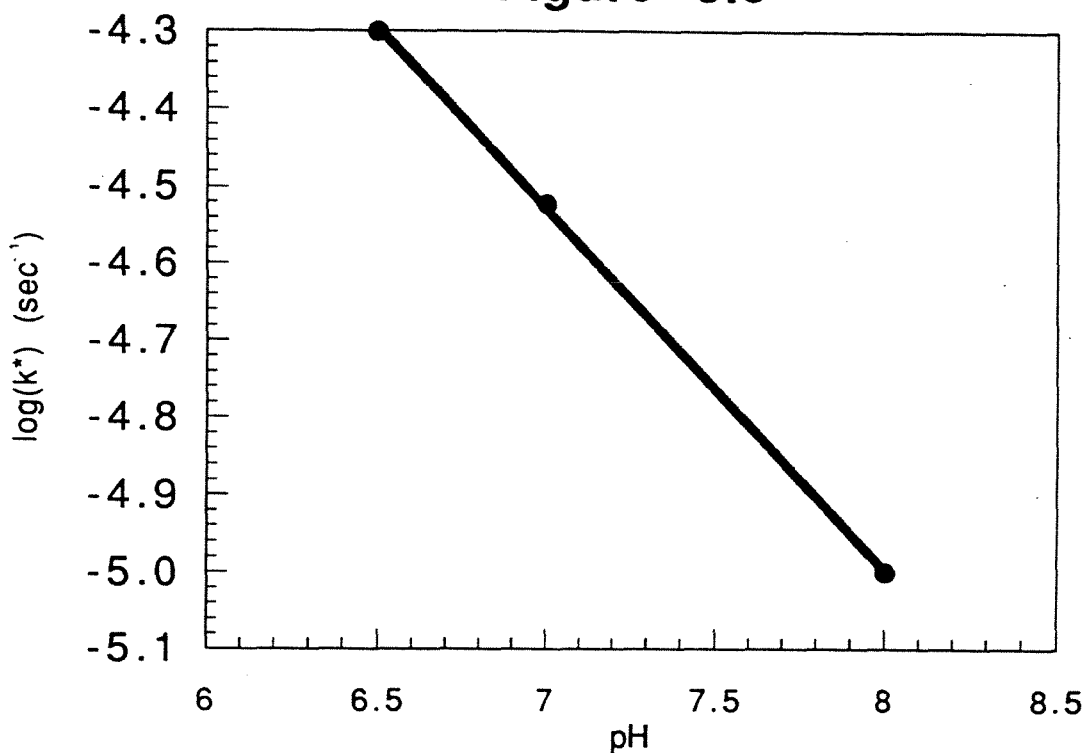


Figure 5.8 Rate constants for dissolution of MnOOH by P_2O_7 . Plot of $\log k$ (s^{-1}) versus pH for three different pHs. $\log k$ was determined by first order fits to the data. At pH 6.5 and 7.0 the solids concentration is 0.5g/l, at pH 8.0 the solids concentration is 1.0g/l. In all three cases the pyrophosphate concentration is 0.05M. The line is a linear fit.

Figure 5.9

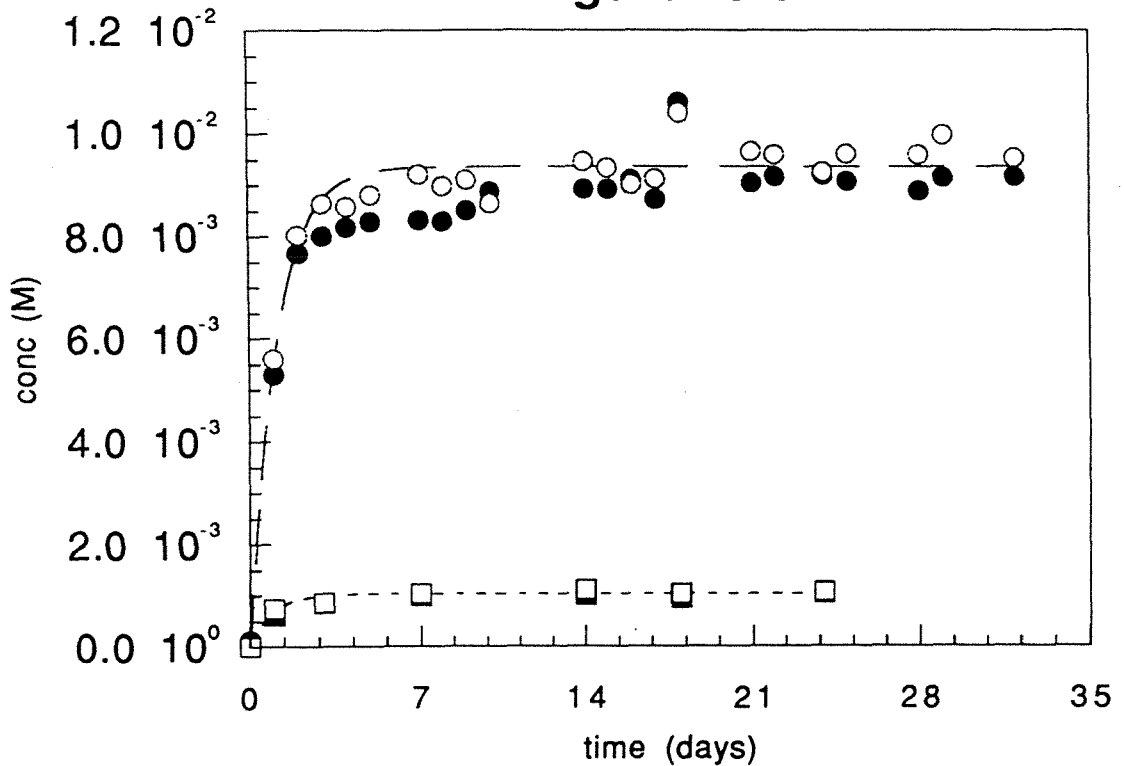


Figure 5.9 Dissolution of MnOOH by P_2O_7 - dependence on solids. Plot of concentrations of total dissolved Mn and $Mn(III)P_2O_7$ versus time for the dissolution of MnOOH solids by P_2O_7 . Two solids concentrations are shown, 1.0 and 0.2g/l. Both total dissolved Mn and $Mn(III)P_2O_7$ are shown. The symbols are: ● - $Mn(III)P_2O_7$ [solids] = 1g/l, ○ - Mn_t [solids] = 1g/l, ■ - $Mn(III)P_2O_7$ [solids] = 0.2g/l, □ - Mn_t [solids] = 0.2g/l. The pH is 8.0 and the pyrophosphate concentration is 0.05M. Lines are first order fits to the data.

Figure 5.10

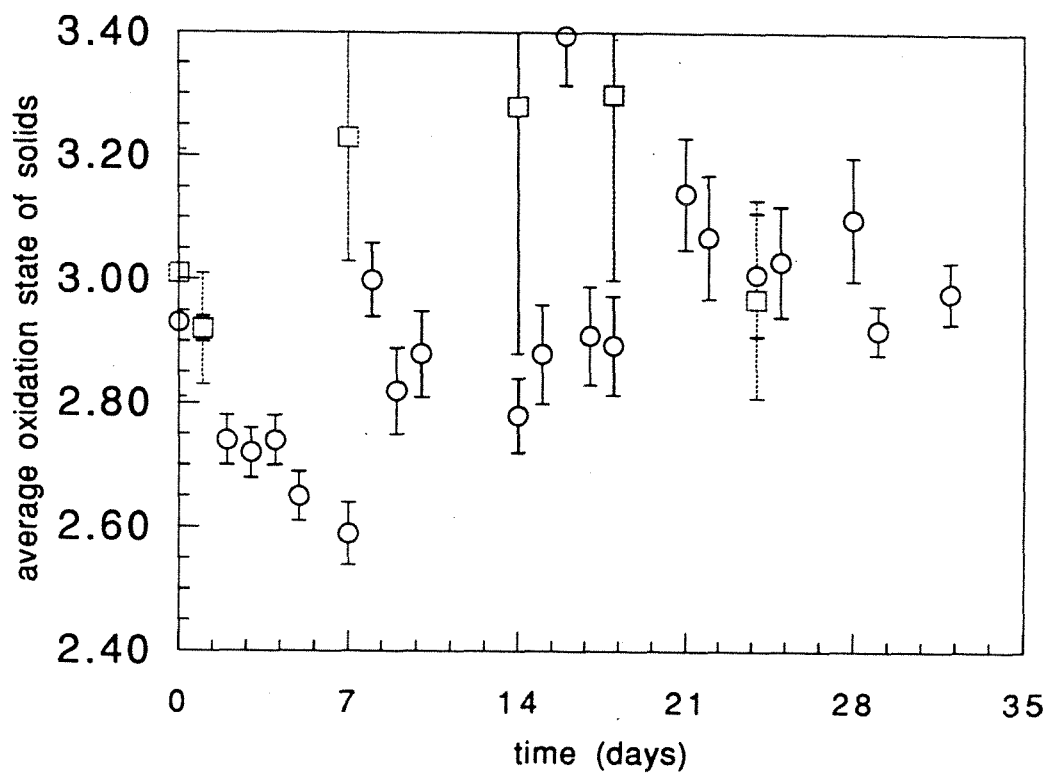


Figure 5.10 Dissolution of MnOOH by P_2O_7 - solids oxidation state. Plot of the average oxidation state of the solids versus time for the dissolution of MnOOH solids by P_2O_7 . Two different solids concentrations are shown: \circ - 1g/l, and \square - 0.2g/l. The pH is 8.0 and the pyrophosphate concentration is 0.05M.

Figure 5.11

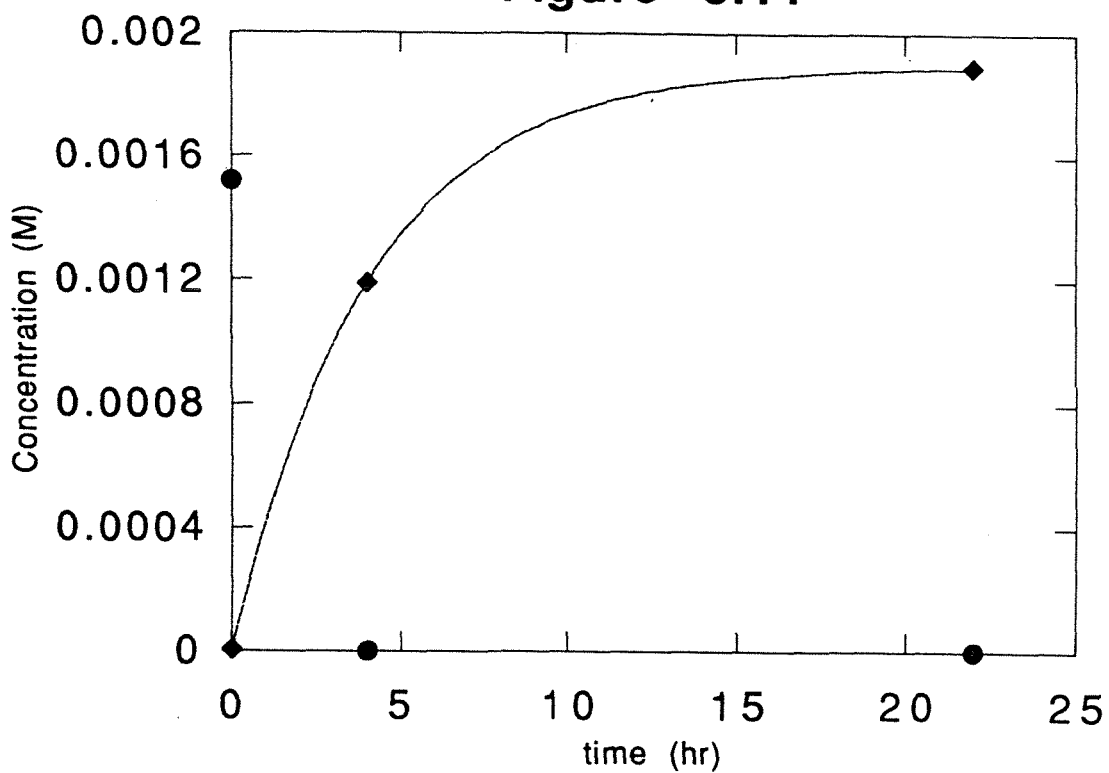


Figure 5.11 Dissolution of MnOOH by EDTA - pH 8.0. Plot of concentrations of total suspended solids and total dissolved Mn versus time for the dissolution of MnOOH by EDTA. Concentration of solids, ●; and total dissolved Mn, ◆; are shown. The pH is 8.0, the solids concentration is 0.5g/l, and the EDTA concentration is 0.025M.

Figure 5.12

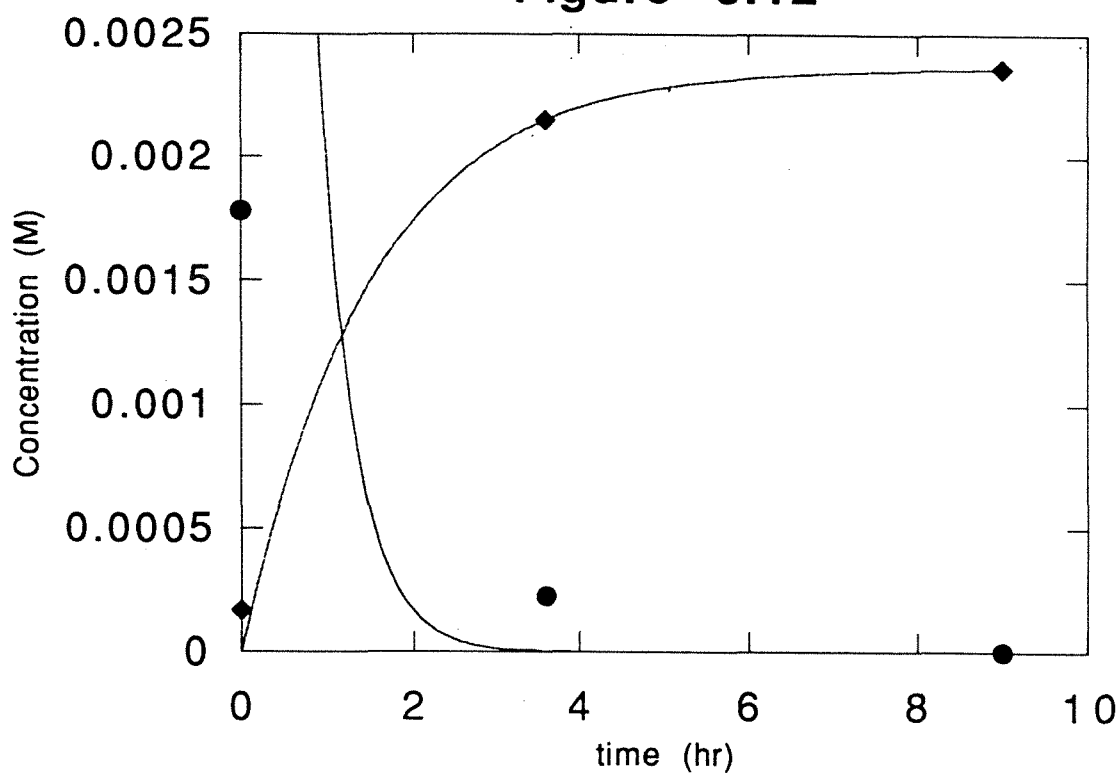


Figure 5.12 Dissolution of MnOOH by EDTA - pH 7.0. Plot of concentrations of total suspended solids and total dissolved Mn versus time for the dissolution of MnOOH by EDTA. Concentration of solids, ●; and total dissolved Mn, ◆; are shown. The pH is 7.0, the solids concentration is 0.5g/l, and the EDTA concentration is 0.05M.

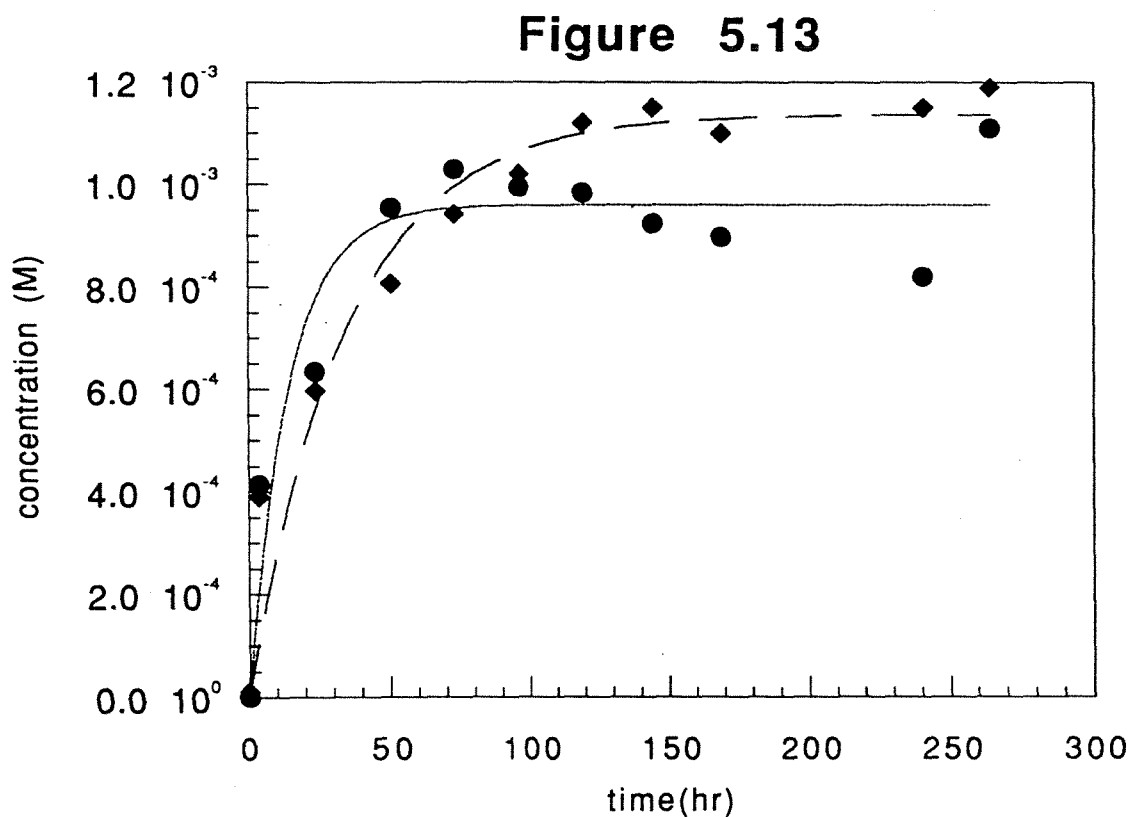


Figure 5.13 Dissolution of MnOOH by CIT - pH 7.8. Plot of concentrations of total dissolved Mn and Mn(III)CIT versus time for the dissolution of MnOOH by CIT. Concentration of Mn(III)CIT, ●; and total dissolved Mn, ◆; are shown. The pH is 7.8, the solids concentration is 0.5g/l, and the CIT concentration is 0.05M.

Figure 5.14

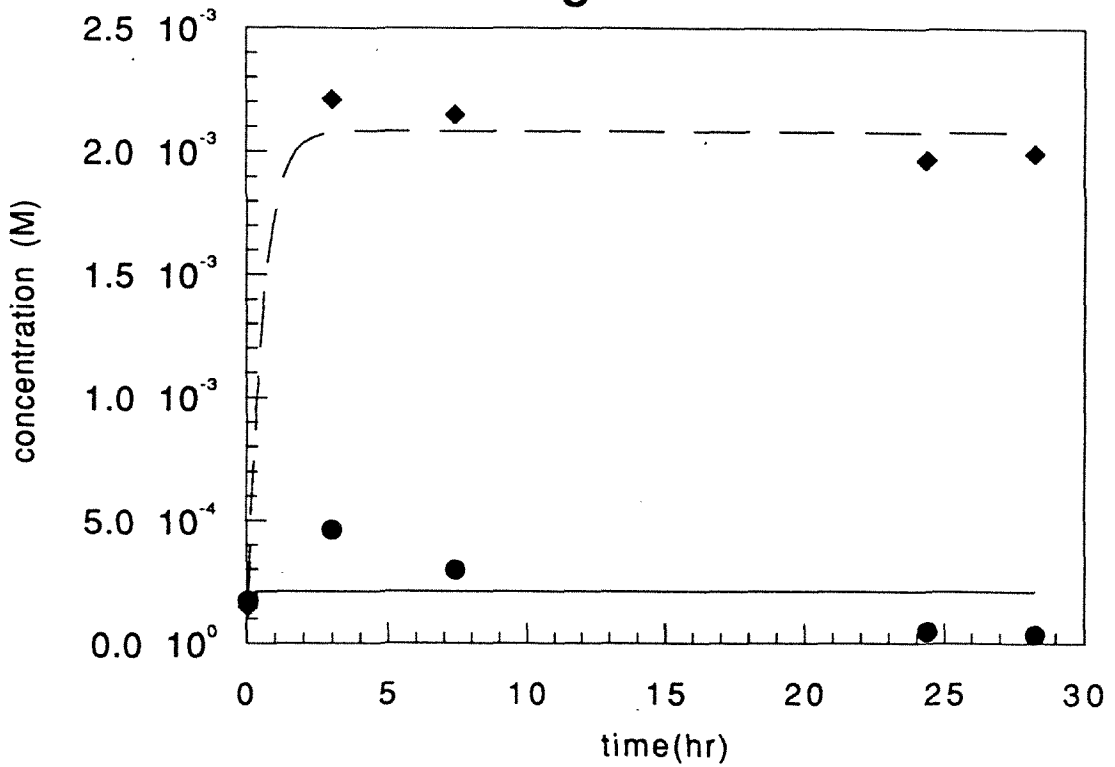


Figure 5.14 Dissolution of MnOOH by CIT - pH 6.3. Plot of concentrations of total dissolved Mn and Mn(III)CIT versus time for the dissolution of MnOOH by CIT. Concentration of Mn(III)CIT, ●; and total dissolved Mn, ◆; are shown. The pH is 6.3, the solids concentration is 0.5g/l, and the CIT concentration is 0.075M.

Figure 5.15

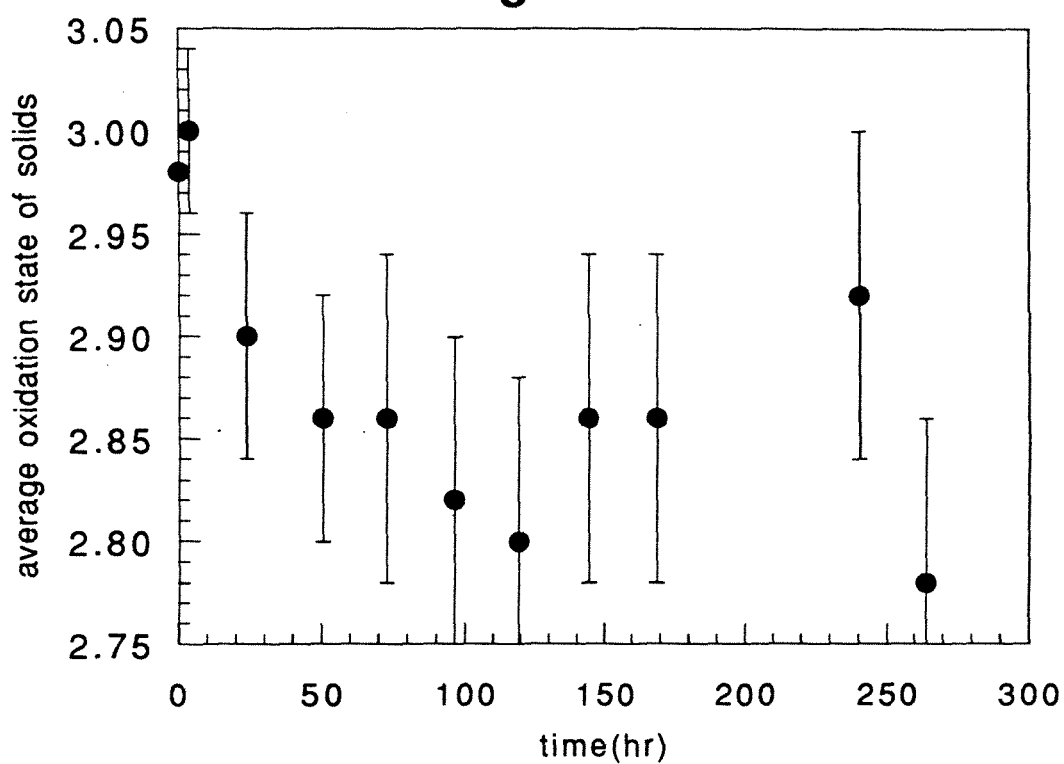


Figure 5.15 Dissolution of MnOOH by CIT - solids oxidation state. Plot of average oxidation state of the solids versus time for the dissolution of MnOOH solids by citrate. The pH is 7.8, the solids concentration is 0.5g/l, and the CIT concentration is 0.05M.

SUMMARY AND CONCLUSIONS

6.1 Important Findings of This Study

6.1.1 Mn Oxidation

The oxidation of Mn(II) was studied at 45, 50, and 60°C at Mn(II) concentrations low enough that the solution was never supersaturated with respect to any solid phase. Rate constants on the order of 10^{-9} s^{-1} were found. An activation energy of $99 \pm 14 \text{ kJ/mol}$ was found. This led to the calculation of a rate constant of $6.9 \pm 0.5 \times 10^{-7} \text{ M}^{-1}\text{s}^{-1}$ for the rate expression

$$\frac{d[\text{Mn}^{2+}]}{dt} = -k \cdot [\text{O}_2] \cdot [\text{Mn}^{2+}] \quad [6.1]$$

at pH 8 and 25°C.

6.1.2 Mn(III)

Rate expressions and rate constants for the disappearance of Mn(III) complexes are given in Table 6.1 for the three ligands studied. The complex of Mn(III) with the $\text{P}_2\text{O}_7^{4-}$ species is the longest lived of the complexes studied, with first order constants on the order of 10^{-7} s^{-1} . While the disappearance rate of Mn(III) P_2O_7 species was observed to depend on both pH and total $\text{P}_2\text{O}_7^{4-}$ concentration, the data are too limited to establish a firm rate law. The kinetic inertness appears greatest at a pH slightly above neutral. Dependence of the loss rate on $[\text{P}_2\text{O}_7^{4-}]$ appears complex, possibly the result of several Mn(III) P_2O_7 complexes with different susceptibility to hydrolysis of the ligand.

The Mn(III)EDTA complex is the shortest lived of the complexes studied. Its disappearance rate constants range from 10^{-3} to 10^{-6} s^{-1} . For the MnEDTA⁻ complex the rate is dependent on the 0.31 power of $[\text{H}^+]$. The fractional dependence is most likely caused by some unknown intermediate complexes which depend on pH. The

reaction rate is somewhat more than proportional to the first power of EDTA concentration. This is believed to be the result of the slowness of the inner sphere electron transfer of the complex as compared to electron transfer from an outer sphere electron donor, the excess EDTA.

The Mn(III)CIT complex displays a more complicated cycle. Rate constants for disappearance of the Mn(III) complex are on the order of 10^{-5} s^{-1} . The rate expression shows a dependence on the 0.2 power of $[\text{H}^+]$ and the 0.1 power of $[\text{CIT}]$. These fractional dependences are due at least in part to the competition between the reduction of the Mn(III) complex and the oxidation of the Mn(II) citrate complex. The rate dependences on pH are obscured somewhat by the difficulty in buffering the citrate experiments. Most of the observations; however, can be explained by a cycle where the Mn(III)CIT complex undergoes an inner sphere electron transfer producing Mn(II) which is then reoxidized to Mn(III) in the presence of oxygen.

6.1.3 MnOOH Dissolution

The rate constants and rate expressions for the dissolution of MnOOH by the ligands used in this study are shown in Table 6.2.

Pyrophosphate caused the slowest of the dissolution reactions. Rate constants were on the order of 10^{-5} s^{-1} . All of the dissolved MnOOH was found to remain in solution as $\text{Mn(III)P}_2\text{O}_7$ species. The dissolution reaction was found to be approximately 0.5 order in $[\text{H}^+]$. This may be the consequence of the unprotonated ligand binding to the surface and releasing a $\text{Mn(III)P}_2\text{O}_7^-$ species to solution.

EDTA was found to dissolve MnOOH the fastest. Rate constants were on the order of 10^{-4} s^{-1} . The dissolution was found to be totally reductive with no evidence for Mn(III) in solution. The reduction by EDTA was found to be 0.4 order in $[\text{H}^+]$. The fractional dependence is likely caused by the adsorption of EDTA to the surface, similar to pyrophosphate. Recently Tian and Stone (1) confirmed the absence of

Mn(III) in solution and detected degradation products of EDTA using capillary electrophoresis.

CIT showed a complex dissolution pattern. The dissolution occurred in two phases. The first phase was a nonreductive dissolution, followed by a second phase of reductive dissolution. Rates constants were on the order of 10^{-4} to 10^{-6} s⁻¹. The dissolution was also found to be approximately first order in [H⁺]. This is probably the result of a outersphere radical reduction pathway becoming rate controlling once the reaction products have accumulated sufficiently.

6.2 Implications of This Study

Figure 6.1a shows the generally accepted cycle of manganese in natural water systems according to the conventional wisdom before Mn(III) was considered as a potential solution phase species. Figure 6.1b shows a proposed new cycle with the possibility of solution phase Mn(III) taken into consideration. This study has addressed several of the additional reactions depicted in Figure 6.1b.

The reduction of solution phase Mn(III)L to Mn(II) species has been measured and it is shown that Mn(III)L complexes can persist in solution on time scales of minutes to months depending on the character of the ligand. Ligands which can easily lose electrons to the Mn(III) react rather rapidly on a time scale of minutes. Complexes of ligands which do not lose electrons to Mn(III) can last for months. Previous studies have not examined the disappearance of a Mn(III)L complex in the absence of external reductants.

The oxidation of Mn(II)L complexes to Mn(III)L complexes has been verified as occurring for citrate in the presence of oxygen. This is a result that was also seen by Guindy et. al., although at much higher pH(2). This study found the oxidation occurs on a time scale of weeks. It has also been shown that Mn(VII) can oxidize Mn(II)L to Mn(III)L on a time scale of minutes. Although Mn(VII) is not present in natural waters other oxidants can exhibit similar reduction potentials. For example

$\text{OH}\cdot$ and H_2O_2 have similar potentials and could be capable of forming Mn(III). Such reactions have been observed in biological systems(3-5).

The ability of ligands to dissolve MnOOH and release Mn(III)L complexes has also been demonstrated. The time scale for this dissolution is on the order of a day. The dissolution reaction of MnOOH by pyrophosphate was studied qualitatively by Kostka et. al. (6).

6.2.1 Surface Waters

The implications of this work for natural waters are many. To answer the question: do Mn(III) complexes exist in natural waters? several factors must be examined. The various species of the system must be considered to determine possible sources of Mn, stabilizing ligands, and oxidants/reductants. In addition the time scale of reactions must be considered to determine how long Mn(III) complexes formed might last.

In surface waters the majority of Mn is found as Mn(II). To produce Mn(III) complexes from Mn(II) in surface waters would require a significant amount of stabilizing ligand and an oxidant. The areas where this is most likely to occur in surface waters are areas of high biological activity or in the surface microlayer. Areas of high biological activity would produce large quantities of organic ligands as well as H_2O_2 , radical species and oxygen produced by the biological activity. The surface microlayer is a layer that has been found to have highly concentrated amounts of organics and metals. It is also the area where dissolved oxygen is likely to be the highest, and radical-producing photochemistry the most active. These areas are capable of producing Mn(III) complexes.

Such complexes once produced would more than likely react with organics or reduced metals in the same area where they were produced and not travel very far. Thus the lifetime of such complexes would more than likely be seconds to minutes rather than days. If the oxidation of Mn(II) to Mn(III) is relatively rapid there could

still be a significant contribution to the redox chemistry of the surface waters. If a cycle were created like that observed in the laboratory for citrate, then catalytic oxidation of organics or reduced metals could occur. This would require the oxidant to be other than oxygen, which has a time scale for oxidation of Mn(II) of days to weeks, even in the presence of surfaces and microbes. Radicals produced by photochemistry or biological activity represent possible oxidants capable of oxidizing Mn(II) to Mn(III) fast enough to produce a catalytic Mn cycle.

There are also some Mn oxides found in surface waters. These result from either oxidation of Mn(II) or deposition from aerosols. Since Mn(II) oxidation has been shown to go through a Mn(III) oxide phase, these Mn oxides represent another possible source of Mn(III) complexes. Again the formation of Mn(III) complexes would have to occur in either the surface microlayer or areas of high biological activity. Such complexes would be short-lived in the absence of a rapid oxidation as described above.

Another area in natural systems where there are likely to be large amounts of Mn(III) stabilizing ligands is in bottom waters and sediments. Since such areas tend to be anoxic, the source of the Mn(III) would have to come from Mn(III) oxides. This is indeed possible if the settling time of the Mn(III) particle is faster than either the reduction time or the time for oxidation to Mn(IV). Once formed, Mn(III) complexes would then go on to react with reductants present. If the time scale of reduction is slow enough there is the possibility that the complexes could diffuse upward above the anoxic/oxic boundary where their lifetime could be longer.

A cycle has already been demonstrated in which Mn oxides settle to the bottom waters, are reduced to Mn(II), diffuse upward to the anoxic/oxic boundary, are reoxidized and settle once again to the bottom waters. Although this cycle has been postulated to involve Mn(IV) oxides, it could very well include Mn(III) intermediates as well, especially since Mn(III) oxides have been found to be the first product of

Mn(II) oxidation. It would seem unlikely that the particles would have time to be oxidized all the way to Mn(IV) before settling back below the anoxic boundary. Thus the area near the oxic/anoxic boundary could be an area where Mn(III) complexes play an important role.

To obtain an idea of the quantitative concentrations and fluxes of Mn(III) possible a simple box model was constructed. Five Mn species: Mn^{2+} , Mn(II)L, Mn(III)L, MnOOH, and MnO_2 were assumed to exist. The processes considered were: oxidation of Mn^{2+} to MnOOH, oxidation of MnOOH to MnO_2 , oxidation of Mn(II)L to Mn(III)L, reduction of MnOOH and MnO_2 to Mn^{2+} , dissolution of MnOOH by ligand, and reduction of Mn(III)L to Mn(II)L. For all the species except Mn^{2+} the concentration was calculated by writing out the change in concentration with respect to time for each species. For example, for MnO_2 :

$$\frac{d[MnO_2]}{dt} = k_{ox2} \cdot [MnOOH] \cdot [O_2] - k_{r2} \cdot [MnO_2] \cdot [R] \cdot [H] \quad [6.2]$$

where k_{ox2} is the rate constant for the oxidation of MnOOH to MnO_2 and k_{r2} is the rate constant for the reduction of MnO_2 to Mn^{2+} by reductant R. The equations were then integrated through time using a $\Delta C/\Delta t$ approach. For example for MnO_2 :

$$\Delta[MnO_2] = (k_{ox2} \cdot [MnOOH] \cdot [O_2] - k_{r2} \cdot [MnO_2] \cdot [R] \cdot [H]) \cdot \Delta t \quad [6.3]$$

time steps of one second were used. $[Mn^{2+}]$ was calculated by using an assumed total Mn and subtracting the concentrations of the other 4 components.

The rate constants and expressions used were obtained from the literature when available, from the present study, or estimated otherwise. Table 6.3 gives the rate constants and rate expressions used for the box model. For the oxidation of Mn^{2+} to MnOOH the rate constant was taken from Davies(7). The same rate was used for

the rate of reduction of both MnOOH and MnO₂ and was taken from Stone(8). The rate constant used was for the reduction of Mn(III,IV) solids by hydroquinone. Although hydroquinone is probably a better reductant than most average organic compounds it was used as it has the best quantified rate expression(for example catechol reduces Mn oxides about ten times faster than hydroquinone while resorcinol is about 1000 times slower and oxalate about 4 to 5 orders of magnitude smaller (8)). A rate constant for the oxidation of MnOOH to MnO₂ could not be found. Therefore it was assumed the rate was first order in MnOOH and O₂. The rate constant assumed would give a half-life of about 1 month for an oxygen concentration in equilibrium with the atmosphere, which is what was observed by Stone(8). An equilibrium constant of 10⁴ M⁻¹ was assumed for the Mn²⁺/Mn(II)L equilibrium. This is typical for many Mn(II)L species. It was assumed that the ligand was strong enough to bind all Mn(III) so that Mn³⁺ is not considered as a species. The rate constants for the reactions of Mn(III)L were taken from this study. The constants for citrate were used as an intermediate value between pyrophosphate and EDTA and as representative of typical organic ligands.

The conditions assumed for the simulation were taken as what might be typical of a surface seawater with biological activity. Two cases were run: one without the Mn(III)L species and one including it. The conditions were pH = 8.0, [O₂] = 2.4 x 10⁻⁴ M, [L] = [R] = 10⁻⁶M, [Ox] = 10⁻⁶M, and Mn_T = 10⁻⁷M. These conditions were assumed to be constant throughout the simulation.

The results of the two cases are shown in Figures 6.2a and 6.2b. It is seen that most of the Mn is in the form of Mn²⁺, with about 1% being Mn(II)L. Both Mn oxides are at much smaller concentrations. This is a result of the slow oxidation and the relatively high concentration of reductant. These results correspond fairly well with what is observed in natural waters and therefore show that the simple model gives results which bear a reasonable similarity to natural systems.

Comparing the results of the run with Mn(III)L and the one without shows a significant difference. Although the concentrations of MnOOH and MnO₂ do not change, Mn(III)L becomes the most significant form of oxidized Mn. The main source of this Mn(III)L is from oxidation of Mn(II)L. Although not all ligands promote the oxidation of Mn(II)L to Mn(III)L as citrate does, and although a micromolar concentration of such a ligand might seem unlikely, it is noted that even if the ligand concentration were 2 orders of magnitude smaller, Mn(III)L would still be the dominant oxidized Mn species. It might be argued that biological oxidation of Mn(II) would give a higher MnOOH concentration. This is true, but the dissolution pathway flux would also increase. Therefore, even though these calculations may not be entirely representative of some natural environments, they do show that Mn(III) complexes can be important species in some natural environments and should be considered when studying natural redox cycles.

6.2.2 Ground Waters

Groundwaters represent another environment where there are potentially significant amounts of Mn(III) stabilizing ligands. Strong oxidants are likely to be much more scarce. The most likely source of oxidant would be radicals or peroxide produced by biological activity. Such oxidants could oxidize Mn(II) to Mn(III) in the presence of stabilizing ligands, which would then oxidize any reductants present. This could produce a cycle as described for surface waters. The area effected by such a cycle would depend on the time scale of loss of the Mn(III) complex. If the stabilizing ligands don't react quickly with Mn(III) it is possible for Mn(III) complexes to migrate through groundwater. If this occurs then these complexes would be a very powerful mobile oxidant.

There are likely to be significant amounts of Mn(III) oxides present in groundwaters either as minerals or as oxidation products formed in more oxic environments. If significant amounts of stabilizing ligand come into contact with the

Mn(III) oxides then Mn(III) complexes will be released. This would be most significant in a case where a nonreducing ligand comes into contact with a Mn(III) oxide in an oxic or mildly anoxic zone. If there are no strong reductants present in the immediate vicinity of release, the Mn(III) complexes could migrate to more anoxic zones and become the major oxidant in such areas. It is conceivable that Mn(III) complexes produced in nitrate or sulfate reducing zones could migrate into more anoxic waters and become significant oxidants.

6.2.3 Other Potential Environments for Mn(III) Complexes

Mn(III) complexes have already been shown to be significant in certain biological systems(9-12). In these systems the Mn(III) complexes act to protect the organisms against powerful oxidants such as superoxide and hydrogen peroxide. Mn(III) is certainly important as a superoxide dismutase of several organisms and may be important in others. Mn(III) may have been even more important in this role in prehistoric environments before the atmospheric levels of oxygen had reached their present level. Much higher levels of UV radiation at that would require organisms to have a defense system against radicals produced by this radiation. Mn is certainly one attractive element to serve this purpose.

Another environment where biological activity and Mn are coupled is in desert varnish(13). Although this is largely a nonaqueous environment there are microenvironments that involve water at the cell wall. Most of the Mn in desert varnish is in the +4 oxidation state, but there is evidence of some Mn below an oxidation state of +4 (14). Mn would most likely have to pass through a Mn(III) phase on its way to becoming Mn(IV) and it is possible that this involves a Mn(III) complex.

A microenvironment that contains high concentrations of Mn and stabilizing ligands is the aerosol. Mn(III) may very well play an important role in the redox

cycling in aerosols. Mn(III) has already been demonstrated to be an intermediate in the Mn catalyzed oxidation of S(IV) (15); it may play a role in other redox reactions as well.

6.3 Directions for Future Research

This study leaves several questions unanswered and opens up several more. These questions and possible approaches to them are listed here.

6.3.1 Mn(II) Oxidation

This study has found a rate of homogenous oxidation of Mn(II) much slower than reported in most previous studies. Problems with evaporation, instability of the leuco crystal violet dye reagent, blank problems, and the possibility of contaminant oxidants from the atmosphere led to a relatively large uncertainty in the rate constants measured. Construction of an air tight reaction vessel to limit evaporation loss and exclude other atmospheric oxidants could help to reduce this uncertainty. Bubbling with pure oxygen also would increase the rate and might give less of a blank problem, as the signal to blank ratio would be higher.

6.3.2 Mn(III) Solution Complexes

Rate expressions for the pyrophosphate complex loss could not be established with the limited data available. Further studies to define the rate law would be helpful. This would involve expanding the experiment to several more pHs and ligand concentrations. It would also be interesting to measure for phosphate hydrolysis product and the Mn(IV) product of disproportionation. If the pyrophosphate hydrolysis is the active loss mechanism, detection of these species would verify the mechanism. Phosphate could be detected using capillary electrophoresis or ion chromatography. Mn(IV) could be detected by filtering the solution, dissolving the filter and measuring Mn.

For EDTA the main challenge lies in the mechanism of reaction and identification of the products. EDTA degradation products could be detected using capillary electrophoresis or ion chromatography. Detection of degradation products would give insight as to the mechanism of the reduction reaction. Analysis of the products both in the presence and absence of oxygen might also be revealing of the mechanism of degradation of EDTA.

The possibility of a cycle for the Mn(III)CIT complex which results in catalytic destruction of citrate is interesting. Although the data of this study suggest that such a cycle exists, it has not been definitively proven. Citrate would need to be measured over time to confirm the cycle. This can be done using capillary electrophoresis. If the loss of citrate were found to be greater than the re-formed Mn(III)CIT that would prove the oxidation of citrate. If product peaks could be identified, that would be helpful in determining both mechanism and stoichiometry. The actual oxidation pathway of the citrate would be crucial to determining how many cycles would be required to destroy the citrate and whether the reaction is actually catalytic.

Another set of interesting question relates to the kinetics of other ligand reactions. If the existence of such complexes in natural systems is to be approached it will be helpful to know the reaction rates for different types of ligands. A class of ligands missing from this study is the aromatic compounds. It would be interesting to examine humic and fulvic type materials as well. Since molar absorptivities are not presently available for such complexes this might require a new technique for Mn(III) detection.

Perhaps the most useful area of research in this area would be development of more sensitive techniques for Mn(III) detection. As natural levels of Mn are usually in the submicromolar range such techniques would be crucial for doing any studies in the natural environment or in trying to simulate natural systems in the laboratory.

Possible techniques for this include polarography, capillary electrophoresis, or electrospray mass spectrometry.

6.3.3 MnOOH Dissolution

For all three ligands investigated more experiments could be done to give a better idea of the rate law. This is especially true in determining the effect of the ligand concentration. More data are needed over a wider range of concentrations. Concentrations in smaller excess than those used in this study should be used to determine if saturation of surface sites was achieved in this study, and what the effect on rate is if the surface sites are not saturated.

Product analysis of any ligand degradation products would be of great interest. This could be done using capillary electrophoresis. It would also be interesting to examine the surface of the solids during the reaction to determine the identity of surface complexes formed, if any, or at least to determine the dissolution pattern of the surface. This might possibly be done using AFM or SEM.

Another very interesting question is the possibility of the reaction noted by the dashed line in Figure 6.1b. That is the formation of Mn(III) complexes from MnO₂. Since MnO₂ is the most stable and one of the most common forms of Mn it would be significant if Mn(III) complexes could form from them. It should be of interest to examine the reaction of MnO₂ with a ligand such as citrate which has the ability both to reduce Mn(IV) to Mn(III) and then to stabilize the Mn(III).

This study has found that Mn(III) complexes can be formed both from solution phase Mn(II) and Mn(III) solids. It has further found that such complexes can be long lived under the proper conditions. The consequences of these facts need to be considered on the natural environment. Such compounds could have a significant effect not only on the kinetics of oxidation in many environments but also on the type of compounds which are capable of being oxidized. Such questions merit further consideration.

References

- (1) Tian, J.; Stone, A. T. Personal Communication **1995**
- (2) Milad, N. E.; Guindy, N. M.; Helmy, F. M. **1971**, *14*, 571 - 580.
- (3) Aitken, M. D.; Irvine, R. L. *Archives of Biochemistry and Biophysics* **1990**, *276*, 405 - 414.
- (4) Glenn, J. K.; Gold, M. H. *Archives of Biochemistry and Biophysics* **1985**, *242*, 329 - 341.
- (5) Kenten, R. H.; Mann, P. J. G. **1952**, *50*, 360 - 369.
- (6) Kostka, J. E.; Luther, G. W.; Nealson, K. H. *Geochimica et Cosmochimica Acta* **1995**, *59*, 885 - 894.
- (7) Davies, S. H. R. PhD Thesis, California Institute of Technology, 1985.
- (8) Stone, A. T. PhD Thesis, California Institute of Technology, 1983.
- (9) Aitken, M. D.; Irvine, R. L. *Archives of Biochemistry and Biophysics* **1990**, *276*, 405 - 414.
- (10) Archibald, F. S.; Fridovich, I. *Archives of Biochemistry and Biophysics* **1982**, *214*, 452 - 463.
- (11) Kenten, R. H.; Mann, P. J. G. **1955**, *61*, 279 - 286.
- (12) Kenten, R. H.; Mann, P. J. G. **1952**, *50*, 360 - 369.
- (13) Potter, R. M.; Rossman, G. R. *Chemical Geology* **1979**, *25*, 79 - 94.
- (14) Rossman, G. R. personal communication **1996**
- (15) Berglund, J.; Fronaeus, S.; Elding, L. I. *Inorganic Chemistry* **1993**, *32*, 4527 - 4538.

Table 6.1
Rate Constants for Mn(III)L Disappearance

Pyrophosphate, $P_2O_7^{4-}$

[Mn] = 0.5mM
[L] = 25mM

pH	rate constant (s^{-1})
6.9	$1.9 \pm 0.2 \times 10^{-7}$
7.3	$1.5 \pm 0.1 \times 10^{-8}$
8.0	$1.2 \pm 0.3 \times 10^{-7}$
8.98	$2.9 \pm 0.2 \times 10^{-8}$

[Mn] = 0.5mM
pH = 7.8

[L] (mM)	rate constant (s^{-1})
12.5	$2.81 \pm 0.08 \times 10^{-7}$
25	$3.6 \pm 0.3 \times 10^{-8}$
50	$3.9 \pm 0.3 \times 10^{-7}$
100	$1.4 \pm 0.2 \times 10^{-7}$

EDTA

Rate Constant Expression for pH > 6:

$$\text{rate constant} = 10^{2.9} [\text{H}^+]^{0.31} [\text{EDTA}]^{1.35}$$

Rate Constants

[Mn] = 0.5mM

[L] = 25mM

pH	rate constant (s ⁻¹)
3.6	$1.67 \pm 0.5 \times 10^{-4}$
4.1	$9. \pm 1 \times 10^{-4}$
5.2	$3.4 \pm 0.1 \times 10^{-3}$
6.0	$3.8 \pm 0.2 \times 10^{-3}$
6.5	$3.7 \pm 0.3 \times 10^{-3}$
6.9	$2.1 \pm 0.1 \times 10^{-3}$
7.3	$1.42 \pm 0.05 \times 10^{-3}$
7.7	$1.08 \pm 0.02 \times 10^{-3}$
9.5	$3.78 \pm 0.07 \times 10^{-4}$

[Mn] = 0.5mM

pH = 6.8

[L] mM	rate constant (s ⁻¹)
0.5	$5.67 \pm 0.5 \times 10^{-6}$
2.5	$8.0 \pm 0.8 \times 10^{-5}$
5.0	$1.7 \pm 0.1 \times 10^{-4}$
25	$1.160 \pm 0.005 \times 10^{-3}$

Citrate

Rate Constant Expression for pH > 6:

$$\text{Rate Constant} = 10^{-0.41} [\text{H}^+]^{0.18} [\text{CIT}]^{-0.13}$$

Rate Constants

$$[\text{Mn}] = 1\text{mM}$$

$$[\text{L}] = 200\text{mM}$$

pH	rate constant (hr ⁻¹)
6.1	$1.6 \pm 0.2 \times 10^{-5}$
6.8	$6.4 \pm 0.8 \times 10^{-6}$
8.5	$3.6 \pm 1 \times 10^{-6}$
9.2	1.86×10^{-6}
9.8	1.92×10^{-6}

$$[\text{Mn}] = 0.5\text{mM}$$

$$\text{pH}_0 = 6.0$$

[L] mM	rate constant (hr ⁻¹)
1.0	1.25×10^{-5}
2.5	9.17×10^{-6}
5.0	9.72×10^{-6}
25	7.78×10^{-6}

Table 6.2
Rate Constants for MnOOH dissolution

Pyrophosphate, $P_2O_7^{4-}$

Rate Constant Expression:

$$\text{rate constant} = 10^{-1.27} [H^+]^{0.46}$$

[L] = 50mM

[solids] (g/l)	pH	rate constant (s^{-1})
0.5	6.5	$5.0 \pm 0.8 \times 10^{-5}$
0.5	7.0	$3.0 \pm 0.08 \times 10^{-5}$
1.0	8.0	$1.0 \pm 0.1 \times 10^{-5}$
0.2	8.0	$1.0 \pm 0.1 \times 10^{-5}$

EDTA

Rate Constant Expression:

$$\text{rate constant} = 10^{-0.74} [H^+]^{0.42}$$

[solids] = 0.5g/l

[L] (mM)	pH	rate constant (s^{-1})
25	8.0	$6.83 \pm 0.05 \times 10^{-5}$
50	7.0	$1.8 \pm 0.8 \times 10^{-4}$

Citrate

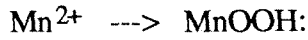
Rate Constant Expression:

$$\text{rate constant} = 10^{4.35} [H^+]^{1.2}$$

[solids] = 0.5g/l

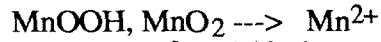
[L] (mM)	pH	rate constant (s^{-1})
50	7.8	$7.8 \pm 1 \times 10^{-6}$
75	6.3	$5.0 \pm 3 \times 10^{-4}$

Table 6.3
Rate constants and expressions used for box model



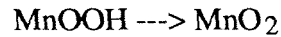
$k = 5.8 \times 10^{13} \text{ M}^{-4} \text{ s}^{-1}$

$$-\frac{d[\text{Mn(II)}]}{dt} = k \cdot [\text{Mn}^{2+}] \cdot [\text{OH}^-]^2 \cdot [\text{O}_2] \cdot [\text{Ox}]$$



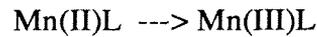
$k = 4.8 \times 10^9 \text{ M}^{-1.46} \text{ s}^{-1}$

$$-\frac{d[\text{Mnox}]}{dt} = k \cdot [\text{Mnox}] \cdot [\text{R}] \cdot [\text{H}^+]^{0.46}$$



$k = 1.5 \times 10^{-3} \text{ M}^{-1} \text{ s}^{-1}$

$$-\frac{d[\text{MnOOH}]}{dt} = k \cdot [\text{MnOOH}] \cdot [\text{O}_2]$$



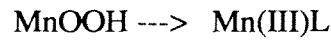
$k = 1.37 \times 10^{-18} \text{ M s}^{-1}$

$$-\frac{d[\text{Mn(II)L}]}{dt} = \frac{k \cdot [\text{Mn(II)L}] \cdot [\text{O}_2]}{[\text{H}^+]^2}$$



$k = 1.3 \times 10^4 \text{ M}^{-1.12} \text{ s}^{-1}$

$$-\frac{d[\text{Mn(III)L}]}{dt} = k \cdot [\text{Mn(III)L}] \cdot [\text{H}^+]^{1.12}$$



$k = 2.2 \times 10^{16} \text{ M}^{-3} \text{ s}^{-1}$

$$-\frac{d[\text{MnOOH}]}{dt} = k \cdot [\text{MnOOH}] \cdot [\text{L}] \cdot [\text{H}^+]^2$$

Figure 6.1a
Mn Cycle without Knowledge of Mn(III) solution species

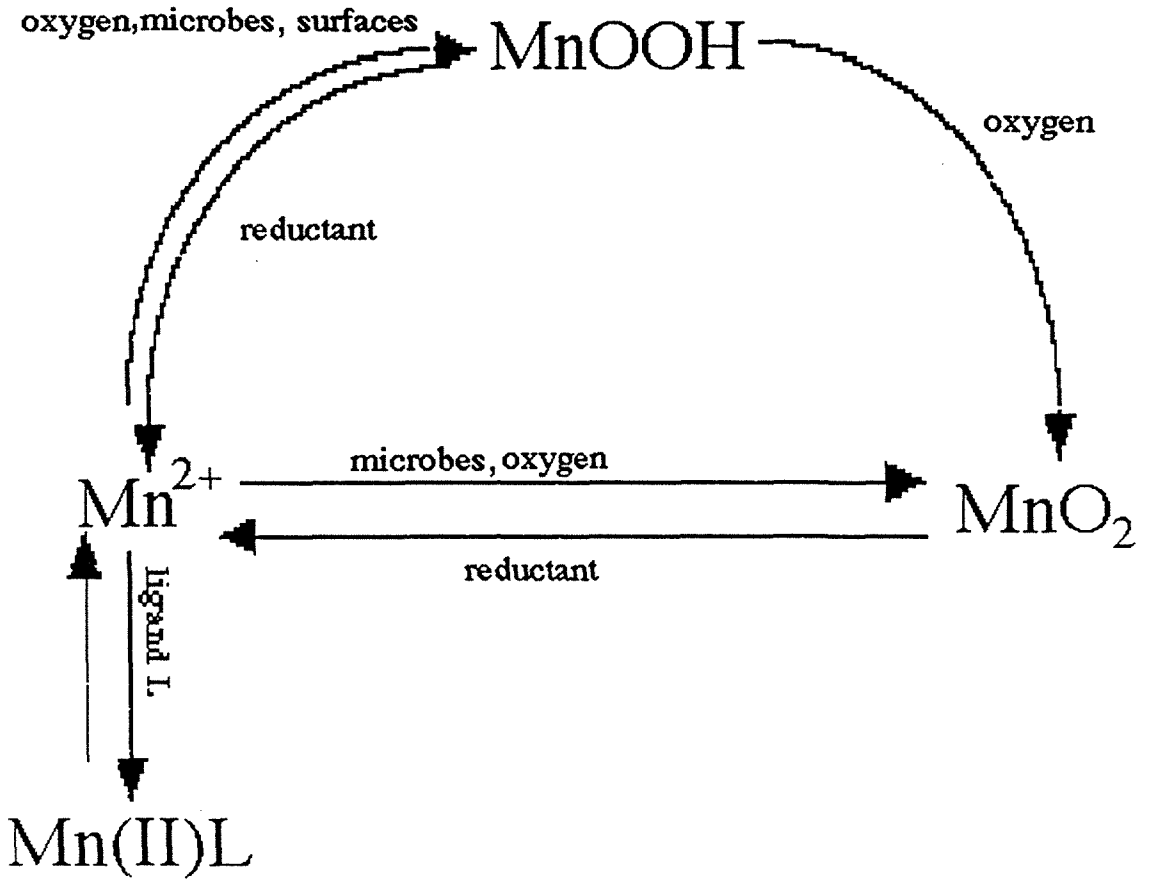


Figure 6.1b
Mn Cycle With Knowledge of Mn(III) solution species

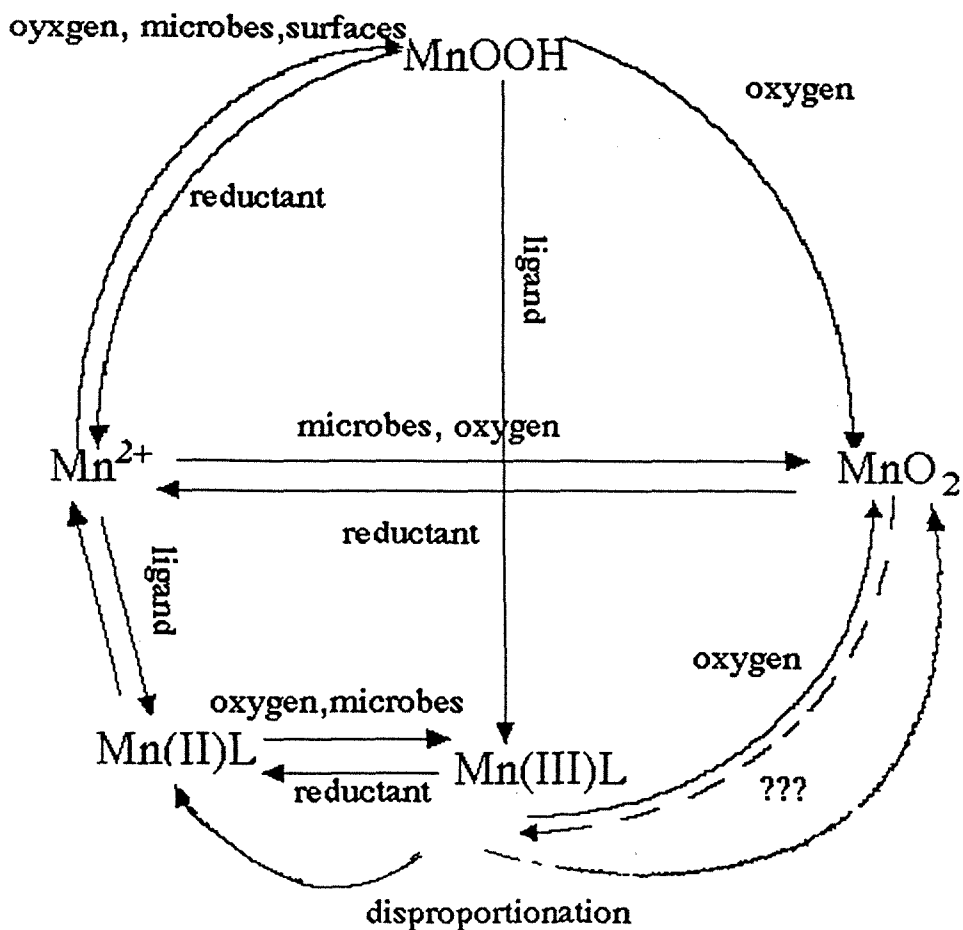


Figure 6.2a

Box Model Results for an Mn(II)-MnOOH-MnO₂ System

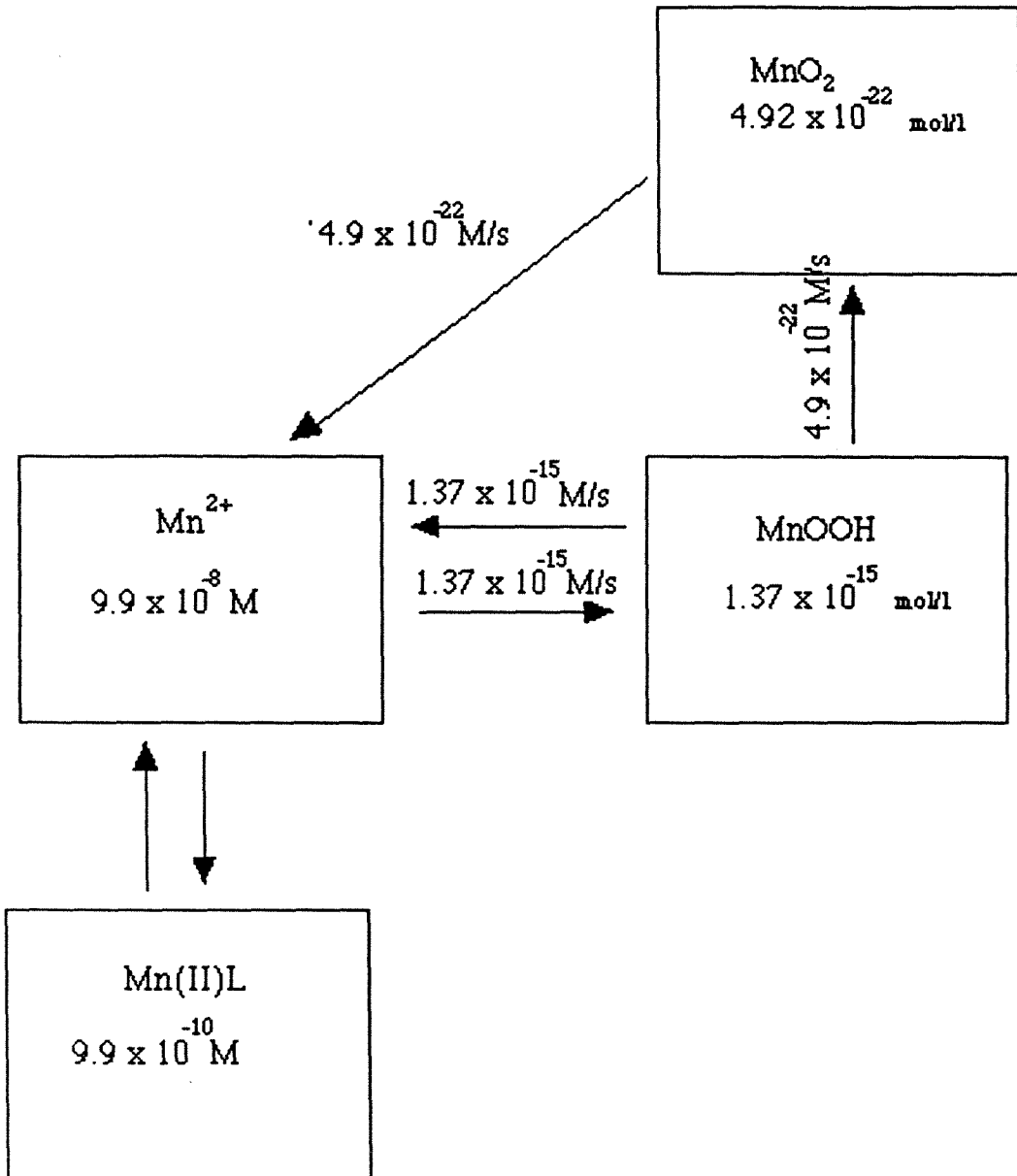
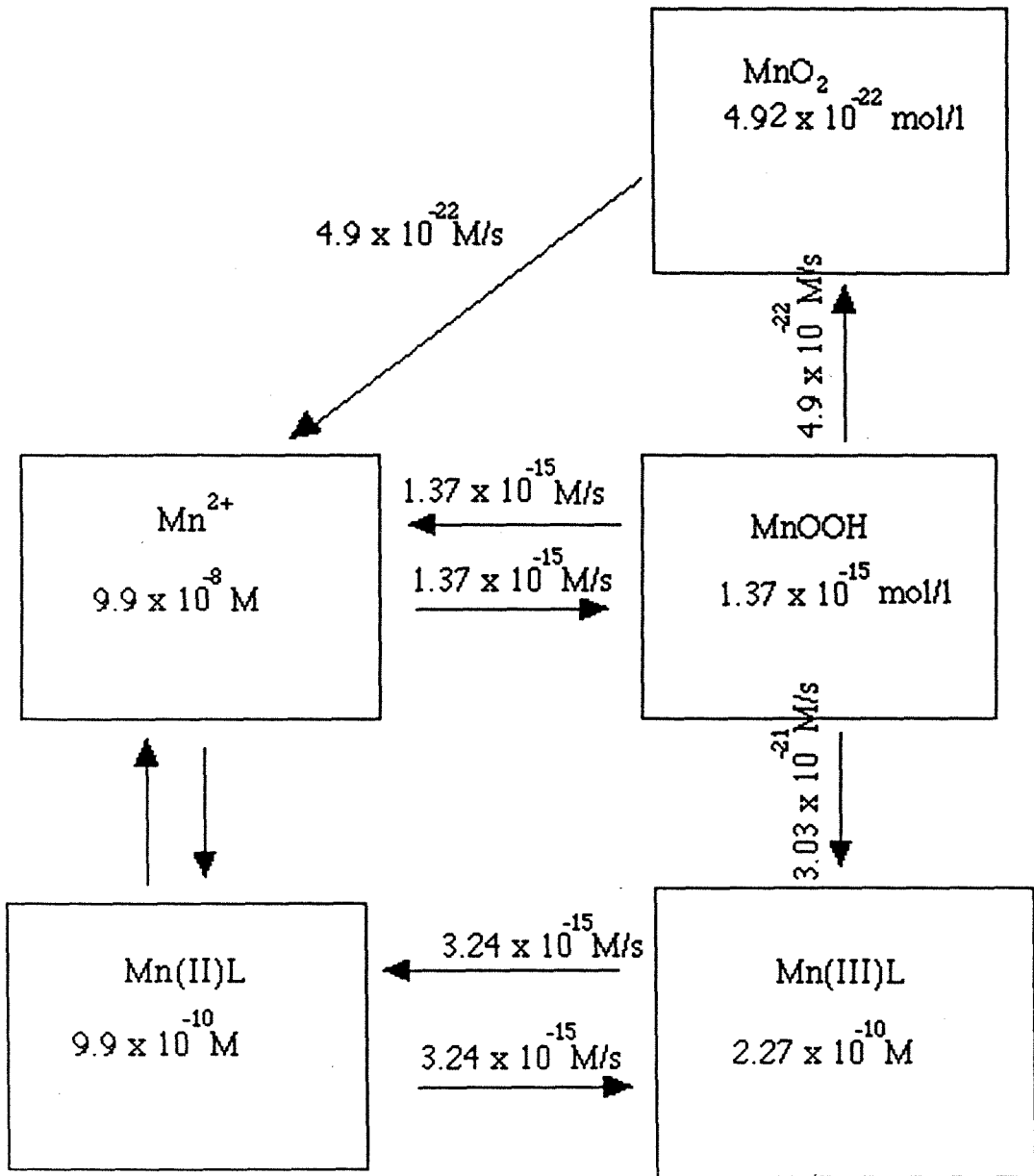


Figure 6.2b
 Box Model Results for an Mn(II)-MnOOH-Mn(III)L-MnO₂ System



Appendix A

Table 1
Acidity Constants of Ligands Used in This Study

Pyrophosphate

Reaction	log Constant ^a
$H_4L \rightleftharpoons H^+ + H_3L^-$	-0.8
$H_3L^- \rightleftharpoons H^+ + H_2L^{2-}$	-2.0
$H_2L^{2-} \rightleftharpoons H^+ + HL^{3-}$	-6.04
$HL^{3-} \rightleftharpoons H^+ + L^{4-}$	-8.37

EDTA

Reaction	log Constant ^a
$H_4L \rightleftharpoons H^+ + H_3L^-$	-2.0
$H_3L^- \rightleftharpoons H^+ + H_2L^{2-}$	-2.69
$H_2L^{2-} \rightleftharpoons H^+ + HL^{3-}$	-6.18
$HL^{3-} \rightleftharpoons H^+ + L^{4-}$	-10.15

Citrate

Reaction	log Constant ^a
$H_3L \rightleftharpoons H^+ + H_2L^-$	-2.85
$H_2L^- \rightleftharpoons H^+ + HL^{2-}$	-4.35
$HL^{2-} \rightleftharpoons H^+ + L^{3-}$	-5.82

^a all constants for 25°C and I = 0.1M

Table 2
Stability Constants of Mn(II) and Mn(III) Complexes

Mn(II)

Reaction	log Constant ^a
$\text{Mn}^{2+} + \text{P}_2\text{O}_7^{4-} \rightleftharpoons \text{MnP}_2\text{O}_7^{2-}$	6.5
$\text{Mn}^{2+} + \text{EDTA}^{4-} \rightleftharpoons \text{MnEDTA}^{2-}$	14.05
$\text{Mn}^{2+} + \text{CIT}^{3-} \rightleftharpoons \text{MnCIT}^-$	2.16
$\text{Mn}^{2+} + \text{OH}^- \rightleftharpoons \text{MnOH}^+$	3.4 ^b
$\text{Mn}^{2+} + \text{HCO}_3^- \rightleftharpoons \text{MnHCO}_3^-$	0.45 ^b

Mn(III)

Reaction	log Constant ^a
$\text{Mn}^{3+} + 2\text{P}_2\text{O}_7^{4-} \rightleftharpoons \text{Mn}(\text{P}_2\text{O}_7^{2-})_2^{5-}$	31.85 ^c
$\text{Mn}^{3+} + \text{P}_2\text{O}_7^{4-} \rightleftharpoons \text{MnP}_2\text{O}_7^-$	16.68 ^c
$\text{Mn}^{3+} + \text{EDTA}^{4-} \rightleftharpoons \text{MnEDTA}^-$	24.75
$\text{Mn}^{3+} + \text{CIT}^{3-} \rightleftharpoons \text{MnCIT}$	14 ^d
$\text{Mn}^{3+} + \text{OH}^- \rightleftharpoons \text{MnOH}^{2+}$	14.4 ^e

^a unless otherwise noted constants for 25°C and I = 0.1M

^b constants for 25°C and I = 0M

^c constants for 25°C and I = 0.3M

^d constant estimated from analogy with Fe complexes

^e constant for 25°C and I = 4M

Table 3
Equilibrium Constants of Mn Solids

Reaction	log Constant
$\text{Mn}^{2+} + 2\text{H}_2\text{O} \rightleftharpoons \text{MnO}_2(\text{s}) + 4\text{H}^+ + 2\text{e}^-$	-41.38
$3\text{Mn}^{2+} + 4\text{H}_2\text{O} \rightleftharpoons \text{Mn}_3\text{O}_4(\text{s}) + 8\text{H}^+ + 2\text{e}^-$	-61.03
$\text{Mn}^{2+} + 2\text{H}_2\text{O} \rightleftharpoons \text{MnOOH}(\text{s}) + 3\text{H}^+ + \text{e}^-$	-25.34
$\text{Mn}^{2+} + \text{CO}_3^{2-} \rightleftharpoons \text{MnCO}_3(\text{s})$	10.30
$\text{Mn}^{2+} + 2\text{OH}^- \rightleftharpoons \text{Mn}(\text{OH})_2(\text{s})$	12.8

Table 4
Band Gap Energy of β -MnO₂

4768 nm